



Cardiff  
Catalysis Institute

---

Sefydliad Catalysis  
Caerdydd

# Catalysis by Gold

**Thesis submitted in accordance with the requirements of Cardiff  
University for the degree of Doctor of Philosophy**

**Scott Patrick Davies**

**2017**

## DECLARATION

This work has not been submitted in substance for any other degree or award at this or any other university or place of learning, nor is being submitted concurrently in candidature for any degree or other award.

Signed .....(candidate)                      Date.....

## STATEMENT 1

This thesis is being submitted in partial fulfillment of the requirements for the degree of .....(insert MCh, MD, MPhil, PhD etc, as appropriate)

Signed .....(candidate)                      Date.....

## STATEMENT 2

This thesis is the result of my own independent work/investigation, except where otherwise stated, and the thesis has not been edited by a third party beyond what is permitted by Cardiff University's Policy on the Use of Third Party Editors by Research Degree Students. Other sources are acknowledged by explicit references. The views expressed are my own.

Signed .....(candidate)                      Date.....

## STATEMENT 3

I hereby give consent for my thesis, if accepted, to be available online in the University's Open Access repository and for inter-library loan, and for the title and summary to be made available to outside organisations.

Signed .....(candidate)                      Date.....

## STATEMENT 4: PREVIOUSLY APPROVED BAR ON ACCESS

I hereby give consent for my thesis, if accepted, to be available online in the University's Open Access repository and for inter-library loans **after expiry of a bar on access previously approved by the Academic Standards & Quality Committee.**

Signed .....(candidate)                      Date.....

# Abstract

The oxidation of benzyl alcohol over supported Au, Pd and AuPd catalysts on a range of metal oxide supports was investigated using a Radley's Starfish Reactor. Reaction conditions such as temperature, solvent, support and metal loading were varied in order to obtain insight into benzyl alcohol oxidation. All catalysts were prepared using the sol immobilisation technique. It was discovered that AuPd bimetallic catalysts were most active for benzyl alcohol oxidation, in a ratio of 1:1 Au:Pd.

Further, substituted benzyl alcohol compounds were oxidised using AuPd catalysts in order to investigate the mechanistic properties of benzyl alcohol oxidation. By conducting the Hammett methodology on a range of substituents, mechanistic insight into the reaction was possible due to the electronic effects substituent groups had on the parent benzyl alcohol molecule. The results from these experiments indicate that a transition state with a formal charge is being created as the reaction proceeds and electron donating groups such as MeO in the *para*- position was able to stabilise this transition state and promote the oxidation reaction, resulting in a higher rate of reaction.

Lastly, cinnamyl alcohol was subjected to the same oxidation reactions as benzyl alcohol in order to assess how a structural variant of benzyl alcohol is affected by varying certain catalytic parameters such as temperature, support and solvent. It was found that cinnamyl alcohol undergoes similar reactions as benzyl alcohol and the major oxidation product is the corresponding cinnamaldehyde. Differing supports had different effects on the oxidation, with disproportionation being suppressed on certain supports. Higher temperature also promoted hydrogenation of cinnamyl alcohol.

# Acknowledgements

I would like to begin by thanking my ever patient supervisors, Graham Hutchings, Stuart Taylor and Dave Knight for their input, help, support and guidance over the last few years. Without their support, this thesis would not have been possible. I'd like to thank Prof. Golunski for being a mentor and for his calm demeanour which reassured a most panicked student.

Special thanks go to Dr Gemma Brett for always seeing the bright side of situations and for going above and beyond the call of duty in her ever diligent support of this thesis. I'd like to thank Dr Peter Miedziak for the support and guidance he has given throughout my time at the CCI. Thanks to Dr Sankar Meenakshisundaram for his enthusiasm and pastoral care and for always showing a passion and dedication to work that was highly infectious. Thanks go to Dr Eva Nowicka for her unique style of friendship, one that defined being a student at the CCI and one that was caring, nurturing and very straight talking.

Thanks to the technicians who are always happy to help and get stuck in to solve your problem and who you can chat to for hours on end and feel like you've known them for a while.

A very special thanks to all the staff at Bute Library, especially Rhi and Lisa who were the best work colleagues anyone could ask for.

I'd like to thank all the friends I have made in the CCI, from old acquaintances to new faces, it was a highlight of the working week to converse with the fellow students in the office.

Thanks go to Charlie for provided much needed entertainment and relief whilst completing this PhD. Special mention goes to Neil Henderson for his exemplary proof reading skills.

Lastly, I'd like to thank my parents as without their constant support and encouragement, I would not have achieved nearly half as much as I have in life.

# Contents

1.	Introduction .....	1
1.1.	Catalysis .....	1
1.2.	Gold Catalysis .....	3
1.2.1.	Preparation Methods.....	4
1.2.2.	Gold catalysts for selective oxidation .....	6
1.3.	Direct synthesis of hydrogen peroxide .....	6
1.4.	Alkene epoxidation .....	8
1.5.	C-H bond activation .....	9
1.6.	Alcohol Oxidation.....	10
1.6.1.	Benzyl Alcohol Oxidation .....	11
1.6.2.	Cinnamyl Alcohol oxidation .....	14
1.7.	CO Oxidation .....	14
1.8.	Acetylene Hydrochlorination .....	15
1.8.1.	Mechanism of acetylene hydrochlorination.....	17
1.9.	Biodiesel Production .....	18
1.9.1.	Glycerol Transformation.....	20
1.9.2.	Glycerol Oxidation.....	21
1.10.	Crotyl Alcohol Oxidation .....	23
1.11.	Aims of the study .....	24
2.	Experimental .....	37
2.1.	Chemicals.....	37
2.2.	Definitions.....	38
2.3.	Definitions.....	38
2.4.	Catalyst Preparation .....	39
2.4.1.	Sol Immobilisation.....	39

2.4.2.	Au, Pd, Au-Pd Catalysts by sol immobilisation .....	39
2.5.	Catalyst Evaluation .....	40
2.5.1.	Oxidation of alcohols in water .....	40
2.5.2.	Solvent free alcohol oxidation .....	40
2.5.3.	Oxidation of alcohols in benzene .....	41
2.5.4.	Oxidation of alcohols in methanol .....	41
2.6.	Catalyst Characterisation .....	41
2.6.1.	X-ray Photoelectron Spectroscopy .....	43
2.6.2.	X-Ray Diffraction .....	47
2.6.3.	Microwave Plasma Atomic Emission Spectrometry .....	48
2.7.	Product Analysis .....	52
2.7.1.	Nuclear Magnetic Spectrometry .....	52
2.7.2.	Gas Chromatography .....	53
2.7.3.	Gas Chromatography/Mass Spectrometry .....	54
3.	Benzyl Alcohol Oxidation .....	57
3.1.	Introduction .....	57
3.2.	Catalyst Characterisation .....	58
3.2.1.	MP-AES Results .....	58
3.2.2.	XPS Analysis .....	59
3.2.3.	TEM Analysis .....	61
3.3.	Catalyst Evaluation .....	61
3.3.1.	Effect of solvent .....	62
3.3.2.	Effect of AuPd Ratio .....	73
3.4.	Summary .....	80
4.	Effect of substituent groups on the oxidation of benzyl alcohol .....	86
4.1.	Introduction .....	86
4.2.	Methoxy group substitution in the <i>para</i> - position .....	88
4.3.	Halide group substitution in the <i>para</i> - position .....	90

4.4.	Effect of Au:Pd ratio and support on the oxidation of 4-Methoxybenzyl alcohol and 4-Fluorobenzyl alcohol .....	93
4.5.	Overall comparison/Hammett plot.....	95
4.6.	Hammett Plot.....	98
5.	Cinnamyl Alcohol Oxidation.....	110
5.1.	Introduction.....	110
5.2.	Effect of support .....	114
5.3.	Effect of temperature .....	127
5.4.	Effect of metal loading .....	131
5.5.	Conclusion.....	133
6.	General Discussion, Conclusion and Future Work.....	140
6.1.	General Discussion and Conclusions .....	140
6.1.1.	Effects of solvent and metal ratio on benzyl alcohol oxidation .....	140
6.1.2.	Effects of substituent groups on the oxidation of benzyl alcohol.....	143
6.1.3.	Effect of Au and Pd ratio on the oxidation of substituted benzyl alcohols ...	144
6.1.4.	Hammett methodology on the reaction of substituted benzyl alcohols.....	144
6.1.5.	Cinnamyl alcohol oxidation and the effect of support .....	145
6.1.6.	Effect of temperature on cinnamyl alcohol oxidation .....	146
6.1.7.	Effect of metal loading on the oxidation of cinnamyl alcohol.....	147
6.2.	Future work .....	147

# Chapter 1

## 1. Introduction

### 1.1. Catalysis

Catalysis is a term that was first used in 1835 by J.J. Berzelius whilst observing certain physical phenomena that at that point, had no explanation<sup>1</sup>. Berzelius had noted that certain compounds seemed to promote the decomposition of other reactants when present in small concentrations. He called this the catalytic force. In modern times, a catalyst is defined as *“a body or material which can induce the phenomenon of catalysis. It enhances the rate of reaction, and while being intimately involved in the reaction sequence, it is regenerated at the end of it”*<sup>2</sup>.

Catalysts have wide ranging applications today, with well-known examples being the Davy lamp and the Haber process. Davy lamps were used by miners to assess the safety of the mines they were operating in and had platinum or palladium wires surrounding a flame. This flame would heat up the wire and when exposed to explosive atmospheres, the flame would go out but the wire would become incandescent, alerting miners to the potential danger. The Haber process<sup>3</sup> is an incredibly important process, developed in the early 20<sup>th</sup> century it fixes nitrogen to allow its use in agriculture as a fertiliser. Without the Haber process, global crop production would be significantly lower and would not be able to sustain the current global population.

Catalysts come in many different forms: heterogeneous, homogeneous, and biological. Homogeneous catalysts are catalysts that operate in the same phase as the reactants, such as a liquid catalyst and liquid reactant; heterogeneous catalysts are catalysts that operate in a different phase to the reactants, such as a supported metal catalyst reacting with liquids or gases as in the case of the Haber process; biological catalysts are usually enzymatic in nature and are present in every living thing such as energy production from consumed food.



For heterogeneous catalysts, the surface chemistry is of key importance in determining their activity and selectivity. Surface chemistry is largely dependent on factors including how easily the reactants can diffuse to the catalyst surface, how strongly reactants adsorb onto the catalyst surface, and how readily they react on the catalyst surface. How easily the products of the reaction desorb from the catalyst surface is also of critical importance as if the products do not desorb they can deactivate the catalyst. This study is concerned only with heterogeneous catalysts due to their wide range of applications.

Catalysts are an important global asset, with estimates suggesting over 90% of all commercially produced chemical products involve catalysis at some point in their manufacture<sup>4</sup>. With such a high penetration rate in global chemical production and with the potential for future global productivity facing new challenges due to resource shortages and an ever-increasing population, the need for more efficient catalysts is high. This need is the driving force behind the search for new, green catalysts that do not use toxic, stoichiometric oxygen sources or other toxic compounds. As this demand continues, the research into heterogeneous catalysts will continue.

As mentioned, the demand and usefulness of catalysts is high. This is due to the nature of how catalysts operate, they can lower the activation energy of reactions which allows the reaction to take place at lower temperatures or over a shorter period of time. This is highlighted in Figure 1-1: under normal circumstances, the reactants X and Y would follow the non-catalysed energy profile which has a high activation energy. This high activation energy would either mean the reaction would need to be conducted under harsh conditions, such as high temperatures and pressures, or mean the reaction is not feasible. By introducing the catalyst, a new, lower energy pathway is available (red) which allows X and Y to form Z at lower temperatures and pressures.

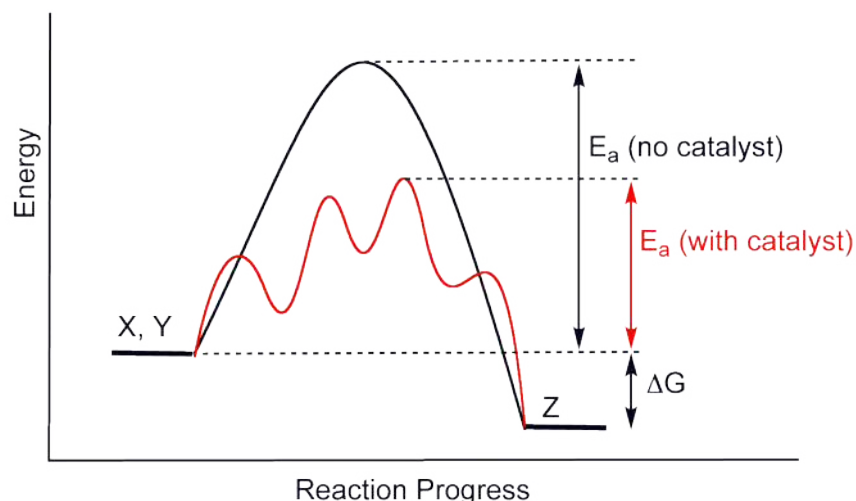


**Figure 1-1 A potential energy diagram showing the exothermic reaction of substrates X and Y to form product Z. Peaks represent transition states. Catalysed pathway is highlighted in red and the non-catalysed pathway in black<sup>5</sup>**

## 1.2. Gold Catalysis

Traditionally, gold has been seen as an inert material with limited catalytic capability. This is reflected in its use as a fashion item and use as an item of value as it was assumed that gold would not tarnish due to its inertness. This opinion has now changed, with Bond *et al.*<sup>6</sup> using  $\text{HAuCl}_4$  as a precursor to a catalyst that was able to hydrogenate olefins. This was then supplemented sometime later by work from Haruta *et al.*<sup>7</sup> who demonstrated gold supported on iron oxide was the most effective catalyst for the low temperature oxidation of CO. The preparation of these catalysts was investigated and this led to the discovery that the size of the gold particles on the metal oxide could be controlled and was key to ensuring an active catalyst.

Research by Hutchings *et al.*<sup>8</sup> demonstrated that supported gold catalysts would be highly effective in the hydrochlorination of ethyne. Both Haruta's and Hutchings's seminal studies began a new era of research into gold catalysis and highlighted the fact this metal was not as inert as it had been assumed for so long. Further work by Haruta *et al.*<sup>9</sup> demonstrated gold supported on  $\text{TiO}_2$  could be used as a catalyst for the oxidation of propene to propene oxide. Since these early studies by Haruta and Hutchings, further research teams have demonstrated gold catalysts as being an ideal candidate for oxidation reactions, such as Prati and Rossi<sup>10</sup>, who showed gold supported on carbon was active for the selective oxidation for ethylene glycol and 1,2-propanediol.

Moving to a point closer in time to present day, Hutchings discovered the next major breakthrough in gold catalysis, observing gold containing catalysts were active for the direct synthesis of hydrogen peroxide under non-explosive conditions<sup>11</sup>.

Throughout the current literature on gold catalysis it has been demonstrated that in order for gold to be catalytically active, it needs to have been formed in nanoparticulate form<sup>12</sup>. It is in this state that gold can catalyse reactions and why, up until recently, it has been considered an inert material as bulk gold is highly unreactive. To control the size of gold particles, various catalytic preparation methods have been designed which is in addition to the considerations of type of support and whether one wants to induce an alloying of the gold catalysts with a secondary metal.

### 1.2.1. Preparation Methods

Gold containing catalysts can be prepared via several different methodologies which each impart varying control over key catalyst features. One of the more basic catalyst preparation methods is the impregnation technique in which a gold precursor solution is stirred with the chosen solid support and subsequently calcined at high temperature. This synthetic preparation of gold catalysts has been used in the study of alcohol oxidation<sup>13</sup> and hydrogen peroxide synthesis<sup>14</sup>. Catalysts prepared via impregnation usually contain large nanoparticle sizes of > 10 nm and are usually inactive for CO oxidation<sup>14</sup>.

Haruta *et al.*<sup>7</sup> developed a new gold catalysis preparation technique called deposition precipitation (DP) which allowed for a higher degree of control over the size of gold nanoparticles synthesised, allowing smaller nanoparticles to be formed. Using the DP method introduced many more variables in the catalyst preparation such as concentration of the metal precursors, pH, stirring time and calcination conditions<sup>6</sup>.

Another synthetic route to gold catalysis is the co-precipitation route<sup>6</sup> in which the metal precursor and metal oxide precursor, typically in the form of a nitrate, are heated and adjusted

to a pH in which precipitation occurs. The resultant solution is filtered to obtain the precipitate, washed, dried and calcined and has similar variable parameters such as the DP method.

Finally, colloidal gold species have been known to exist for quite some time and early exploits of synthesising gold colloids involved solutions of  $\text{HAuCl}_4$  being reduced with toxic white phosphorus to produce a colloidal solution of metallic gold<sup>15</sup>. These colloids were observed to have a broad size distribution and consisted mainly of large particles of gold<sup>16</sup>. As gold particle size is of critical importance in synthesising active catalysts, a new synthetic technique involving colloids was discovered and subsequently named the sol immobilisation technique.

Sol immobilisation is a relatively new catalyst synthesis method which involves the generation of a gold colloid which is immobilised onto a support using a polymer to act as a stabiliser for the nanoparticles once they are stuck on the support material. Before the stabilising ligand is added to the sol, the metal cation species are reduced using  $\text{NaBH}_4$  to take the oxidation state of gold from  $3+$  to  $0$ . Using sol immobilisation, a very narrow size distribution is able to be achieved, with gold particle sizes ranging between  $2 - 10 \text{ nm}$ <sup>17</sup>. Using this technique, gold nanoparticles have been immobilised over a range of metal oxide supports such as  $\text{TiO}_2$ ,  $\text{ZrO}_2$  and  $\text{Al}_2\text{O}_3$  by stirring in water, acidified to pH 2 using  $\text{HCl}$ . This is below the isoelectric point of the support material, enabling the nanoparticles to stick to its surface. These catalysts were observed to be active for CO oxidation without calcination which contrasts with gold catalysts prepared via DP and impregnation.

Sol immobilisation has also allowed researchers to create bimetallic catalysts containing  $\text{AuPd}$ <sup>18</sup> and  $\text{AuPt}$ <sup>19</sup> nanoparticles supported on metal oxides. These bimetallic catalysts have been observed to be higher in activity compared to their monometallic analogues, demonstrating a synergistic effect between the two metals. It has been shown that bimetallic catalysts prepared via sol immobilisation are predominantly random alloys<sup>17</sup>.

### 1.2.2. Gold catalysts for selective oxidation

Gold catalysts have been shown to be active for a variety of oxidation reactions, from alcohol oxidation, CO oxidation and hydrogen peroxide synthesis<sup>20</sup>. These gold catalysts have been observed to be more stable and selective than traditional catalysts based on platinum and palladium<sup>19</sup>. As gold has a high electrode potential, it is resistant to oxygen and other poisons which traditionally deactivate conventional catalysts.

### 1.3. Direct synthesis of hydrogen peroxide

Hydrogen peroxide ( $\text{H}_2\text{O}_2$ ) is a simple molecule with a myriad of uses, both in the home in products such as hair dye and industrially in paper bleaching<sup>21</sup>. Hydrogen peroxide is considered to be a green reagent due to its breakdown product being water and is used as a replacement to stoichiometric oxidants such as sodium percarbonate, which has significant toxicity issues that need considering when used industrially<sup>22</sup>.

Hydrogen peroxide, whilst considered a green chemical itself, is not currently produced in environmentally benign ways as its production is only viable on an industrially large scale. Hydrogen peroxide is currently produced using the anthraquinone cycle, which is only economical at large scale and also produces hydrogen peroxide in concentrations far exceeding the concentrations required at the point of use<sup>23</sup>. Additionally, as the anthraquinone cycle is an industrial process in large chemical plants there is a transportation element which needs consideration regarding the hydrogen peroxide synthesised using this production method. If hydrogen peroxide could be produced locally and in concentrations closer to the desired usage concentration, advantages would include less environmental impact from  $\text{H}_2\text{O}_2$  production.

The first patent awarded for the direct synthesis of hydrogen peroxide was awarded to Henkel and Weber<sup>24</sup> who demonstrated its direct synthesis using a palladium based catalyst. This direct synthetic route was not widely used due to the difficulty translating this method to an industrial scale. This difficulty arose from two factors that affected the discovery, one being that  $\text{H}_2/\text{O}_2$  gas mixtures are explosive over a wide range of concentrations and the second

being catalysts effective for the synthesis of hydrogen peroxide are also effective combustion and hydrogenation catalysts. The first issue can be overcome by diluting the hydrogen or oxygen gases with an inert gas such as CO<sub>2</sub> or N<sub>2</sub> in order to operate at a concentration which is not within the explosive region of the two gases<sup>25, 26</sup>. To overcome the second issue, researchers would need to improve H<sub>2</sub> utilisation towards the H<sub>2</sub>O<sub>2</sub> synthetic route as opposed to the hydrogenation and combustion routes which would produce unwanted side reaction products such as water. Previous research has suggested H<sub>2</sub> utilisation can be improved via kinetic control of the reaction<sup>27</sup>.

Within a heterogeneous catalytic system, due to having more than one phase present in the system, active sites on the catalyst can influence differing reaction pathways to a varying degree which introduces some flexibility into the system<sup>28, 29</sup>. Pospelove *et al.*<sup>30</sup> demonstrated that addition of an acid such as HCl to supported Pd catalysts can improve H<sub>2</sub>O<sub>2</sub> yield due to its inhibition of the base-catalysed decomposition of hydrogen peroxide. Later, Choudhary *et al.*<sup>31</sup> compared the effectiveness of a series of acids on the inhibition of H<sub>2</sub>O<sub>2</sub> decomposition using a 5 wt% Pd/C catalyst in an aqueous reaction medium. This study led to a distinction within the types of acid used in H<sub>2</sub>O<sub>2</sub> synthesis, oxyacids such as acetic acid and halide acids such as HCl. It was found that halide acids produced a strong suppression effect on H<sub>2</sub>O<sub>2</sub> decomposition.

Halide salts were investigated to understand which halide had the greatest positive impact on the selectivity towards the desired H<sub>2</sub>O<sub>2</sub> product. It was found F<sup>-</sup> generated the greatest influence on H<sub>2</sub> conversion, followed by no halide, Cl<sup>-</sup>, and Br<sup>-</sup>. I<sup>-</sup> was found to be extremely detrimental to the catalyst and resulted in extensive surface poisoning<sup>32, 33, 34</sup>. Consequently, it can be said that Br<sup>-</sup> is the greatest promoter of H<sub>2</sub>O<sub>2</sub> selectivity due to its minimal influence on H<sub>2</sub> conversion since F<sup>-</sup> promoted side and consecutive reaction pathways within the catalytic system. Burch *et al.*<sup>35</sup> suggested the promotion effects of halide ions were not related to their electronegativity but due to their *sigma*- and *pi*- donation effects with overall coordination ability decreasing down the halogen series.

The first group to demonstrate the potential of H<sub>2</sub>O<sub>2</sub> production directly from oxygen and hydrogen was Hutchings *et al.*<sup>36</sup> who demonstrated the ability to directly synthesise H<sub>2</sub>O<sub>2</sub> from hydrogen and oxygen using Au supported on Al<sub>2</sub>O<sub>3</sub>. The rate of reaction over this catalyst was found to be more than 4 times the rate of a palladium catalyst. Discovered at the same time

was a synergistic effect which occurred upon alloying Au and Pd together. The bimetallic AuPd/Al<sub>2</sub>O<sub>3</sub> catalyst activity was almost three times the activity of the corresponding Au only catalyst (Table 1-1)

**Table 1-1 Formation of H<sub>2</sub>O<sub>2</sub> from the reaction H<sub>2</sub>/O<sub>2</sub> over Au, Pd and AuPd catalysts**

Catalyst	Solvent	Temperature (°C)	Pressure (Mpa)	O <sub>2</sub> /H <sub>2</sub> mol ratio	H <sub>2</sub> O <sub>2</sub> mmol g(catalyst) <sup>-1</sup> h <sup>-1</sup>
Au/Al <sub>2</sub> O <sub>3</sub>	methanol	5	3.7	1.2	1530
Au:Pd(1:1)/Al <sub>2</sub> O <sub>3</sub>	methanol	5	3.7	1.2	4460
Pd/Al <sub>2</sub> O <sub>3</sub>	methanol	5	3.7	1.2	370

Hutchings and co-workers expanded the above study to include TiO<sub>2</sub> as a support<sup>14</sup> which was shown to be superior in activity compared to the alumina support for the synthesis of hydrogen peroxide from H<sub>2</sub> and O<sub>2</sub>. Again, the work demonstrated the bimetallic AuPd catalysts were much more active than the monometallic equivalents. The preparation technique of the catalysts was also investigated and showed that impregnation catalysts were more active than catalysts produced via DP.

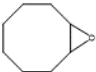
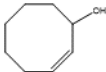
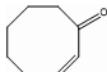
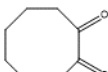
Other supports have been investigated to support AuPd catalysts such as zeolites<sup>37</sup>, carbon, and silica<sup>38</sup>. On the carbon support, it was found the AuPd nanoparticles had a different structure to the other supports. AuPd nanoparticles on carbon possessed random homogeneous alloys whereas the TiO<sub>2</sub> support produced core shell AuPd nanoparticles with a Pd rich shell and an Au rich core.

## 1.4. Alkene epoxidation

Supported gold catalysts have been demonstrated to be effective catalysts for the epoxidation of alkenes if a sacrificial reductant is present which will aid the activation of molecular oxygen. Haruta and co-workers<sup>39, 40</sup> found that Au/TiO<sub>2</sub> prepared using the DP method was selective for the epoxidation of propene, however, initial selectivity was low but was further improved by changing the support from TiO<sub>2</sub> to Ti containing zeolites<sup>41</sup>. More recent studies<sup>42</sup> have

demonstrated that sacrificial hydrogen is not necessary under certain conditions and using catalytic amounts of peroxides could initiate the oxidation of alkenes with O<sub>2</sub>. Investigating the oxidation of cyclooctane with a range of Au catalysts in mild reaction conditions with a peroxide (Table 1-2), the active gold catalysts promotes the idea that the reaction can be deemed “more green” due to not using sacrificial H<sub>2</sub>. The yield obtained in these reactions was comparable to supported gold catalysts using sacrificial H<sub>2</sub><sup>43</sup>.

**Table 1-2 A range of substrates used to show the rate of epoxidation with a range of Au catalysts<sup>42</sup>**

Catalyst	TBHP	Conversion	Selectivity				
	(g)	(%)					
1%Au/Graphite	0.12	7.9	81.2	9.3	4.1	0.5	95.1
1%Au/Graphite	0.02	7.1	79.2	6.8	3.0	0.5	89.5
1%Au/Graphite	0.002	1.3	82.6	7.4	2.1	0.6	92.7
no catalyst	0.008	2.0	trace	0.0	0.0	0.0	-
graphite	0.008	2.3	trace	0.0	0.0	0.0	-

**Reaction conditions: 0.12 g catalyst, *cis*-cyclooctane (10 ml, 0.066 mol), 80 °C, 24 h, in a stirred autoclave with 3 bar O<sub>2</sub>. TBHP = *tert*-butylhydroperoxide.**

## 1.5. C-H bond activation

The activation of the C-H bond in alkanes is of significant commercial interest as it would impart industry with the capability to produce many beneficial molecules from alkanes at a much more economical rate than what is currently possible. Current attention has been directed on the activation of cyclohexane to form cyclohexanol and cyclohexanone which has been a significant challenge<sup>44</sup>. The aerobic oxidation of cyclohexane is of importance due to its use in the production of nylon-6 and nylon-6-6 of which worldwide production exceeds 10<sup>6</sup> tonnes per annum<sup>45</sup>.

Commercially, these two nylon compounds are produced at 150 – 160 °C with cobalt naphthenate as an initiator for radical oxidation, leading to selectivity of around 70 – 85% at around 4% conversion. Operating at high conversion leads to total oxidation and consequently, commercial nylon production is designed to operate at low conversion. By



designing a catalyst that can operate at higher conversion rates would lead to an economically advantageous impact. Previous work<sup>46, 47</sup> has demonstrated  $\mu_3$ -oxo-bridged Co/Mn cluster complexes are very selective as homogeneous catalysts for alkane activation as well as aluminophosphates substituted with  $\text{Mn}^{\text{II}}$ ,  $\text{Co}^{\text{III}}$  and  $\text{Fe}^{\text{III}}$  ions giving high selectivity when operated at 130 °C. These reactions have been used as the benchmark with which to compare the activity of gold catalysts and their ability to activate alkanes.

Work by Zhao *et al.*<sup>48, 49</sup> has shown that gold can activate cyclohexane at 150 °C with selectivity around 90% being achieved with Au/ZSM-5. An initial induction period was observed with this catalyst but catalyst reusability was demonstrated showing how robust gold catalysts can be.

Xu *et al.*<sup>50</sup> demonstrated cyclohexane activation at lower temperatures than previously encountered. At temperatures below 100 °C and using molecular oxygen as an oxidant in a gold catalyst system, Au/C catalysts were compared with supported Pt and Pd catalysts. The Au/C catalysts were comparable in activity to previous catalysts found to be highly effective for epoxidation of alkanes<sup>51</sup>. Selectivity for cyclohexanone and cyclohexanol was very high at low conversion but this declined rapidly at higher conversion values and longer reaction times.

## 1.6. Alcohol Oxidation

The oxidation of primary alcohols to aldehydes is an important laboratory procedure<sup>52</sup>. Aldehydes are valuable as both an intermediate allowing industry to convert them to more useful chemicals, and are important within the perfumery industry. Often, primary alcohol oxidations are carried out with stoichiometric oxygen donors such as chromate or permanganate however, these reagents are expensive and have a negative environmental impact. Given this limitation, there is intense research into alternative systems which can utilise molecular oxygen directly. Au nanocrystals have been shown to be highly effective for the oxidation of alcohols with  $\text{O}_2$  in aqueous base however, it has been shown that gold without the presence of base can be highly effective for the oxidation of alcohols<sup>45</sup>. Seminal work in the area of alcohol oxidation was conducted by Rossi, Prati and co-workers<sup>53</sup> who have demonstrated gold nanoparticles as being highly effective for alcohol oxidation. Within these systems, base was necessary for catalyst activity as it is surmised that it is important for the

first hydrogen abstraction step in the catalytic mechanism which is a departure from Pd and Pt catalysts which do not need basic conditions to operate.

Corma *et al.*<sup>54, 55</sup> showed that Au/CeO<sub>2</sub> catalysts are active for the selective oxidation of alcohols to aldehydes and ketones as well as the oxidation of aldehydes to acids under relatively mild conditions, without solvent, using molecular O<sub>2</sub> as the oxidant and without the requirement of the addition of base. The results from these studies were shown to be comparable to or to exceed the activity of previously reported Pd catalysts<sup>56</sup>. The activity of these catalysts was assigned to the Au/CeO<sub>2</sub> catalyst stabilising a reactive peroxy intermediate from O<sub>2</sub>. Subsequent research by Enache *et al.*<sup>57</sup> has demonstrated that alloying Pd with Au in supported Au/TiO<sub>2</sub> catalysts enhances the activity of alcohol oxidation in solvent free conditions.

### 1.6.1. Benzyl Alcohol Oxidation

Benzyl alcohol is used as a model reaction for the oxidation of aromatic alcohols<sup>58</sup>. Jana *et al.*<sup>59</sup> and Choudhary *et al.*<sup>60</sup> demonstrated Au/U<sub>3</sub>O<sub>8</sub> as a highly promising catalyst for solvent-free selective oxidation of benzyl alcohol with high selectivity to benzaldehyde. In Choudhary *et al.*'s study, the Au/U<sub>3</sub>O<sub>8</sub> catalyst was synthesised via impregnation which resulted in large Au particle sizes whereas homogeneous deposition-precipitation synthesised catalysts with small gold nanoparticles. Choudhary *et al.* demonstrated that U<sub>2</sub>O<sub>3</sub> catalyst achieved better process performance when it contained higher Au loading and smaller Au nanocrystals<sup>60</sup>. With an increasing reaction period or temperature, benzyl alcohol oxidation was increased but selectivity slightly decreased with the formation of benzyl benzoate beginning in the system. When solvent was used, such as toluene or *p*-xylene, activity of the catalyst was decreased and so the solvent-free condition was preferred when using this catalyst.

Hutchings *et al.*<sup>61</sup> further demonstrated supported gold catalysts could be used for benzyl alcohol oxidation and used a wide range of supports and different preparation methods for the synthesis of the catalysts. The catalyst with the highest conversion was found to be gold catalysts prepared via co-precipitation and supported on iron oxide. Highest selectivity to benzaldehyde was achieved on TiO<sub>2</sub> supported gold catalysts prepared via the impregnation method.

Choudhary *et al.*<sup>62</sup> prepared a wide range of gold catalysts and tested them for benzyl alcohol oxidation (Table 1-3) and found the most effective supports for gold catalysts to be ZrO<sub>2</sub>, MnO<sub>2</sub>, Sm<sub>2</sub>O<sub>3</sub> and Al<sub>2</sub>O<sub>3</sub> when comparing the supports in terms of turn over frequency (TOF (h<sup>-1</sup>)).

**Table 1-3 A range of supports used to study the oxidation of benzyl alcohol to benzaldehyde as reported by Choudhary *et al.*<sup>621</sup>**

Nano-gold Catalyst	Conc. Of gold (wt%)	Gold Particle Size/nm	Conversion of benzyl alcohol	Selectivity (%)		Benzaldehyde yield (%)	TOF/mol g(Au) <sup>-1</sup> h <sup>-1</sup>
				Benzaldehyde	Benzylbenzoate		
Au/MgO	7.50	8.9 ± 0.7	51.00	86.00	14.00	43.90	0.34
Au/CaO	4.70	9.6 ± 1.2	33.30	91.30	8.60	30.40	0.38
Au/BaO	5.30	7.10	43.50	81.50	18.50	35.50	0.39
Au/Al <sub>2</sub> O <sub>3</sub>	6.40	3.6 ± 1.1	68.90	65.00	35.00	44.80	0.41
Au/ZrO <sub>3</sub>	3.00	4.5 ± 1.2	50.70	87.00	13.00	44.10	0.85
Au/La <sub>2</sub> O <sub>3</sub>	6.50	n.d.	51.60	68.80	31.30	35.50	0.32
Au/Sm <sub>2</sub> O <sub>3</sub>	4.20	7.9 ± 0.5	44.40	75.00	25.00	33.30	0.46
Au/Eu <sub>2</sub> O <sub>3</sub>	6.60	n.d.	37.50	87.50	12.50	32.40	0.29
Au/U <sub>3</sub> O <sub>8</sub>	8.00	9.4 ± 3.2	53.00	95.00	5.00	50.40	0.37
Au/MnO <sub>2</sub>	4.10	6.1 ± 1.7	39.70	88.80	11.10	34.50	0.49
Au/Fe <sub>2</sub> O <sub>3</sub>	6.10	5.8 ± 0.3	16.20	100.00	-	16.20	0.15
Au/CoO	7.10	5.7 ± 1.3	28.30	95.20	4.80	26.70	0.22
Au/NiO	6.20	23.1 ± 3.7	32.00	78.00	22.00	25.00	0.23
Au/CuO	6.80	11.7 ± 2.6	27.00	69.00	31.00	18.00	0.16
Au/ZnO	6.60	5.90 <sup>a</sup>	40.50	92.80	7.20	37.60	0.33

<sup>a</sup>Rate of the formation of benzaldehyde per unit mass of the deposited gold per unit time

Enache *et al.*<sup>63</sup> investigated the synergy that exists when Au is added to Pd resulting in either an alloy or core shell nanoparticle. For titania based AuPd catalysts prepared via impregnation, the initial activity of the bimetallic catalysts was higher than that for the corresponding Au/TiO<sub>2</sub> catalyst but lower than the corresponding Pd/TiO<sub>2</sub> catalyst. At extended reaction times the bimetallic catalyst exceeded the conversion obtained for Pd/TiO<sub>2</sub> catalyst and achieved a significantly higher selectivity towards the desired benzaldehyde product.

The Au:Pd ratio was also investigated by Enache *et al.*<sup>64</sup> (Table 1-4) using TiO<sub>2</sub> as a support. The highest activity was achieved with a bimetallic AuPd ratio of 1:1 wt. ratio of Au:Pd. Again,

<sup>1</sup> Reprinted from Catalysis Today, 122 3-4, Hutchings et al., Copyright 2007, with permission from Elsevier

the Pd/TiO<sub>2</sub> catalyst has the highest initial rate of reaction but demonstrated deactivation at extended reaction times and was the least selective to the desired benzaldehyde product. The monometallic Au/TiO<sub>2</sub> catalyst was the most selective but was also the least active for the oxidation reaction. It was noted that the more gold rich the AuPd/TiO<sub>2</sub> catalysts became, the higher their selectivity towards benzaldehyde.

**Table 1-4<sup>2</sup> The effect of AuPd ratio on the rate of benzyl alcohol oxidation<sup>64</sup>**

Catalyst	TOF (h <sup>-1</sup> )	
	Au-Pd catalysts	Au-Pd physical mixtures
5%Au/TiO <sub>2</sub>	33700	33700
4%Au-1%Pd/TiO <sub>2</sub>	47600	42300
3%Au-2%Pd/TiO <sub>2</sub>	48700	50800
2.5Au-2.5%Pd/TiO <sub>2</sub>	65400	55100
2%Au-3%Pd/TiO <sub>2</sub>	65100	59400
1%Au-4%Pd/TiO <sub>2</sub>	64000	67900
5%Pd/TiO <sub>2</sub>	76500	76500

Determined after 30 minutes of reaction

Dimitratos *et al.*<sup>65</sup> demonstrated sol immobilisation catalysts were effective alcohol oxidation catalysts, investigating the effect of metal order in generating the sol. The effects of seeding were investigated within an AuPd/TiO<sub>2</sub> catalytic system. The following effects were investigated:

- Simultaneous formation of the metal sols for both metals
- Generation of a Pd seed sol, reduction of a sol, addition of Au sol and a further reduction of the sols
- Generation of Au sol, reduction of sol, addition of Pd sol and a further reduction of the sols

Dimitratos *et al.* demonstrated that within this system, the order of metal addition within the catalyst preparation was not a significant contributor to catalyst activity or selectivity.

Li *et al.*<sup>61</sup> demonstrated that multiple products can be produced from benzyl alcohol oxidation due to many mechanisms being in operation within the system. The main product from benzyl alcohol oxidation is benzaldehyde. Another possible product arises from the possibility of

<sup>2</sup> Reprinted from Catalysis Today, 122 3-4, Hutchings et al., Copyright 2007, with permission from Elsevier

decarbonylation to form benzene<sup>66</sup>, with another possible product being benzyl benzoate. Benzyl benzoate is produced from a condensation reaction between benzaldehyde and benzyl alcohol, generating a hemiacetal which is unstable and further oxidises to an ester<sup>61</sup>. Dibenzyl ether is an additional side product the formation of which is promoted via acid-base sites on catalyst surfaces. Lastly, benzyl alcohol can also undergo disproportionation to form benzaldehyde and toluene in equal measures.

### 1.6.2. Cinnamyl Alcohol oxidation

Cinnamyl alcohol is a white, crystalline solid aromatic alcohol at room temperature and is used in the perfume industry as a deodorant. It can be oxidised to several oxidation products such as cinnamaldehyde which has a pleasant odour. Sheldon *et al.*<sup>67</sup> demonstrated cinnamyl alcohol oxidation using a Pd(II) bathophenanthroline complex with sodium acetate in water at 30 bar air. At 80 °C, Sheldon and co-workers achieved total conversion of cinnamyl alcohol with 80% selectivity to cinnamaldehyde. For gold based catalysts, it was Corma *et al.*<sup>54</sup> who demonstrated cinnamyl alcohol oxidation was possible by using Au/CeO<sub>2</sub> in 1 bar O<sub>2</sub>. After 7 hours, conversion of 66% was achieved with selectivity to the desired cinnamaldehyde at 73%. With cinnamyl alcohol shown to be oxidised using monometallic Au and Pd catalysts, Hutchings *et al.*<sup>68</sup> oxidised cinnamyl alcohol using toluene as a solvent with 2.5%Au+2.5Pd/TiO<sub>2</sub> at 190 °C and observed a TOF (h<sup>-1</sup>) of 97 mol kg<sup>-1</sup> h<sup>-1</sup> with 1 atm O<sub>2</sub> showing cinnamyl alcohol could be oxidised using AuPd bimetallic catalysts.

## 1.7. CO Oxidation

The oxidation of CO at ambient temperatures using supported Au catalysts was of key importance and as previously mentioned, was investigated by Haruta<sup>7</sup> and co-workers who demonstrated this reaction could occur at low temperatures, such as 203 K. Even though this discovery was made over 20 years ago, there is still ongoing debate as to how gold is catalysing this reaction and active research continues to identify the active site for the catalyst, the role the support plays in CO oxidation and if the presence of moisture in the reaction affects CO oxidation<sup>69, 70</sup>. Several reaction mechanisms have been proposed for this reaction, such as the one by Bond-Thomson<sup>71</sup> who proposed Au atoms at the metal-support interface represents the active site for CO oxidation.

Hutchings and co-workers<sup>72</sup> applied advanced electron microscopy techniques to Au/FeO<sub>x</sub> catalysts and identified clusters of Au particles of roughly 0.5 nm in diameter as being responsible for CO oxidation activity. Theoretical study has also indicated via DFT calculations that Au clusters are responsible for catalytic activity<sup>73</sup>. These publications indicate that Au clusters containing 10 atoms are the key to activity.

Further work by Goodman *et al.*<sup>74</sup> compared the activity of model Au/TiO<sub>2</sub> catalysts and showed they had a TOF (h<sup>-1</sup>) maxima for CO oxidation when Au clusters of 3.5 nm in diameter and 3 atoms thick were present. This represented the Au clusters as partially losing their metallic character and forming discrete energy band-gaps, something the authors related to the catalyst's activity. This work was based on model Au model catalysts and Haruta *et al.*<sup>40</sup> stated that the ratio of metallic Au atoms on the surface relative to the number of Au atoms at the metal support interface is a more reasonable interpretation, of which an optimum value is obtained at 3.5 nm average cluster diameter.

## 1.8. Acetylene Hydrochlorination

Acetylene hydrochlorination is traditionally achieved using a mercury chloride catalyst supported on activated carbon. This catalyst readily undergoes deactivation<sup>75, 76</sup> which results in decreased activity and the leaching of toxic mercury from the catalyst. Due to these significant environmental concerns, a new green catalyst is desired to lessen the impact acetylene hydrochlorination has on the environment.

Shinoda *et al.*<sup>77</sup> investigated the activity of a wide range of carbon supported metal chloride catalysts for acetylene hydrochlorination and were able to correlate the activity of the catalysts with the electron affinity of the metal cation over the metal valence. Subsequently, Hutchings<sup>8</sup> correlated the activity of supported metal chloride catalysts with their standard electrode potential due to the assumption the reaction is proceeding via a two electron process. The resultant data from this investigation suggested gold should be the most active metal for this reaction, an assumption that was later confirmed<sup>78</sup> (Figure 1-2).

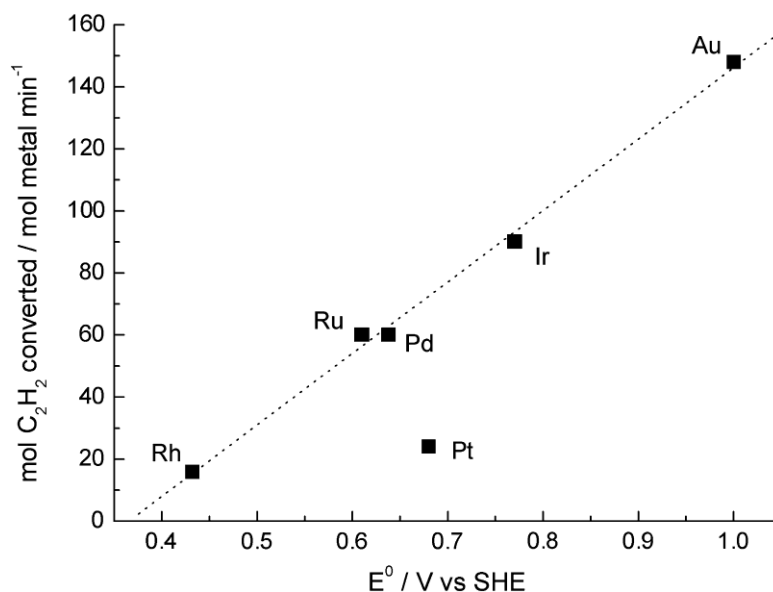


**Figure 1-2<sup>3</sup> Correlation of initial acetylene hydrochlorination activity with standard electrode potential for supported metal chlorides**

It was also reported that not only do Au catalysts have the highest activity for this reaction, their selectivity towards the desired vinyl chloride monomer (VCM) compound is greater than 99.5%, higher than other catalysts which usually demonstrate a secondary hydrochlorination reaction whereby dichloromethane is produced. Au catalysts still suffer from the deactivation issues that mercury catalysts possess. Nkosi *et al.*<sup>79</sup> determined that although metal leaching from the catalyst was the main deactivation for hydrochlorination catalysts, this was not the case for Au based catalysts.

Nkosi *et al.* also investigated how temperature effected acetylene hydrochlorination and found that at 100 °C, deactivation was minimised, and deactivation was observed as mainly a result of deposition of carbonaceous residue on the catalyst surface. At higher temperatures, deactivation was ascribed to the reduction of cationic  $Au^{n+}$  to  $Au^0$ . Whilst deactivation was minimised at 100 °C, the activity of the catalyst is too low to be considered useful and so temperatures of around 180 °C continue to be used.

<sup>3</sup> Reprinted from Journal of Catalysis, 257 1, Hutchings et al., Copyright 2008, with permission from Elsevier

### 1.8.1. Mechanism of acetylene hydrochlorination

Kinetic studies into acetylene hydrochlorination have indicated the reaction is first order with respect to acetylene and HCl<sup>79</sup> with formation of a  $C_2H_2/Au/HCl$  complex being suggested. Conte *et al.*<sup>80</sup> conducted a range of experiments in order to further explore the mechanism of acetylene hydrochlorination and catalyst deactivation. Sequential exposure of catalyst to the individual reactants prior and during reaction discovered that exposure to HCl enhanced activity whereas acetylene lead to catalyst deactivation. It was also discovered increasing the HCl: $C_2H_2$  ratio in the reactant gas feed increased catalytic activity.

Due to acetylene's symmetrical nature, it is difficult to obtain mechanistic data directly and so substituted alkynes are used instead to allow product differentiation. It was found that activity was affected by steric hindrance of the substrates. Deuterated studies led to the conclusion acetylene hydrochlorination proceeds via anti-addition of HCl across the carbon-carbon triple bond.

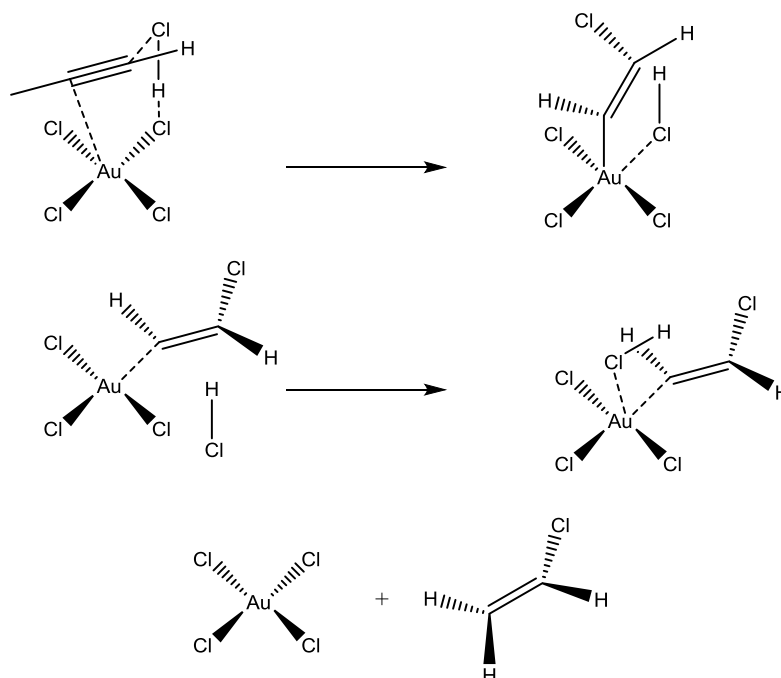


**Figure 1-3 Mechanism for the hydrochlorination of acetylene using an Au/C catalyst<sup>81</sup>**



## 1.9. Biodiesel Production

Throughout the work on Au catalysts, the aim has been to produce a green catalyst that is less environmentally impactful. From the very beginning of Industry, energy has been a vital necessity to produce economic output for the benefit of society. In the beginning, coal was the major source of energy with petroleum overtaking in popularity towards the end of the twentieth century.

The depletion of fossil fuels presents a massive challenge for future generations due to our current reliance on its derivatives and having no resilience in place to offset dwindling supplies. One aspect of petroleum substitution that is receiving attention is that of biofuels, which are fuels created from bio-renewable sources such as corn or sugarcane. Biofuels aim to be carbon neutral, by absorbing an amount of carbon from the atmosphere that is equal to the amount of carbon produced from biofuel combustion. Biofuels are also cleaner than traditional fuels, often containing lower levels of sulphur, soot and aromatics<sup>82</sup>.

Biodiesel can be produced from the trans-esterification of triglycerides, which are found in organic matter such as plants as well as some animal fats. Biodiesel has become the most commonplace biofuel within the European Union and is key to the EU's emissions targets. Biodiesel's properties are similar to traditional diesel, potentially helping to avoid large infrastructure changes to the current fuel distribution systems in place. When biodiesel is combusted in car engines, it results in far less engine wear. This is in addition to other advantages such as cost, availability and improved lubrication<sup>83</sup>.

Emissions of biodiesel display a 99% reduction in SO emission as well as a 20% reduction in CO, 32% reduction in hydrocarbon and 50% reduction in soot emission. Particulates are also reduced by up to 39%. Biodiesel is also biodegradable, something which traditional fuel is not. Following a biodiesel fuel spillage, after 3 weeks, 90% of the spilled biodiesel will have degraded, greatly reducing any long term impact the spill may have had on the environment<sup>84</sup>.

Due to these advantages, the worldwide production of biofuel has increased from 11.4 million litres in 1991 to 3.9 billion litres in 2005<sup>85</sup> with indication that there has been a net reduction of

greenhouse gas emission for biodiesel, which also includes the generation of greenhouse gases from the production of biodiesel from agriculture, bio-refining and consumption<sup>86</sup>.

Biofuels are not without controversy, whilst they offer a green alternative to traditional fuel sources, they also have a significant impact of their own. As biodiesel is produced from crop normally used for food production, increasing demand for biofuel is encouraging farmers to convert their food crops to biodiesel crops, reducing the amount of available food. Consequently, as food production is reduced, this leads to food unavailability which will have the effect of increasing food prices in areas of poverty. Biodiesel crops are in direct competition with food farmers who rely on agriculture for a steady income. Additionally, conversion of non-agricultural land and forestry to biodiesel farming land is a contributing factor in ongoing deforestation around the globe. In Malaysia, rain forest and peat lands are being displaced and the Amazon is being deforested for soybean production. This leads to a significant impact on the local wildlife and continues the ongoing threat to certain species of animal. The clearing of these areas is also a source of significant greenhouse gas emission<sup>87</sup>.

From one molecule of triglyceride, three molecules of ester are produced<sup>88</sup> (Figure 1-4). Yield is typically 10% by weight of glycerol. Due to an EU directive, it is mandated that 5.75% of travel fuels must be bio-derived which has had the effect of increasing production and subsequent price reduction in biofuels. As biofuel is now relatively cheap, focus is being directed at whether glycerol can be used as a source of value adding chemicals due to it being a by-product of biofuel production.

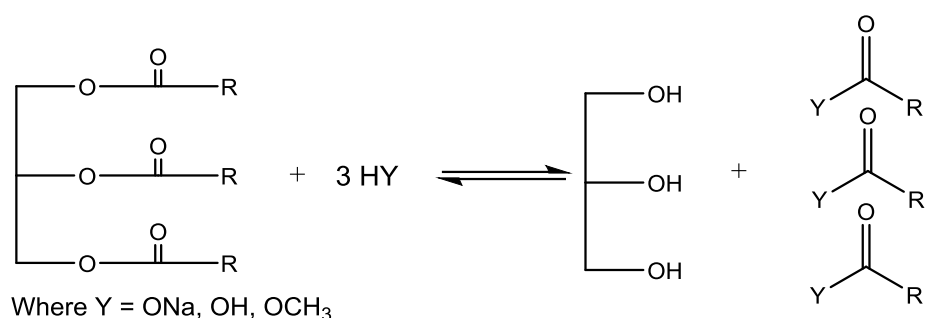


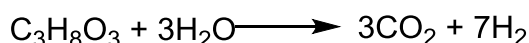
**Figure 1-4 Production of biodiesel<sup>76</sup>**

Glycerol has a number of uses in its original form, such as cosmetics, pharmaceuticals and food<sup>89</sup>. In these uses, glycerol needs to be of high purity due to human use but the glycerol produced during biofuel production is not of a high enough grade to be used directly, often

containing water, methanol, fatty acids and unrelated triglyceride compounds. Due to methanol being present, crude glycerol from biofuel production is considered a hazardous waste product which imposes certain limits on its disposal. Purification of crude glycerol usually involves neutralisation with phosphoric acid followed by separation of the components in a vacuum to remove the methanol content. After this process, glycerol is approximately 80 – 90% pure and is sold to glycerol purification plants for further treatment to get the purity up to about 99.5 – 99.7%. This is an expensive process with current projections indicating worldwide demand for glycerol will not exceed the production volume of the chemical. To avoid any reduction in glycerol purification, and to increase demand for glycerol, the need for an alternative glycerol process to utilise the functional molecule is currently being researched.

### 1.9.1. Glycerol Transformation

The possibility of producing fuel from glycerol has attracted significant interest leading to the investigation of whether glycerol can be used as an alternative to syngas, especially as a source of hydrogen. Hydrogen gas has a number of industrial uses such as use in fuel cells and the Haber process<sup>90</sup>. The global demand for hydrogen is expected to increase in the immediate future and so a bio-renewable source would be very a very welcome addition. Glycerol can be converted to hydrogen and carbon monoxide in aqueous phase reforming<sup>91</sup>. This reforming process is achieved at relatively low temperatures of around 225 – 300 °C by using a Pt-Re catalyst in a one pot synthesis, as shown in Equation 1-1.



**Equation 1-1 Formation of Hydrogen and Carbon Dioxide from Glycerol**

Syngas can be used for a variety of reactions such as methanol synthesis or the Fischer-Tropsch process and if it can be replaced with glycerol, these two processes will be able to have some environmentally green aspect to them. The formation of syngas from glycerol can be directly used in the Fischer-Tropsch reaction if a single two bed reactor is used<sup>92</sup> and can be conducted at temperatures as low as 225 °C.

## 1.9.2. Glycerol Oxidation

Glycerol can be oxidised by several heterogeneous catalysts to produce a variety of compounds that have applications in polymers, cosmetics, food additives and organic synthesis. It was Rossi and Prati<sup>93</sup> who first demonstrated the ability of Au catalysts to oxidise glycerol in the presence of base to glyceric acid as the primary product. These C3 oxidation products are highly desirable but undergo C – C bond cleavage during reaction to compounds such as tartronic acid and glycolic acid (Figure 1-5).

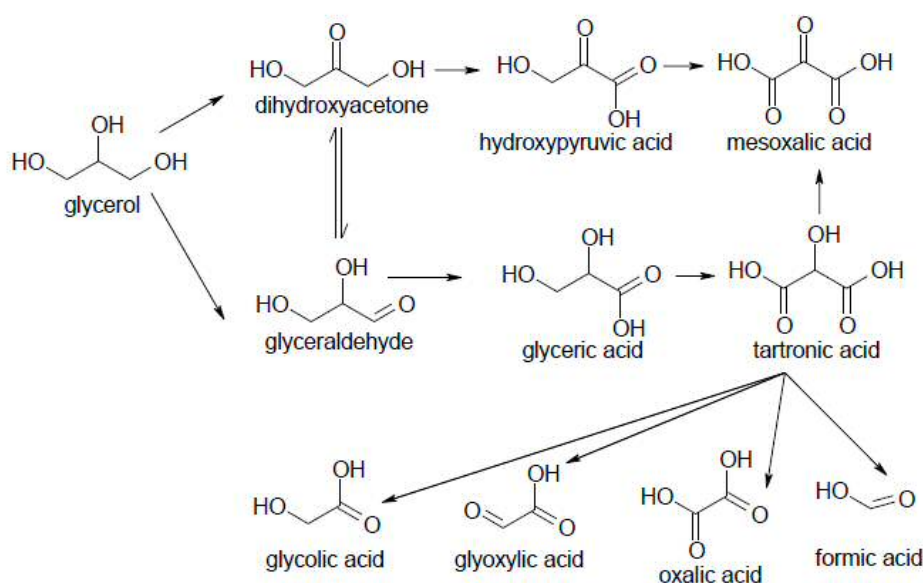


**Figure 1-5 Reaction pathway of Glycerol**

Another route to the C2 compound glycolic acid is via fragmentation of glyceric acid, which can further fragment into the C1 compound formic acid. Carrettin *et al.*<sup>94</sup> demonstrated Au/graphite catalysts can oxidise glycerol to glycerate with 100% selectivity by using O<sub>2</sub> as the oxidant under mild conditions with yields approaching 60%. Selectivity was found to be dependent on the glycerol/NaOH ratio used in the reaction with high selectivity to glyceric acid observed with high concentrations of NaOH. Decreasing the glycerol concentration and increasing the mass of the catalyst along with the concentration of O<sub>2</sub> led to the formation of tartronic acid via consecutive oxidation of glyceric acid, which is stable under the reaction conditions reported.

Under comparable conditions to the Au/graphite catalysts in Carrettin's work, catalysts based on Pd/C and Pt/C always produce other C3 and C2 products in addition to the glyceric acid. The role of base was investigated in-depth by Carrettin *et al.*<sup>95</sup> and its effect on Au, Pd and Pt catalysts for the oxidation of glycerol. Although glycerol oxidation proceeded without the need for a base, the rate was highly improved when one was used. Bases tested include NaOH, NaNO<sub>3</sub>, KOH and LiOH. The selectivity was improved when NaNO<sub>3</sub>, KOH and LiOH were used while NaOH also improved the yield of glyceric acid obtained. The addition of NaNO<sub>3</sub> resulted in no significant effect on glycerol conversion compared to the reaction without base however, selectivity to oxalic acid was 85% whereas the reaction with no base had a selectivity to oxalic acid of 57.4%. Oxalic acid was not detected when using other bases previously mentioned. Carrettin *et al.* concluded that the addition of OH<sup>-</sup> was important for glycerol activation as the absence of base in Au/C systems prevents glycerol from undergoing H-abstraction, a necessary first step for the conversion of glycerol, or slows down glycerol conversion within Pd/C and Pt/C systems.

Prati *et al.*<sup>19</sup> synthesised bimetallic AuPd and AuPt catalysts supported on carbon which showed a marked increase in catalyst activity when compared to either of the monometallic Au and Pd catalysts supported on carbon for the oxidation of glycerol. It was suggested the increase in activity was due to the alloying of the nanoparticles, which was further demonstrated by using bimetallic catalysts that did not contain alloyed metals as their activity was noticeably lower. Selectivity to glyceric acid increased when bimetallic AuPd catalysts were used. The trend in selectivity for the AuPd/C catalysts was similar to the Au/C catalyst whereby the second highest selectivity was towards the C3 product tartronic acid. This trend was also observed when graphite was used as a catalyst support<sup>96</sup>.

Later research focused on the size of the bimetallic AuPd nanoparticles and how it affected the oxidation of glycerol<sup>18</sup>. These particles were synthesised using the sol immobilisation technique and supported on carbon. Small nanoparticles were again shown to be highly active as when the nanoparticle sizes increased, catalyst activity decreased.

## 1.10. Crotyl Alcohol Oxidation

Crotyl alcohol is an allylic alcohol and under oxidation produces crotonaldehyde which has industrial relevance. Kawanami *et al.*<sup>97</sup> demonstrated Au/TiO<sub>2</sub> can oxidise crotyl alcohol to crotonaldehyde with a conversion of 57% and selectivity of 94% using molecular oxygen and supercritical CO<sub>2</sub> as a solvent. Kawanami and co-workers suggested the reaction could stabilise the aldehyde compound being generated. Hutchings *et al.*<sup>57</sup> demonstrated that bimetallic AuPd catalysts gave high TOF (h<sup>-1</sup>) values of 12600 h<sup>-1</sup> using AuPd/TiO<sub>2</sub> which again demonstrates the improvement in activity when bimetallic catalysts are used.

Hou *et al.*<sup>98</sup> used PVP-stabilised 1:3 AuPd nanoparticles which were more active for crotyl alcohol oxidation and selectivity. Balcha *et al.*<sup>99</sup> further studied the synthesis of PVP bimetallic AuPd nanoparticles using co-reduction and sequential reduction routes for aerobic oxidation of crotyl alcohol to the corresponding aldehyde at room temperature. Balcha's study suggested that sequentially reduced particles have significantly Pd rich surfaces and an Au core. AuPd core shell nanoparticles of ratio 1:3 Au:Pd were shown to be the most effective at promoting crotyl alcohol oxidation and achieved this with a high selectivity.

Hutchings *et al.*<sup>100</sup> reported the solvent free oxidation of crotyl alcohol using AuPd in differing ratios supported on graphite. When the catalysts were gold rich, the oxidation of crotyl alcohol to crotonaldehyde was preferred. When the catalysts were Pd rich, crotyl alcohol underwent isomerisation. A mechanism for crotyl alcohol oxidation was proposed and is shown in Figure 1-6.

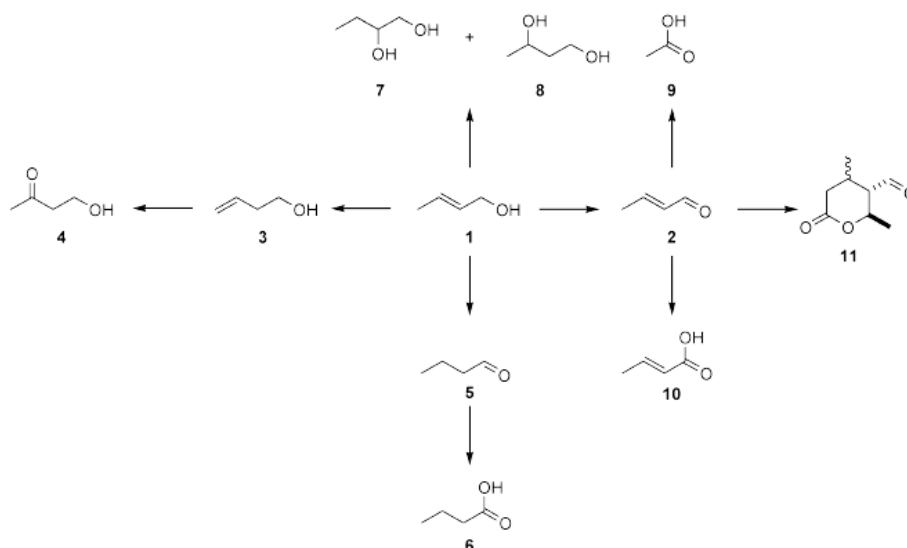


**Figure 1-6 Proposed catalytic cycle for crotyl alcohol oxidation. Crotyl Alcohol (1), 2-butenal (2), 3-butenol (3), 4-hydroxybutan-2-one (4), butanal (5), butanoic acid (6), butane-1,3-diol (7), butane-1,2-diol (8), acetic acid (9), 2-butenic acid (10) and lactone (11)<sup>100</sup>.**

## 1.11. Aims of the study

As described above, the effect of bimetallic AuPd and support is an important consideration for many organic oxidation reactions. Catalyst preparation methods are important but are not the subject of investigation for the purposes of this study, catalyst preparation is exclusively via sol immobilisation. The two alcohols that will be investigated will be benzyl alcohol and cinnamyl alcohol, with benzyl alcohol extended to include several substituted benzyl alcohol derivatives. In summary, the study's aims are:

1. Assess effect of metal loading on benzyl alcohol oxidation
2. Assess impact of substituents on the aromatic ring of benzyl alcohol
3. Assess impact catalyst parameters have on cinnamyl alcohol oxidation

## Chapter 1 References

1. Berzelius M. On a new force acting in the formation of organic compounds. *Journal of the Franklin Institute* 1836, **22**(5): 331-334.
2. Bowker M. *The basis and applications of heterogeneous catalysis*. New York : Oxford University Press, 1998.
3. Patil BS, Wang Q, Hessel V, Lang J. Plasma N<sub>2</sub>-fixation: 1900–2014. *Catalysis Today* 2015, **256**, **Part 1**: 49-66.
4. Sá J, Szlachetko J. Heterogeneous Catalysis Experiments at XFELs. Are we Close to Producing a Catalysis Movie? *Catalysis Letters* 2014, **144**(2): 197-203.
5. Catalysis Scheme. [cited August 2015] Available from:  
<https://upload.wikimedia.org/wikipedia/commons/1/15/CatalysisScheme.png>
6. Moreau F, Bond GC, Taylor AO. Gold on titania catalysts for the oxidation of carbon monoxide: control of pH during preparation with various gold contents. *Journal of Catalysis* 2005, **231**(1): 105-114.
7. Haruta M, Kobayashi T, Sano H, Yamada N. Novel Gold Catalysts for the Oxidation of Carbon Monoxide at a Temperature far Below 0 °C. *Chemistry Letters* 1987, **16**(2): 405-408.
8. Hutchings GJ. Vapor phase hydrochlorination of acetylene: Correlation of catalytic activity of supported metal chloride catalysts. *Journal of Catalysis* 1985, **96**(1): 292-295.
9. Tsubota S, Haruta M, Kobayashi T, Ueda A, Nakahara Y. Preparation of Highly Dispersed Gold on Titanium and Magnesium Oxide. In: G. Poncelet PAJPG, Delmon B (eds). *Studies in Surface Science and Catalysis*, vol. Volume 63. Elsevier, 1991, pp 695-704.



10. Prati L, Rossi M. Gold on Carbon as a New Catalyst for Selective Liquid Phase Oxidation of Diols. *Journal of Catalysis* 1998, **176**(2): 552-560.
11. Landon P, Collier PJ, Papworth AJ, Kiely CJ, Hutchings GJ. Direct formation of hydrogen peroxide from  $H_2/O_2$  using a gold catalyst. *Chemical Communications* 2002(18): 2058-2059.
12. Brett GL, Miedziak PJ, Knight DW, Taylor SH, Hutchings GJ. Gold-Based Nanoparticulate Catalysts for the Oxidative Esterification of 1,4-Butanediol to Dimethyl Succinate. *Topics in Catalysis* 2014, **57**(6): 723-729.
13. Enache DI, Hutchings GJ, Taylor SH, Raymahasay S, Winterbottom JM, Mantle MD, Sederman AJ, Gladden LF, Chatwin C, Symonds KT, Stitt EH. Multiphase hydrogenation of resorcinol in structured and heat exchange reactor systems: Influence of the catalyst and the reactor configuration. *Catalysis Today* 2007, **128**(1–2): 26-35.
14. Edwards JK, Solsona BE, Landon P, Carley AF, Herzing A, Kiely CJ, Hutchings GJ. Direct synthesis of hydrogen peroxide from  $H_2$  and  $O_2$  using  $TiO_2$ -supported Au–Pd catalysts. *Journal of Catalysis* 2005, **236**(1): 69-79.
15. Faraday M. The Bakerian Lecture: Experimental Relations of Gold (and Other Metals) to Light. *Philosophical Transactions of the Royal Society of London* 1857, **147**(0): 145-181.
16. Wiesner J, Wokaun A. Anisometric gold colloids. Preparation, characterization, and optical properties. *Chemical Physics Letters* 1989, **157**(6): 569-575.
17. Dimitratos N, Lopez-Sanchez JA, Anthonykutti JM, Brett G, Carley AF, Tiruvalam RC, Herzing AA, Kiely CJ, Knight DW, Hutchings GJ. Oxidation of glycerol using gold-palladium alloy-supported nanocrystals. *Physical Chemistry Chemical Physics* 2009, **11**(25): 4952-4961.

18. Dimitratos N, Lopez-Sanchez J, Lennon D, Porta F, Prati L, Villa A. Effect of Particle Size on Monometallic and Bimetallic (Au,Pd)/C on the Liquid Phase Oxidation of Glycerol. *Catalysis Letters* 2006, **108**(3-4): 147-153.
19. Bianchi CL, Canton P, Dimitratos N, Porta F, Prati L. Selective oxidation of glycerol with oxygen using mono and bimetallic catalysts based on Au, Pd and Pt metals. *Catalysis Today* 2005, **102–103**: 203-212.
20. Wang J, Kondrat SA, Wang Y, Brett GL, Giles C, Bartley JK, Lu L, Liu Q, Kiely CJ, Hutchings GJ. Au–Pd Nanoparticles Dispersed on Composite Titania/Graphene Oxide-Supports as a Highly Active Oxidation Catalyst. *ACS Catalysis* 2015, **5**(6): 3575-3587.
21. Hydrogen peroxide: innovations in chemical pulp bleaching. *TAPPI Journal* 1991, **74**(1).
22. Vaino AR. Sodium Percarbonate as an Oxygen Source for MTO Catalyzed Epoxidations. *The Journal of Organic Chemistry* 2000, **65**(13): 4210-4212.
23. Crole DA, Freakley SJ, Edwards JK, Hutchings GJ. Direct synthesis of hydrogen peroxide in water at ambient temperature. *Proceedings of the Royal Society of London A: Mathematical, Physical and Engineering Sciences* 2016, **472**(2190).
24. Henkel H, Weber W, inventors; Google Patents, assignee. Manufacture of hydrogen peroxid. 1914.
25. DeClippeir GEMJ, Cahen RM, Van Thillo H, Debras GLG, inventors; Google Patents, assignee. Process for preparing crystalline silicas. 1988.
26. Edwards JK, Thomas A, Carley AF, Herzing AA, Kiely CJ, Hutchings GJ. Au-Pd supported nanocrystals as catalysts for the direct synthesis of hydrogen peroxide from H<sub>2</sub> and O<sub>2</sub>. *Green Chemistry* 2008, **10**(4): 388-394.

27. Taramasso M, Perego G, Notari B, inventors; Google Patents, assignee. Preparation of porous crystalline synthetic material comprised of silicon and titanium oxides. 1983.
28. Todorovic R, Meyer RJ. A comparative density functional theory study of the direct synthesis of  $\text{H}_2\text{O}_2$  on Pd, Pt and Au surfaces. *Catalysis Today* 2011, **160**(1): 242-248.
29. Piccinini M, Ntainjua N E, Edwards JK, Carley AF, Moulijn JA, Hutchings GJ. Effect of the reaction conditions on the performance of Au-Pd/ $\text{TiO}_2$  catalyst for the direct synthesis of hydrogen peroxide. *Physical Chemistry Chemical Physics* 2010, **12**(10): 2488-2492.
30. Pospelova TA, Kobozev NI. *Russian Journal of Physical Chemistry A* 1961, **35**.
31. Choudhary VR, Samanta C, Choudhary TV. Factors influencing decomposition of  $\text{H}_2\text{O}_2$  over supported Pd catalyst in aqueous medium. *Journal of Molecular Catalysis A: Chemical* 2006, **260**(1–2): 115-120.
32. Choudhary VR, Samanta C, Jana P. Decomposition and/or hydrogenation of hydrogen peroxide over Pd/ $\text{Al}_2\text{O}_3$  catalyst in aqueous medium: Factors affecting the rate of  $\text{H}_2\text{O}_2$  destruction in presence of hydrogen. *Applied Catalysis A: General* 2007, **332**(1): 70-78.
33. Choudhary VR, Jana P. Direct oxidation of  $\text{H}_2$  to  $\text{H}_2\text{O}_2$  over Br and F-promoted Pd/ $\text{Al}_2\text{O}_3$  in aqueous acidic medium: Influence of the concentration of Br and F and the method of incorporation of the two halogens in the catalyst on their beneficial synergetic effect on the net  $\text{H}_2\text{O}_2$  formation. *Applied Catalysis A: General* 2007, **329**: 79-85.
34. Choudhary VR, Jana P. Synergetic effect of two halogen promoters present in acidic reaction medium or catalyst on the  $\text{H}_2\text{O}_2$  formation (in  $\text{H}_2$ -to- $\text{H}_2\text{O}_2$  oxidation) and destruction over Pd/C (or  $\text{Al}_2\text{O}_3$ ) catalyst. *Journal of Catalysis* 2007, **246**(2): 434-439.

35. Burch R, Ellis PR. An investigation of alternative catalytic approaches for the direct synthesis of hydrogen peroxide from hydrogen and oxygen. *Applied Catalysis B: Environmental* 2003, **42**(2): 203-211.
36. Landon P, Collier PJ, Carley AF, Chadwick D, Papworth AJ, Burrows A, Kiely CJ, Hutchings GJ. Direct synthesis of hydrogen peroxide from H<sub>2</sub> and O<sub>2</sub> using Pd and Au catalysts. *Physical Chemistry Chemical Physics* 2003, **5**(9): 1917-1923.
37. Li G, Edwards J, Carley AF, Hutchings GJ. Direct synthesis of hydrogen peroxide from H<sub>2</sub> and O<sub>2</sub> using zeolite-supported Au catalysts. *Catalysis Today* 2006, **114**(4): 369-371.
38. Li G, Edwards J, Carley AF, Hutchings GJ. Direct synthesis of hydrogen peroxide from H<sub>2</sub> and O<sub>2</sub> using zeolite-supported Au-Pd catalysts. *Catalysis Today* 2007, **122**(3-4): 361-364.
39. Hayashi T, Tanaka K, Haruta M. Selective Vapor-Phase Epoxidation of Propylene over Au/TiO<sub>2</sub> Catalysts in the Presence of Oxygen and Hydrogen. *Journal of Catalysis* 1998, **178**(2): 566-575.
40. Haruta M, Daté M. Advances in the catalysis of Au nanoparticles. *Applied Catalysis A: General* 2001, **222**(1-2): 427-437.
41. Nijhuis TA, Huizinga BJ, Makkee M, Moulijn JA. Direct Epoxidation of Propene Using Gold Dispersed on TS-1 and Other Titanium-Containing Supports. *Industrial & Engineering Chemistry Research* 1999, **38**(3): 884-891.
42. Hughes MD, Xu Y-J, Jenkins P, McMorn P, Landon P, Enache DI, Carley AF, Attard GA, Hutchings GJ, King F, Stitt EH, Johnston P, Griffin K, Kiely CJ. Tunable gold catalysts for selective hydrocarbon oxidation under mild conditions. *Nature* 2005, **437**(7062): 1132-1135.

43. Sinha AK, Seelan S, Okumura M, Akita T, Tsubota S, Haruta M. Three-Dimensional Mesoporous Titanosilicates Prepared by Modified Sol–Gel Method: Ideal Gold Catalyst Supports for Enhanced Propene Epoxidation. *The Journal of Physical Chemistry B* 2005, **109**(9): 3956-3965.
44. Hill CL, Weinstock IA. Homogeneous catalysis: On the trail of dioxygen activation. *Nature* 1997, **388**(6640): 332-333.
45. Hashmi ASK, Hutchings GJ. Gold Catalysis. *Angewandte Chemie International Edition* 2006, **45**(47): 7896-7936.
46. Chavan SA, Srinivas D, Ratnasamy P. Oxidation of Cyclohexane, Cyclohexanone, and Cyclohexanol to Adipic Acid by a Non-HNO<sub>3</sub> Route over Co/Mn Cluster Complexes. *Journal of Catalysis* 2002, **212**(1): 39-45.
47. Raja R, Sankar G, Thomas JM. Powerful Redox Molecular Sieve Catalysts for the Selective Oxidation of Cyclohexane in Air. *Journal of the American Chemical Society* 1999, **121**(50): 11926-11927.
48. Zhao R, Ji D, Lv G, Qian G, Yan L, Wang X, Suo J. A highly efficient oxidation of cyclohexane over Au/ZSM-5 molecular sieve catalyst with oxygen as oxidant. *Chemical Communications* 2004(7): 904-905.
49. Lü G, Zhao R, Qian G, Qi Y, Wang X, Suo J. A Highly Efficient Catalyst Au/MCM-41 for Selective Oxidation Cyclohexane Using Oxygen. *Catalysis Letters* 2004, **97**(3-4): 115-118.
50. Xu Y-J, Landon P, Enache D, Carley A, Roberts MW, Hutchings G. Selective conversion of cyclohexane to cyclohexanol and cyclohexanone using a gold catalyst under mild conditions. *Catalysis Letters* 2005, **101**(3-4): 175-179.
51. Yap N, Andres RP, Delgass WN. Reactivity and stability of Au in and on TS-1 for epoxidation of propylene with H<sub>2</sub> and O<sub>2</sub>. *Journal of Catalysis* 2004, **226**(1): 156-170.

52. Brink G-Jt, Arends IWCE, Sheldon RA. Green, Catalytic Oxidation of Alcohols in Water. *Science* 2000, **287**(5458): 1636-1639.
53. Porta F, Prati L, Rossi M, Coluccia S, Martra G. Metal sols as a useful tool for heterogeneous gold catalyst preparation: reinvestigation of a liquid phase oxidation. *Catalysis Today* 2000, **61**(1–4): 165-172.
54. Abad A, Concepcion P, Corma A, Garcia H. A collaborative effect between gold and a support induces the selective oxidation of alcohols. *Angew Chem Int Ed Engl* 2005, **44**(26): 4066-4069.
55. Corma A, Domine ME. Gold supported on a mesoporous CeO<sub>2</sub> matrix as an efficient catalyst in the selective aerobic oxidation of aldehydes in the liquid phase. *Chemical Communications* 2005(32): 4042-4044.
56. Mori K, Hara T, Mizugaki T, Ebitani K, Kaneda K. Hydroxyapatite-Supported Palladium Nanoclusters: A Highly Active Heterogeneous Catalyst for Selective Oxidation of Alcohols by Use of Molecular Oxygen. *Journal of the American Chemical Society* 2004, **126**(34): 10657-10666.
57. Enache DI, Edwards JK, Landon P, Solsona-Espriu B, Carley AF, Herzing AA, Watanabe M, Kiely CJ, Knight DW, Hutchings GJ. Solvent-Free Oxidation of Primary Alcohols to Aldehydes Using Au-Pd/TiO<sub>2</sub> Catalysts. *Science* 2006, **311**(5759): 362-365.
58. Nijhuis TA, Kreutzer MT, Romijn ACJ, Kapteijn F, Moulijn JA. Monolithic catalysts as efficient three-phase reactors. *Chemical Engineering Science* 2001, **56**(3): 823-829.
59. Choudhary VR, Jha R, Jana P. Solvent-free selective oxidation of benzyl alcohol by molecular oxygen over uranium oxide supported nano-gold catalyst for the production of chlorine-free benzaldehyde. *Green Chemistry* 2007, **9**(3): 267-272.

60. Choudhary VR, Dumbre DK. Solvent-free selective oxidation of benzyl alcohol to benzaldehyde by tert-butyl hydroperoxide over  $U_3O_8$ -supported nano-gold catalysts. *Applied Catalysis A: General* 2010, **375**(2): 252-257.
61. Li G, Enache D, Edwards J, Carley A, Knight D, Hutchings G. Solvent-free oxidation of benzyl alcohol with oxygen using zeolite-supported Au and Au–Pd catalysts. *Catalysis Letters* 2006, **110**(1-2): 7-13.
62. Choudhary VR, Dhar A, Jana P, Jha R, Uphade BS. A green process for chlorine-free benzaldehyde from the solvent-free oxidation of benzyl alcohol with molecular oxygen over a supported nano-size gold catalyst. *Green Chemistry* 2005, **7**(11): 768-770.
63. Enache D, Knight D, Hutchings G. Solvent-free Oxidation of Primary Alcohols to Aldehydes using Supported Gold Catalysts. *Catalysis Letters* 2005, **103**(1-2): 43-52.
64. Enache DI, Barker D, Edwards JK, Taylor SH, Knight DW, Carley AF, Hutchings GJ. Solvent-free oxidation of benzyl alcohol using titania-supported gold–palladium catalysts: Effect of Au–Pd ratio on catalytic performance. *Catalysis Today* 2007, **122**(3–4): 407-411.
65. Dimitratos N, Lopez-Sanchez JA, Morgan D, Carley AF, Tiruvalam R, Kiely CJ, Bethell D, Hutchings GJ. Solvent-free oxidation of benzyl alcohol using Au-Pd catalysts prepared by sol immobilisation. *Physical Chemistry Chemical Physics* 2009, **11**(25): 5142-5153.
66. Dai Y, Wu X-P, Tang Y, Yang Y, Gong X-Q, Fan J. Selectivity switching resulting in the formation of benzene by surface carbonates on ceria in catalytic gas-phase oxidation of benzyl alcohol. *Chemical Communications* 2016, **52**(13): 2827-2830.
67. Brink G-Jt, Arends IWCE, Hoogenraad M, Verspui G, Sheldon RA. Catalytic Conversions in Water. Part 23: Steric Effects and Increased Substrate Scope in the Palladium-Neocuproine Catalyzed Aerobic Oxidation of Alcohols in Aqueous Solvents. *Advanced Synthesis & Catalysis* 2003, **345**(12): 1341-1352.

68. Conte M, Budroni G, Bartley JK, Taylor SH, Carley AF, Schmidt A, Murphy DM, Girgsdies F, Ressler T, Schlögl R, Hutchings GJ. Chemically Induced Fast Solid-State Transitions of  $\omega$ -VOPO<sub>4</sub> in Vanadium Phosphate Catalysts. *Science* 2006, **313**(5791): 1270-1273.
69. Daté M, Haruta M. Moisture Effect on CO Oxidation over Au/TiO<sub>2</sub> Catalyst. *Journal of Catalysis* 2001, **201**(2): 221-224.
70. Daté M, Okumura M, Tsubota S, Haruta M. Vital Role of Moisture in the Catalytic Activity of Supported Gold Nanoparticles. *Angewandte Chemie International Edition* 2004, **43**(16): 2129-2132.
71. Bond G, Thompson D. Gold-catalysed oxidation of carbon monoxide. *Gold Bulletin* 2000, **33**(2): 41-50.
72. Herzing AA, Kiely CJ, Carley AF, Landon P, Hutchings GJ. Identification of Active Gold Nanoclusters on Iron Oxide Supports for CO Oxidation. *Science* 2008, **321**(5894): 1331-1335.
73. Lopez N, Nørskov JK. Catalytic CO Oxidation by a Gold Nanoparticle: A Density Functional Study. *Journal of the American Chemical Society* 2002, **124**(38): 11262-11263.
74. Valden M, Lai X, Goodman DW. Onset of Catalytic Activity of Gold Clusters on Titania with the Appearance of Nonmetallic Properties. *Science* 1998, **281**(5383): 1647-1650.
75. Zhang H, Li W, Li X, Zhao W, Gu J, Qi X, Dong Y, Dai B, Zhang J. Non-mercury catalytic acetylene hydrochlorination over bimetallic Au-Ba(ii)/AC catalysts. *Catalysis Science & Technology* 2015, **5**(3): 1870-1877.
76. Hutchings GJ, Grady DT. Hydrochlorination of acetylene: The effect of mercuric chloride concentration on catalyst life. *Applied Catalysis* 1985, **17**(1): 155-160.



77. Shinoda K. The Vapour-Phase Hydrochlorination of Acetylene Over Metal Chlorides Supported on Activated Carbon. *Chemistry Letters* 1975, **4**(3): 219-220.
78. Conte M, Carley AF, Attard G, Herzing AA, Kiely CJ, Hutchings GJ. Hydrochlorination of acetylene using supported bimetallic Au-based catalysts. *Journal of Catalysis* 2008, **257**(1): 190-198.
79. Nkosi B, Adams MD, Coville NJ, Hutchings GJ. Hydrochlorination of acetylene using carbon-supported gold catalysts: A study of catalyst reactivation. *Journal of Catalysis* 1991, **128**(2): 378-386.
80. Qin G, Song Y, Jin R, Shi J, Yu Z, Cao S. Gas-liquid acetylene hydrochlorination under nonmercuric catalysis using ionic liquids as reaction media. *Green Chemistry* 2011, **13**(6): 1495-1498.
81. Conte M, Carley AF, Heirene C, Willock DJ, Johnston P, Herzing AA, Kiely CJ, Hutchings GJ. Hydrochlorination of acetylene using a supported gold catalyst: A study of the reaction mechanism. *Journal of Catalysis* 2007, **250**(2): 231-239.
82. Rahmat N, Abdullah AZ, Mohamed AR. Recent progress on innovative and potential technologies for glycerol transformation into fuel additives: A critical review. *Renewable and Sustainable Energy Reviews* 2010, **14**(3): 987-1000.
83. Haseeb ASMA, Fazal MA, Jahirul MI, Masjuki HH. Compatibility of automotive materials in biodiesel: A review. *Fuel* 2011, **90**(3): 922-931.
84. Körbitz W. Biodiesel production in Europe and North America, an encouraging prospect. *Renewable Energy* 1999, **16**(1-4): 1078-1083.
85. Pacific Food System Outlook 2006 - 2007: The Future Role of Biofuels. [cited August 2016] Available from:

[https://web.archive.org/web/20090116220246/http://www.pecc.org/food/pfso-singapore2006/PECC\\_Annual\\_06\\_07.pdf](https://web.archive.org/web/20090116220246/http://www.pecc.org/food/pfso-singapore2006/PECC_Annual_06_07.pdf)

86. Law EA, Meijaard E, Bryan BA, Mallawaarachchi T, Koh LP, Wilson KA. Better land-use allocation outperforms land sparing and land sharing approaches to conservation in Central Kalimantan, Indonesia. *Biological Conservation* 2015, **186**: 276-286.
87. Fargione J, Hill J, Tilman D, Polasky S, Hawthorne P. Land Clearing and the Biofuel Carbon Debt. *Science* 2008, **319**(5867): 1235-1238.
88. Behr A, Eilting J, Irawadi K, Leschinski J, Lindner F. Improved utilisation of renewable resources: New important derivatives of glycerol. *Green Chemistry* 2008, **10**(1): 13-30.
89. Zhou C-H, Beltramini JN, Fan Y-X, Lu GQ. Chemoselective catalytic conversion of glycerol as a biorenewable source to valuable commodity chemicals. *Chemical Society Reviews* 2008, **37**(3): 527-549.
90. Valliyappan T, Bakhshi NN, Dalai AK. Pyrolysis of glycerol for the production of hydrogen or syn gas. *Bioresource Technology* 2008, **99**(10): 4476-4483.
91. Pagliaro M, Rossi M. *The Future of Glycerol: New Usages for a Versatile Raw Material*, 2008.
92. Simonetti DA, Rass-Hansen J, Kunkes EL, Soares RR, Dumesic JA. Coupling of glycerol processing with Fischer-Tropsch synthesis for production of liquid fuels. *Green Chemistry* 2007, **9**(10): 1073-1083.
93. Biella S, Prati L, Rossi M. Selective Oxidation of D-Glucose on Gold Catalyst. *Journal of Catalysis* 2002, **206**(2): 242-247.

94. Carrettin S, McMorn P, Johnston P, Griffin K, Hutchings GJ. Selective oxidation of glycerol to glyceric acid using a gold catalyst in aqueous sodium hydroxide. *Chemical Communications* 2002(7): 696-697.
95. Carrettin S, McMorn P, Johnston P, Griffin K, Kiely CJ, Hutchings GJ. Oxidation of glycerol using supported Pt, Pd and Au catalysts. *Physical Chemistry Chemical Physics* 2003, **5**(6): 1329-1336.
96. Dimitratos N, Villa A, Bianchi CL, Prati L, Makkee M. Gold on titania: Effect of preparation method in the liquid phase oxidation. *Applied Catalysis A: General* 2006, **311**: 185-192.
97. Wang X, Kawanami H, Dapurkar SE, Venkataramanan NS, Chatterjee M, Yokoyama T, Ikushima Y. Selective oxidation of alcohols to aldehydes and ketones over TiO<sub>2</sub>-supported gold nanoparticles in supercritical carbon dioxide with molecular oxygen. *Applied Catalysis A: General* 2008, **349**(1-2): 86-90.
98. Hou W, Dehm NA, Scott RWJ. Alcohol oxidations in aqueous solutions using Au, Pd, and bimetallic AuPd nanoparticle catalysts. *Journal of Catalysis* 2008, **253**(1): 22-27.
99. Balcha T, Strobl JR, Fowler C, Dash P, Scott RWJ. Selective Aerobic Oxidation of Crotyl Alcohol Using AuPd Core-Shell Nanoparticles. *ACS Catalysis* 2011, **1**(5): 425-436.
100. Bawaked S, He Q, Dummer NF, Carley AF, Knight DW, Bethell D, Kiely CJ, Hutchings GJ. Selective oxidation of alkenes using graphite-supported gold-palladium catalysts. *Catalysis Science & Technology* 2011, **1**(5): 747-759.

# Chapter 2

## 2. Experimental

### 2.1. Chemicals

Chemicals were used as received and are as follows with information on their source and purity:

- Benzyl Alcohol (Extra Pure, SLR, Fisher Scientific)
- Cinnamyl Alcohol (98%, Sigma Aldrich)
- 4-Methoxybenzyl Alcohol (98%, Sigma Aldrich)
- 4-Chlorobenzyl Alcohol (99%, Sigma Aldrich)
- 4-Fluorobenzyl Alcohol (97% Sigma Aldrich)
- 4-Bromobenzyl Alcohol (99% Sigma Aldrich)
- Water (HPLC, Fisher Scientific)
- Benzene ( $\geq 99\%$  Sigma Aldrich)
- Toluene (HPLC, Fisher Scientific)
- Methanol (HPLC, Fisher Scientific)
- Titania (Degussa P25)
- Magnesium Oxide (nanoscale corporation)
- Graphite (Sigma Aldrich)
- Activated Carbon (Darco G60)
- Zinc Oxide (nano)
- Sodium Borohydride (98% Sigma Aldrich)
- Palladium Chloride (Johnson Matthey)
- Gold (III) Chloride (s) ( $\sim 52\%$  Au Basis, Sigma Aldrich, hydrated with HPLC water in lab)

## 2.2. Definitions

---

**Equation 2-1** Equation showing how conversion (%) was calculated when analysing reaction results

---



---

**Equation 2-2** Equation showing how selectivity (%) was calculated when analysing reaction results

---



---

**Equation 2-3** Equation showing how turnover frequency (TOF ( $\text{h}^{-1}$ )) was calculated when analysing reaction results

---

## 2.3. Definitions

<u>Acronym</u>	<u>Definition</u>
TOF ( $\text{h}^{-1}$ )	Turnover Frequency
TOF	Time of Flight
PVA	Polyvinyl Alcohol
NMR	Nuclear Magnetic Resonance
SEM	Scanning Electron Microscope
XPS	X-ray Photoelectron Spectroscopy
PES	Photoelectron Spectroscopy
NIST	National Institute of Standards and Technology
XRD	X-ray Diffraction
MP-AES	Microwave Plasma – Atomic Emission Spectroscopy
ICP-OES	Inductively Coupled Plasma – Optical Emission Spectroscopy
AAS	Atomic Absorption Spectroscopy
ICP	Inductively Coupled Plasma
RF-ICP	Radio Frequency – Inductively Coupled Plasma
GC	Gas Chromatograph/Chromatography
GC/MS	Gas Chromatography/Mass Spectrometry

Acronym	Definition
FID	Flame Ionisation Detector

## 2.4. Catalyst Preparation

### 2.4.1. Sol Immobilisation

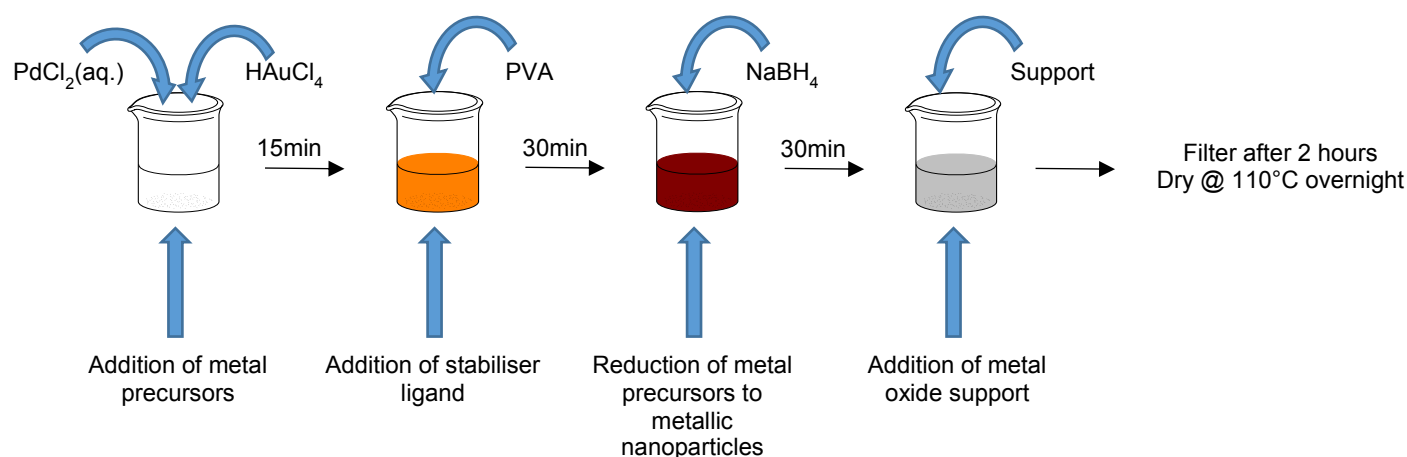


**Figure 2-1 Diagram outlining sol immobilisation technique for the synthesis of AuPd catalysts**

The sol immobilisation technique is a fairly new technique of catalyst preparation first pioneered by Dimitratos *et al.*<sup>1</sup>. This method involves creating a stabilised metal-based colloid and immobilising the particles on a metal oxide support (Figure 2-1). Using gold as an example, it is usually used in the Au(III) state from the compound  $\text{HAuCl}_4 \cdot x\text{H}_2\text{O}$  so before the immobilisation step, it needs to be reduced from Au(III) to Au(0). Once this has occurred, the metal oxide support can be added to immobilise the Au. The pH of the solution may need to be adjusted to ensure the solution's isoelectric point is lower than that of the support with  $\text{H}_2\text{SO}_4$  being the acid of choice to achieve this aim.

### 2.4.2. Au, Pd, Au-Pd Catalysts by sol immobilisation

Combinations of monometallic and bimetallic catalysts were prepared using the sol immobilisation technique on  $\text{TiO}_2$  or  $\text{MgO}$ . The detailed procedure for the preparation of 1wt%AuPd (1:1 mol)/support (2 g) (1%w/w) is as follows: a colloid was formed by adding a

stabilising ligand, polyvinyl alcohol (PVA), to an aqueous solution (800 ml) of  $\text{HAuCl}_4 \cdot x\text{H}_2\text{O}$  (1.123 ml of a 9.8 mg/ml solution) and palladium chloride (1.66 ml of a 6 mg/ml solution). The metal salts were reduced after 30 minutes using  $\text{NaBH}_4$  (x ml of 0.1M solution). The solution was left for 30 minutes to equilibrate before adding the metal oxide support (1.98 g). After 1 hour, the solution was acidified (except for  $\text{MgO}$  and  $\text{ZnO}$  supports) using concentrated  $\text{H}_2\text{SO}_4$ . After an additional one hour, the solution was filtered and washed with fresh, deionised water (1 l), and dried (16 h,  $110^\circ\text{C}$ ).

## 2.5. Catalyst Evaluation

The substrates used in this study were benzyl alcohol, cinnamyl alcohol, 4-fluorobenzyl alcohol, 4-chlorobenzyl alcohol, 4-bromobenzyl alcohol, 4-methoxybenzyl alcohol, 3,4-dimethoxybenzyl alcohol and 3,4,5-trimethoxybenzyl alcohol.

### 2.5.1. Oxidation of alcohols in water

All reactions were carried out in a Radleys® Starfish™ reactor using a multipot insert to allow the operation of 5 simultaneous reactions. A 50 ml glass reactor was charged with an aqueous solution of the chosen alcohol (0.200 g), catalyst (0.02 g) and water (5 ml). The reactor was then purged by flowing oxygen for 30 seconds, sealed, and pressurised with  $\text{O}_2$  (2 bar gauge (g)). The oxygen inlet was left open to replenish any  $\text{O}_2$  consumed in the reaction. The reactor was then heated to the required temperature. The stirrer speed set to 1000 rpm. The reaction was left for the required amount of time. Samples were centrifuged to remove any solid particulates. Once centrifuged, a sample was taken and analysed via NMR spectrometry.

### 2.5.2. Solvent free alcohol oxidation

All reactions were carried out in a Radleys® Starfish™ reactor using a multipot insert to allow the operation of 5 simultaneous reactions. A 50 ml glass reactor was charged with the chosen alcohol (1 g) and catalyst (0.02 g). The reactor was then purged with oxygen for 30 seconds, sealed, and pressurised with  $\text{O}_2$  (2 bar gauge (g)). The oxygen inlet was left open to replenish

any O<sub>2</sub> consumed in the reaction. The reactor was then heated to the required temperature and the stirrer speed set to 1000 rpm. The reaction was left for the required amount of time. Samples were centrifuged to remove any solid particulates. Once centrifuged, a sample was taken and analysed via NMR spectrometry or gas chromatography (GC).

### 2.5.3. Oxidation of alcohols in benzene

All reactions were carried out in a Radleys® Starfish™ reactor using a multipot insert to allow the operation of 5 simultaneous reactions. A 50 ml glass reactor was charged with a solution of the chosen alcohol (0.200 g), catalyst (0.02 g) and benzene (5 ml). The reactor was then purged with oxygen for 30 seconds, sealed, and pressurised with O<sub>2</sub> (2 bar gauge (g)). The oxygen inlet was left open to replenish any O<sub>2</sub> consumed in the reaction. The reactor was then heated to the required temperature. The stirrer speed set to 1000 rpm. The reaction was left for the required amount of time. Samples were centrifuged to remove any solid particulates. Once centrifuged, a sample was taken and analysed via NMR spectrometry.

### 2.5.4. Oxidation of alcohols in methanol

All reactions were carried out in a Radleys® Starfish™ reactor using a multipot insert to allow the operation of 5 simultaneous reactions. A 50 ml glass reactor was charged with an aqueous solution of the chosen alcohol (0.200 g), catalyst (0.02 g) and methanol (5 ml). The reactor was then purged with oxygen for 30 seconds, sealed, and pressurised with O<sub>2</sub> (2 bar gauge (g)). The oxygen inlet was left open to replenish any O<sub>2</sub> consumed in the reaction. The reactor was then heated to the required temperature. The stirrer speed set to 1000 rpm. The reaction was left for the required amount of time. Samples were centrifuged to remove any solid particulates. Once centrifuged, a sample was taken and analysed via NMR spectrometry.

## 2.6. Catalyst Characterisation

In this section, the two main experimental techniques that were used in this experiment will be explained. These techniques are scanning electron microscopy (SEM) and x-ray



photoelectron spectroscopy (XPS). These two techniques are surface science techniques, each having their own advantages and disadvantages which will be explained in their respective sections.

Spectroscopy is defined as the study of physical systems by the electromagnetic radiation with which they interact or that they produce and spectrometry is the measurement of such radiations as a means of obtaining information about the systems and their components<sup>2</sup>. This basic definition however, hides a very complex technique that has proved very useful for the physical chemist.

At the end of the last century, scientists were discovering that matter could not take up energy in a continuous manner, as previous theories had suggested. In 1900 Max Planck published the idea that the energy of an oscillator is discontinuous and that any change in its energy content can occur only by means of a jump between two distinct energy states. A single molecule in space contains many different classes of energy; rotational energy since it rotates about its centre of gravity; vibrational energy due to the periodic displacement of its atoms from their equilibrium positions; electronic energy since the electrons associated with each atom or bond are in constant motion.

It is these energies that have become recognised as having distinct regions, it is quantized and a molecule can exhibit a range of these energy levels (Figure 2-2). Transitions from one energy level to another are possible between these energy levels. This sudden transition involves a finite amount of energy equal to or exceeding the energy difference between the two energy levels.

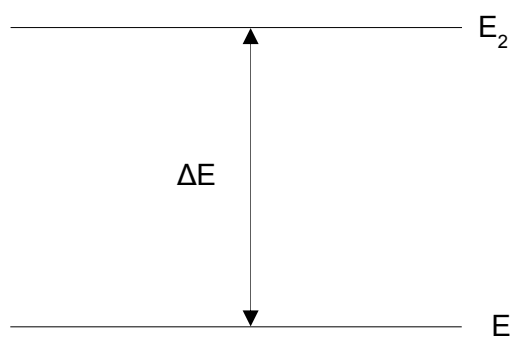


**Figure 2-2** Diagram showing two discrete energy levels within an atomic system.  $\Delta E$  is the energy difference between the energy levels  $E_1$  and  $E_2$

The suffixes one and two distinguish between two different energy levels and are designated quantum numbers. Transitions can take place between level 1 and level 2 provided the appropriate amount of energy  $\Delta E = E_2 - E_1$  can be either absorbed or emitted from the system. Planck suggested this energy can be provided by electromagnetic radiation and that the frequency of this radiation can be expressed as  $\nu = \Delta E / h$  Hz which equates to  $\Delta E = h\nu$  where energy is expressed in joules and  $h$  is Planck's constant.

If we take a molecule in state 1, the ground state, and shine a beam of radiation onto it, and the frequency,  $\nu$ , is equal to  $\Delta E$  then energy will be absorbed by the system and the molecule will jump to state 2, the so called excited state. If a detector is set to detect the change in energy of the incident beam, it will be seen that only a specific region will have decreased in intensity. This is the basis of absorption spectroscopy. The molecule can only stay in the excited state for a very short amount of time before which the excess energy taken on by the molecule is emitted. This is emission spectroscopy whereby a detector measures the radiation given off by the molecule. The emitted radiation will have the energy per Equation 2-4.

---

**Equation 2-4 Equation to identify the emission energy of a molecule exposed to spectroscopic investigation**

### 2.6.1. X-ray Photoelectron Spectroscopy

XPS is an important analytical technique which can be used to characterise heterogeneous catalysts. XPS has been used in this thesis to describe the Au and Pd species present within the AuPd nanoparticles supported on metal oxides and these results are described in later chapters. An overview of XPS is given to contextualise this data.

An atom is made up of negatively charged particles, called electrons, and positively charged elements called protons (neutrons are also present, but will be disregarded since in photoelectron techniques discussed, its role is not required).

Since an electron is a charged particle, its orbit around the nucleus will induce a magnetic field whose intensity and direction will depend upon the electron velocity and on the radius of the orbit. These two quantities are characterised by the orbital angular momentum which is quantized as the electron can only travel in a well-defined orbital (the s, p, d, f...orbital). This characteristic is assigned the quantum number  $l$  – the angular momentum quantum number, which can take on the values 0, 1, 2, 3...which correspond to which shell the electron is occupying. Where  $l = 0$  corresponds to s sub shell, 1 corresponds to the p sub shell and so forth.

Another property of an orbiting electron is the electron spin; it can be either positive or negative which can also contribute to an inherent magnetic field. This in turn is termed the spin momentum and has the spin quantum number  $s$  which takes the value  $\pm \frac{1}{2}$ . Taking account of these two factors, the total electronic angular momentum is a combination of  $s$  and  $l$  and is a vector sum of the two momenta. This summation can occur in two ways however, through j-j coupling and L-S (Russel-Saunders) coupling.

### 2.6.1.1. Photoelectron Spectroscopy

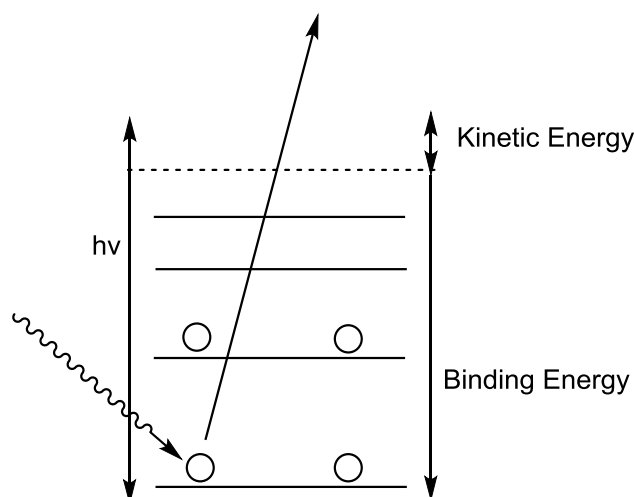


**Figure 2-3 Basic principle of photoelectron spectroscopy**

XPS is a technique that probes atomic and molecular electronic energy levels, which are influenced by the coupling techniques mentioned before. XPS relies upon the photoelectric effect summarised in Figure 2-3. Each electron (the circles) is held in place by the nucleus

with a characteristic binding energy. A photon (squiggly line) approaches the system and collides with an electron, this energy is transferred to the electron and if this is greater than the binding energy, the electron will leave the atom and carry the excess energy away. This results in the leaving electron having a certain kinetic energy and velocity, which can be defined in Equation 2-5 and Equation 2-6:

**Equation 2-5 Indicating how photon energy is related to binding energy and kinetic energy**

or

**Equation 2-6 Equation indicating an electron's binding energy is related to the energy of an incoming photon minus its kinetic energy**

By knowing the energy of the monochromatic exciting radiation, the binding energies of the electrons in the atom being examined and identified, based on the kinetic energies with which they leave with. Electrons can be ejected from either the core or valence levels of an atom depending on the energy of the incident radiation. For XPS analysis, electrons from the core shell of the atom are ejected and this requires excitation radiation of sufficiently high energy. In this case, the X-Ray beam is produced by electron bombardment of a clean metal target such as Al or Mg, resulting in emission of radiation at very specific energy ( $k_{\alpha}$  for Al occurs at 1486.6 eV).

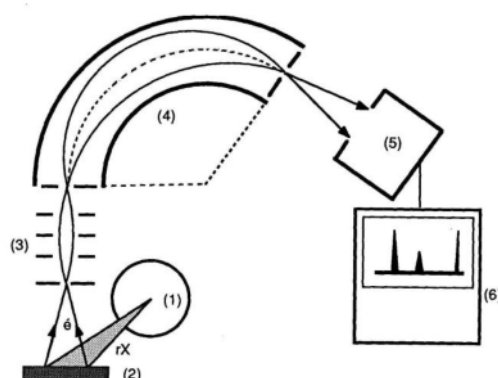


**Figure 2-4 Diagrammatic representation of an XPS hemispherical analyser<sup>3</sup>, (1) x-ray tube, (2) Sample, (3) Focusing system, (4) Spectrometer, (5) Detector, (6) Data recorder.**

Experimentally, the detection of electrons must occur at high vacuum as electrons are chemically active. Imaging solid samples is relatively straight forward and has no pumping problems, however, liquid and gaseous samples present great difficulty, but can be done. Once the electrons are emitted from the sample, they are analysed by a hemispherical analyser (Figure 2-4).

Once the monochromatic x-ray source has fallen onto the sample, the ejected electron travels between a pair of electrically charged hemispherical plates which act as an energy filter. The resultant current which is measured by an electron multiplier, indicated the number of electrons ejected from the surface with that kinetic energy.

XPS spectra contain peaks which have different intensities depending on which orbital the electron is ejected from; they can also display a chemical shift analogous to NMR spectroscopy. This is due to non-equivalent atoms of the same element present in the sample. These electrons have measurable different binding energies (BE's) which can arise from: difference in oxidation state, difference in molecular environment, difference in lattice site etc. The physical basis of chemical shift is based on a model which displays reliable results. These chemical shifts can be looked up in various databases (NIST) and used to identify the chemical environment the atom is in from which the ejected electron originated.

Spectra can also display multiplet splitting which occurs if the initial state atom contains unpaired electrons. Upon photoemission, the electron may interact, through its spin moment, with the spin of the additional unpaired electron in the core level of the atom from which the photoelectron left. Parallel or anti parallel spins give final states which differ in energy by 1-2 eV.

An experimental problem in XPS is that electrically insulating samples may charge during the measurement due to photoelectrons leaving the sample. The potential the sample acquires is determined by the photoelectric current of electrons leaving the sample, the current through the sample holder towards the sample and the flow of Auger and secondary electrons from the source window onto the sample. Due to the positive charge on the sample, all XPS peaks in the spectrum shift by the same amount to higher binding energies.

To counteract this, calibration is carried out using the binding energy of a known compound. In the case of XPS run at Cardiff, this is done by using the always present carbon contamination, with a C 1s binding energy of 284.7 eV. In addition to shifting, peaks may broaden when the sample charges inhomogeneously leading to a reduced signal-to-noise ratio and resolution. This charging phenomenon is of concern in monochromatic XPS equipment like that found at Cardiff. This is due to the source being at a large distance from the sample and hence the electrons from the source do not reach the sample. The use of a flood gun which sprays low energy electrons onto the sample and some mounting techniques may overcome this.

XPS can also recognise how particles are dispersed upon a support. If there are two samples, one with high dispersion and one with low, the intensities of the peaks will be different in each case. When the particles are small, almost all of the atoms are at the surface while the support is covered to a large extent. In this case XPS measures a high intensity from the particles but a relatively low intensity for the support. For a low level of dispersion, the opposite will be true.

## 2.6.2. X-Ray Diffraction

XRD is a bulk crystalline technique that probes powdered, crystalline samples such as catalysts. It is possible to identify crystalline phases present in the catalyst and establish particle sizes within a powder sample. To produce the X-rays, a copper target is bombarded with high energy electrons releasing characteristic  $K\alpha$  (8.04 keV, 0.154 nm) and  $K\beta$  X-rays when the electrons in the copper target return to the ground state from their excited state. The  $K\beta$  X-rays are filtered out while the remaining  $K\alpha$  photons are elastically scattered by atoms in the powdered sample.

The scattered X-Rays are measured using a moving detector and x-rays that are in phase with the catalyst sample interfere constructively to give higher intensity reflections. To calculate lattice spacing,  $d$ , the Bragg's Law equation (Equation 2-7), which relates wavelength of the X-rays ( $\lambda$ ), the angle between incident X-rays and the normal angle ( $\theta$ ), and the order of reflection ( $n$ ) is used.

Equation 2-7 Bragg's law<sup>4</sup> equation for calculating lattice spacing via powder XRD.

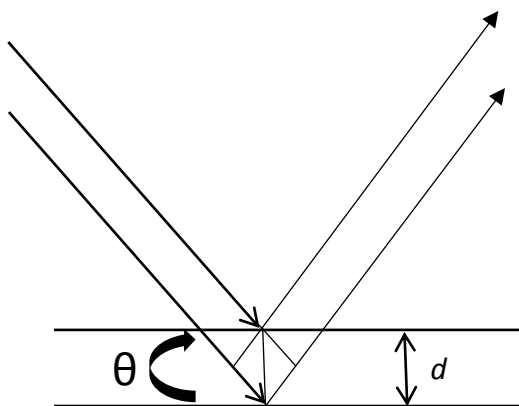


Figure 2-5 Diagrammatical representation of Bragg's law

### 2.6.2.1. Characterization and phase analysis of catalysts

XRPD spectra were acquired using an X'Pert PanAlytical diffractometer operating at 40 kV and 30 mA selecting the Cu K<sub>α</sub> radiation using a Ni filter. Detailed set-up conditions were: soller slits 0.04 radians, mask 15 mm, divergence and receiving slits ¼ °, step scan mode from 10 to 80 ° 2θ in 33 min. Analysis of the spectra was carried out using X'Pert HighScore Plus software for the full pattern analysis.

### 2.6.3. Microwave Plasma Atomic Emission Spectrometry

Spectroscopic methods based on atomic emission are a well-defined area of chemistry, with such techniques as ICP-OES, AAS, and the relatively new technique of MP-AES. Indeed, the two techniques of ICP-OES and MP-AES are relatively similar in their operation, differing in how they produce the analytical plasma each technique is based upon. At present, inductively coupled plasma operating at either 27 MHz or 40 MHz is the plasma of choice for analytical chemistry. Even with ICP methods, microwave plasma generation has been an area of interest

for a while and MP-AES is the result of this research, generating plasma at a frequency of 2.455 GHz. Prior to this, microwave sources of plasma have had worse detection limits than ICP-OES and much more challenging sample handling requirements, two disadvantages MP-AES has eliminated.

An electrical plasma suitable as an emission source must display several key characteristics, these being:

- aerosolised sample introduction
- suitable plasma temperature
- suitable power levels
- suitable thermal coupling and residence time

These criteria allow desolvation, volatisation, atomisation and excitation of the sample if they are within suitable parameters. Introduction of sample should also not exhibit destabilising effects, allowing a stable spectroscopic emission and not extinguishing the plasma.

### 2.6.3.1. Electric field excited plasma

A plasma formed by the action of a uniform axial electric field can be considered being made up of several parallel filaments aligned with the electric field direction. Each filament experiences the same voltage drop along its length and acts as a resistor, dissipating power. The power dissipated in each filament is given by Equation 2-8 where  $V$  = voltage across the plasma filaments (volts) and  $R$  = resistance of the plasma filament (ohms).

#### **Equation 2-8 Equation indicating how to calculate power dissipated in each MP-AES filament**

In the case of plasma filaments, as temperature increases so does the level of ionisation and this reduces the resistance of the filament. If the resistance is reduced of the filament, power dissipation is increased which raises the temperature in a self-reinforcing feedback loop which causes the plasma filament to collapse to a thin rod. This is not ideal as sample introduction to such a thin rod is not optimised as the sample will undergo rapid heating and expansion.



This expansion creates a pressure gradient which deflects the sample away from the plasma filament, preventing entrainment. This problem was overcome by Greenfield *et al.*<sup>2</sup> who recognised creating an RF-ICP as a toroid with a cooler centre could facilitate sample introduction. An aerosolised sample introduced coaxially towards this central core undergoes maximum expansion around its circumference, compressing the gas stream and guiding it into the core.

Further advances in plasma filament generation with electric fields were proposed by Okamoto and others but one major drawback of electric field generated plasmas is that their detection limits are considerably worse than that of the standard ICP-OES suggesting sample atomisation and excitation could be further improved and are the cause for low detection limits.

### 2.6.3.2. Magnetic field excited plasma

Work by Hammer *et al.*<sup>5</sup> investigated the possibility of sustaining a microwave plasma by coupling energy from an axial magnetic field. By using Faraday's law, an induced voltage would be created around the magnetic field which is capable of accelerating ions, subsequently coupling energy into the plasma supporting its continuation. A plasma supported in this way cannot collapse into a rod like a plasma excited solely by an electric field. Instead, the microwave supported plasma will expand to the maximum possible radius. Research indicated this expansion could be controlled by careful design of the torch assembly.

### 2.6.3.3. Microwave generation

Microwaves are part of the electromagnetic spectrum and unlike an electric field, which travels along wires, it is necessary to employ a structure called a waveguide to transmit the microwave energy (Figure 2-6). This waveguide is a hollow rectangular metal section with an electric field aligned to the height of the waveguide and the magnetic field aligned with the width of the waveguide. The field generated is supported by induced currents flowing through the walls.

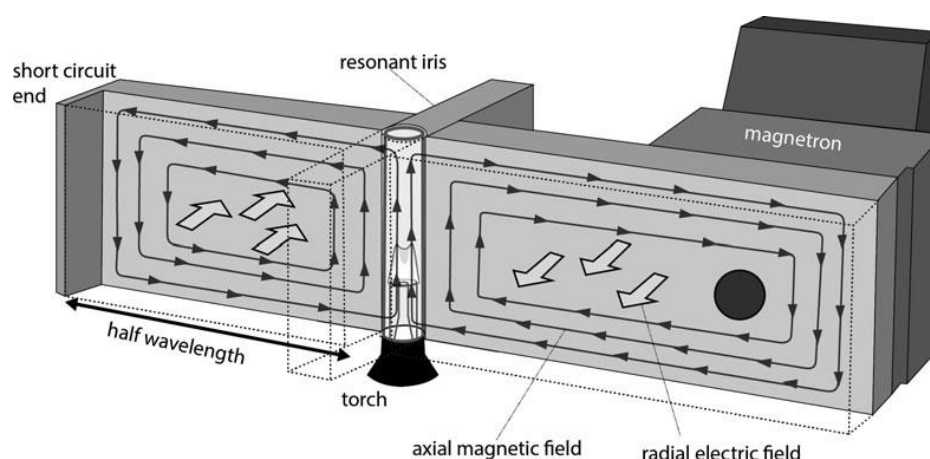


**Figure 2-6<sup>4</sup> Schematic representation of waveguide in an MP-AES, sample is placed within the torch at the centre of the waveguide<sup>6</sup>**

#### 2.6.3.4.MP-AES Operation

Ignition of plasma is achieved using a 300 W or greater microwave source and injecting a spark by briefly switching the carrier gas supply to argon and then switching back to nitrogen. Plasma destabilisation as seen in ICP-OES was not observed for magnetically coupled microwave plasma. Sample is introduced in a spray chamber fed by a peristaltic pump. The wavelength of the plasma will change as sample is introduced through it and using a detector, characteristic emission wavelengths for an element will be observed. A basic diagrammatic representation of the MP-AES equipment used is shown in Figure 2-7.

<sup>4</sup> Used under license from John Wiley and Sons

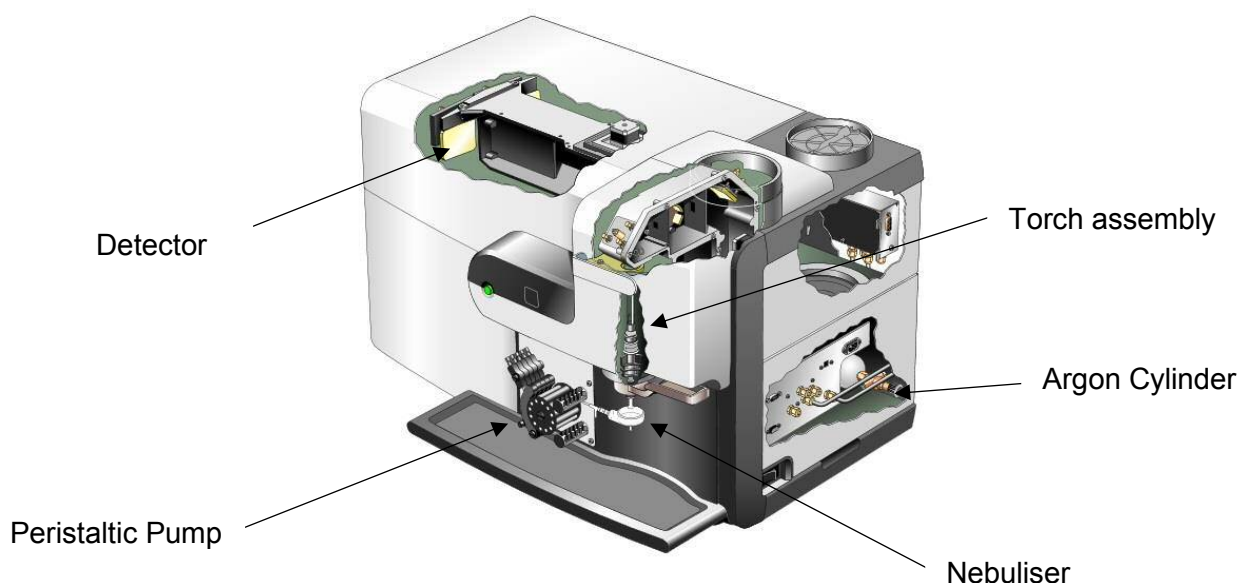


**Figure 2-7 Diagrammatic of MP-AES spectrometer (Agilent 4100 MP-AES)**

## 2.7. Product Analysis

### 2.7.1. Nuclear Magnetic Spectrometry

In 1946, two research groups independently observed nuclear magnetic resonance signals for the first time for which they were jointly awarded the Nobel Prize for physics in 1952. Since their discovery, NMR has become the ubiquitous tool for every chemist in their everyday lives and has progressed from one-dimensional analysis to two-dimensional or three-dimensional analysis. The nuclide of interest in this thesis is  $^1\text{H}$  as its resonance is one of the most important for molecule identification and quantisation.

#### 2.7.1.1. Experimental

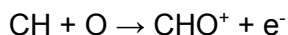
The  $^{13}\text{C}$  and  $^1\text{H}$  NMR spectra were obtained using a Bruker Avance 400 MHz or 500 MHz DPX spectrometer, equipped with Silicon Graphics workstation running X win 1.3 with results reported in ppm with number of protons, multiplicity and assignment. All chemical shifts for  $^1\text{H}$  NMR were recorded in deuterated chloroform ( $d\text{-CDCl}_3$ ).

### 2.7.2. Gas Chromatography

GC is a commonly used method for the separation of chemical mixtures. Firstly, liquid or gas samples are vaporised in an injection port in which an inert carrier gas, helium, is used to transport the now gaseous sample through the chromatographic column that is inside the GC oven. The sample is separated into its constituent parts by way of chemical interactions with the GC column, known as the stationary phase. At the end of the column is a flame ionisation detector (FID) where the products are combusted with air and hydrogen to produce cations which are analysed with an anode detector.

The helium carrier gas is compatible with a wide range of detectors, resulting in good resolution and separation of sample peaks. For a liquid sample, the sample is injected through a rubber septum on an injection port which is heated to above the boiling point of the analyte material. The stationary phase is usually made up of a viscous liquid, chemically bonded to the inside of a capillary column or in the case of a packed column, on the surface of solid particles (or the solid particles themselves). In general, non-polar columns are used to separate non-polar mixtures and polar columns, polar solutions.

In an FID, the separated components of the solution are combusted in a mixture of air and hydrogen gases. Carbon (except carbonyl and carboxyl) atoms produce CH radicals which it has been suggested form  $\text{CHO}^+$  ions in the flame, Equation 2-9.



**Equation 2-9 Decomposition of carbon in a FID detector during GC analysis**

The number of ions produced is proportional to the number of carbon atoms entering the flame. Electrons flow from the anode to the cathode where they neutralise the  $\text{CHO}^+$  in the flame, this creates a current which is the detection signal.

### 2.7.2.1. Experimental

GC analysis was carried out using a Varian 3800 chromatograph equipped with a CP8400 autosampler and a CP-wax 52 column. Products were identified by comparison with authentic samples. For the quantification of the amounts of reactants consumed and products generated, an external calibration method was used.

### 2.7.3. Gas Chromatography/Mass Spectrometry

GC/MS can be used to separate and identify chemical components in a volatile solution. The compounds are separated by gas chromatography as described above, subsequently; each component is identified by ionisation and detection in mass spectrometry. Mass spectrometry is complimentary to GC since the levels of analyte used in both are very low, each analyte will elute at different times allowing for a time resolved mass spectra.

As molecules leave the GC they are ionised by electron ionisation. A hot filament emits electrons which are then accelerated through a potential. These electrons interact with the molecules from the GC causing ionisation, usually by the loss of an electron. If one electron is removed the remainder of the molecule is a positively charged molecular ion. This ion may have enough energy to undergo further fragmentation.

A positively charged plate repels the ions towards the analyser tube. The ions are then separated by their mass to charge ratios ( $m/z$ ). The two most common types of detector are the time of flight detector (TOF) and the quadrupole mass analyser. In the TOF, ions are accelerated by an electric field resulting in all ions having the same kinetic energy. The velocities at which these ions reach the detector can be used to calculate their mass since lighter ions will travel faster than heavier ones.

The second technique, the quadrupole analyser, separates ions of differing mass to charge ratio with the application of an oscillating electric field. The quadrupole consists of four metal rods which have a current applied across them along with alternating radio frequencies. The movement of the ions through the poles depends upon the electric fields as only specific  $m/z$

ratios will have a stable trajectory through the detector. As the fields change ions of differing  $m/z$  can reach the detector.

The separated ions can be detected by several methods including an electron multiplier and Faraday cup. An electron multiplier uses a vacuum tube to multiply charges. A charged particle collides with an emissive material which induces the emission of secondary electrons. These electrons are accelerated to strike a second diode to create more electrons. This greatly amplifies the signal received.

The Faraday cup uses the production of a current to detect the ions. The ions strike a metal plate, the transfer of charge between the two creates a small current. The size of this current is dependent on the number of ions which can therefore be determined.

## Chapter 2 References

1. Dimitratos N, Lopez-Sanchez JA, Morgan D, Carley A, Prati L, Hutchings GJ. Solvent free liquid phase oxidation of benzyl alcohol using Au supported catalysts prepared using a sol immobilization technique. *Catalysis Today* 2007, **122**(3–4): 317-324.
2. Greenfield S, Jones IL, Berry CT. High-pressure plasmas as spectroscopic emission sources. *Pure and Applied Chemistry* 1964, **89**(1064): 713-720.
3. Le Commissariat à l'énergie atomique et aux énergies alternative. X-ray photoelectrons spectroscopy (XPS). 2016 [cited 2016 August]Available from: [http://iramis.cea.fr/Phoce/Vie\\_des\\_labos/Ast/ast\\_sstechnique.php?id\\_ast=508](http://iramis.cea.fr/Phoce/Vie_des_labos/Ast/ast_sstechnique.php?id_ast=508)
4. Atkins PW, Paula JD. *Elements of Physical Chemistry*. Oxford University Press, 2009.
5. Hammer MR. A magnetically excited microwave plasma source for atomic emission spectroscopy with performance approaching that of the inductively coupled plasma. *Spectrochimica Acta Part B: Atomic Spectroscopy* 2008, **63**(4): 456-464.
6. Wiedenbeck M, Bédard LP, Bugoi R, Horan M, Linge K, Merchel S, Morales LFG, Savard D, Souders AK, Sylvester P. GGR Biennial Critical Review: Analytical Developments Since 2012. *Geostandards and Geoanalytical Research* 2014, **38**(4): 467-512.

# Chapter 3

## 3. Benzyl Alcohol Oxidation

### 3.1. Introduction

The oxidation of primary alcohols to their corresponding aldehydes is an important process, both in the laboratory and industrially, as aldehydes are valuable both as chemical intermediates and components in the perfume industry<sup>1</sup>. They are also of interest as a replacement source of fine chemicals due to the future limited supply of petroleum remaining, as this dwindling supply is leading to a continual rise in petroleum price<sup>2</sup>. It has been shown that supported Au and AuPd catalysts are an effective system for the selective oxidation of benzyl alcohol in the liquid phase<sup>3</sup>. The oxidation of benzyl alcohol can be carried out over a wide range of reaction conditions. This has resulted in benzyl alcohol being chosen as a model compound for catalytic oxidation reactions, allowing the screening of new catalysts. The results from these reactions can then be used to compare the screened catalyst to existing systems and can help benchmark the catalyst's activity. The reaction pathway for benzyl alcohol oxidation is shown in Figure 3-1<sup>4</sup> indicating the expected product distribution via oxidation using AuPd catalysts supported on carbon.



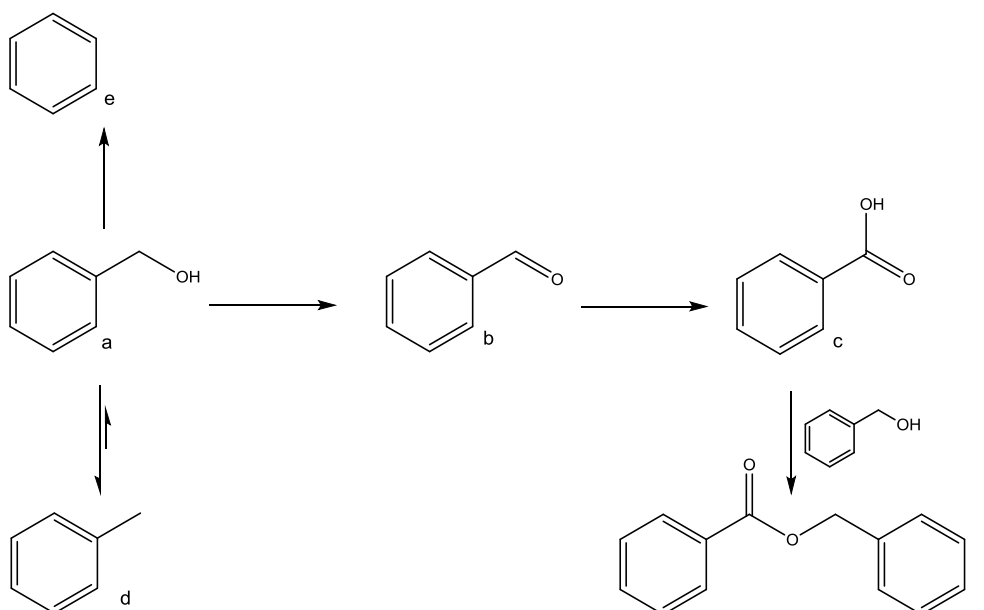


**Figure 3-1 Solvent free catalytic oxidation of benzyl alcohol using AuPd catalysts supported on carbon, potential products include benzyl alcohol (a), benzaldehyde (b), benzoic acid (c), toluene (d), benzene (e) and benzyl benzoate (f)<sup>4</sup>**

The oxidation of benzyl alcohol will typically yield benzaldehyde as the major product. If the catalyst is highly active, it can sequentially oxidise the benzaldehyde to benzoic acid and further to benzyl benzoate<sup>4</sup>.

## 3.2. Catalyst Characterisation

### 3.2.1. MP-AES Results

AuPd on TiO<sub>2</sub> catalysts were subjected to MP-AES testing to ascertain the metal loading of the catalysts. The results, shown in Table 3-1, show that catalysts with varying molar ratios of Au: Pd were synthesised and that most of the catalysts prepared had the expected amount of AuPd loading. Total weight percentages were within the expected range, apart from 0.5:9.5 AuPd/TiO<sub>2</sub> and Pd/TiO<sub>2</sub>. Even with this phenomenon, the expected ratios of Au to Pd were achieved. This may mean there was incomplete digestion of the AuPd nanoparticles in aqua regia before MP-AES analysis was conducted.

The possibility that not all the metal sol was successfully immobilised onto the metal oxide also exists but the ratio of Au to Pd being the expected value suggests the metal mixing during the catalyst synthesis was sufficient to produce the desired nanoparticle composition.

**Table 3-1 Differing AuPd molar ratios on 1%AuPd/TiO<sub>2</sub> as determined by MP-AES**

Molar Metal Ratio		MP-AES ppm		wt.% Catalyst/50ml		Total wt.% Metal	Expected Ratio	Actual Ratio
Au	Pd	Au	Pd	Au	Pd			
1	0	18.71	0	0.93	0	0.93	1.0 Au	1.0 Au
9.5	0.5	18.63	0.54	0.93	0.03	0.96	0.03	0.03
9	1	17.56	1.05	0.87	0.05	0.93	0.06	0.06
1	1	12.15	7.11	0.6	0.35	0.96	0.54	0.59
1	2	8.66	9.43	0.43	0.47	0.9	0.24	0.92
0.5	9.5	1.37	12.8	0.07	0.64	0.71	0.1	0.11
0	1	0	10.5	0	0.59	0.59	1.0 Pd	1.0 Pd

### 3.2.2. XPS Analysis

XPS analysis of the 1%AuPd/TiO<sub>2</sub> catalysts showed that in each of the catalysts, there existed metallic Au<sup>0</sup> as demonstrated by the Au<sub>f7/2</sub> peak being observed at 83.4 eV<sup>5</sup>. The analysis also indicated metallic Pd<sup>0</sup> is present by the presence of the Pd<sub>3d5/2</sub> transition, with a binding energy of 335 eV<sup>6</sup>. Also detected via XPS was Pd<sup>2+</sup> due to the presence of a Pd<sub>3d5/2</sub> peak with a binding energy of 343 eV observed in the spectra. This would suggest that the metals are indeed being reduced during the addition of NaBH<sub>4</sub> during the catalyst preparation. Two XPS scans were taken in succession of each other and the intensities of each scan were the same. This rules out any Pd<sup>n+</sup> or Au<sup>n+</sup> species being present as the intensity of the second scan would be lower, due to the electron beam reducing cationic species.

The metallic ratio for the 1:1 AuPd/TiO<sub>2</sub> catalyst is indicated to be close to 1:1 from the XPS measurements, suggesting that the catalysts are metallic in nature. In previous work, it has been found that the sol-immobilisation method can make core-shell morphology catalysts but the procedure for making them is different to the protocol used in this work. By adjusting the

reduction step, so that one metal is added first, reduced, and then the second metal is added and reduced, a core-shell catalyst is made.

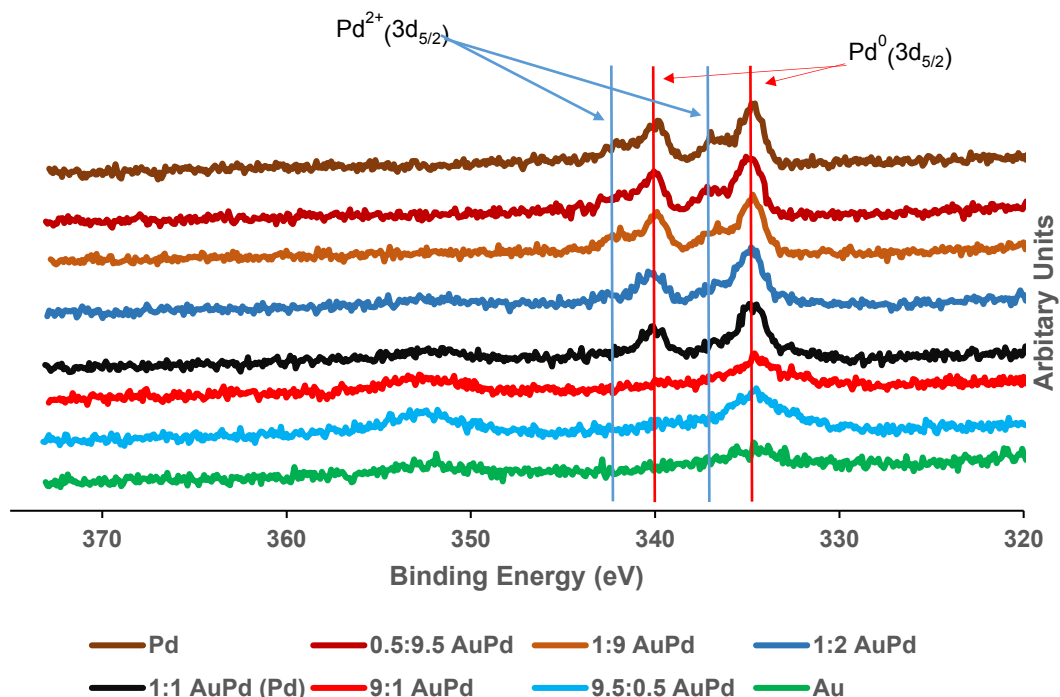


Figure 3-2 Palladium (Pd(3d)) region XPS spectra of varying AuPd ratios supported on  $\text{TiO}_2$

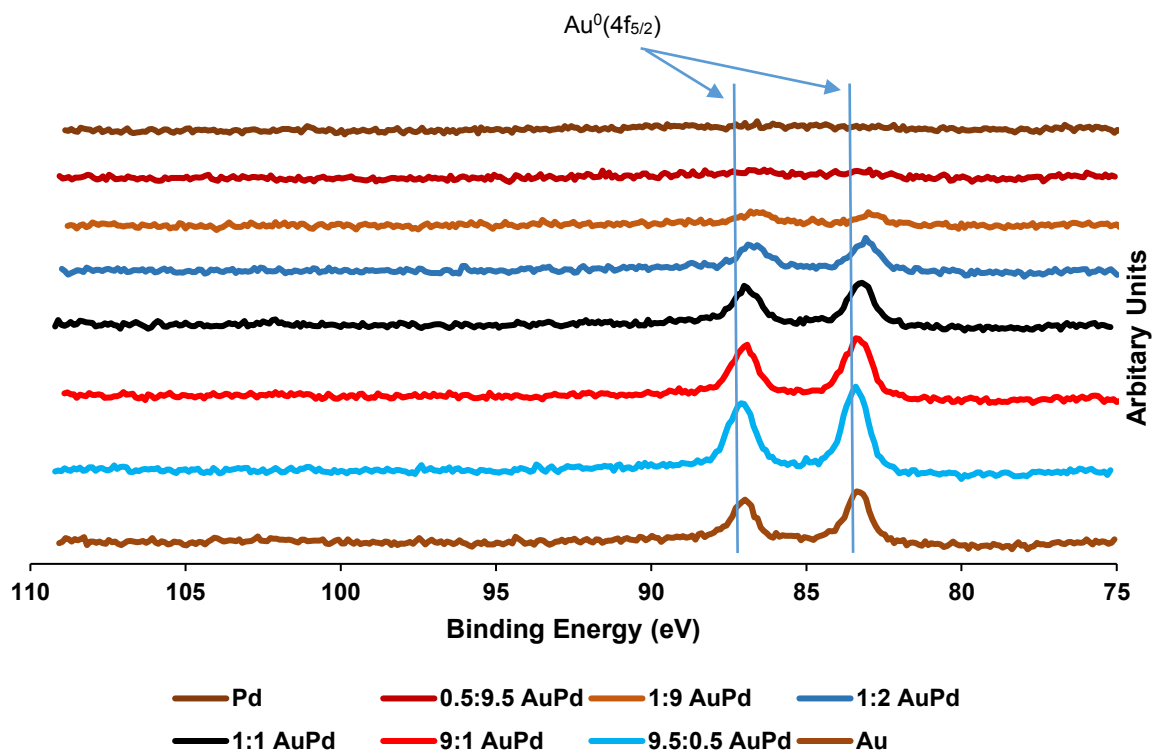


Figure 3-3 Gold (Au(4f)) region XPS spectra of varying AuPd ratios supported on  $\text{TiO}_2$

XPS analysis of the  $\text{TiO}_2$  support showed that there was not a 1:2 ratio for  $\text{Ti}:\text{O}_2$  but that oxygen was slightly in excess. This observation seemingly arises from the presence of the stabiliser ligand used to make the AuPd supported catalysts, namely polyvinyl alcohol (PVA). This PVA ligand stabilises the AuPd nanoparticles via steric interaction as it surrounds the AuPd nanoparticles but this stabilisation effect comes at a cost of activity. PVA stabilised catalysts are less active than tetrakis(hydroxymethyl)phosphonium chloride (THPC) stabilised catalysts but offer a good narrow size distribution when compared to THPC which produces slightly larger nanoparticles than PVA, shown in work by Prati *et al.*<sup>7</sup>. It is also possible to remove this PVA ligand with no significant loss of catalytic activity as demonstrated by Hutchings *et al.*<sup>8</sup>, something that future work could focus on.

### 3.2.3. Transmission Electron Microscopy Analysis

Nanoparticle dispersion was investigated using Transmission Electron Microscopy (TEM) which indicated a narrow size distribution of nanoparticles, with a mean diameter of 4 nm over a range of 1-9 nm when supported on  $\text{TiO}_2$ <sup>6</sup>. Hutchings *et al.*<sup>6</sup> also investigated the thermal stability of the supports by calcining AuPd catalyst for 3 h at 400 °C. It was found that the nanoparticles on  $\text{TiO}_2$  exhibited increased thermal stability after the calcination step, whilst some sintering had occurred it was minimal and the particle size distribution wasn't significantly altered. This was compared with Darco-G60 Carbon support where there was significant nanoparticle sintering with an increase in particle size distribution from a narrow size distribution to a broad size distribution of between 1-70 nm. This sintering had a detrimental impact on catalyst activity but not selectivity. Selectivity remained high towards the benzaldehyde product but activity was decreased by a factor of 2 for the AuPd catalyst on  $\text{TiO}_2$  but an order of magnitude for the C supported catalyst. On activated carbon support, TEM revealed that the nanoparticles were forming face centred cubic structures.

## 3.3. Catalyst Evaluation

For a detailed procedure of catalyst testing, please consult back to chapter 2.

### 3.3.1. Effect of solvent

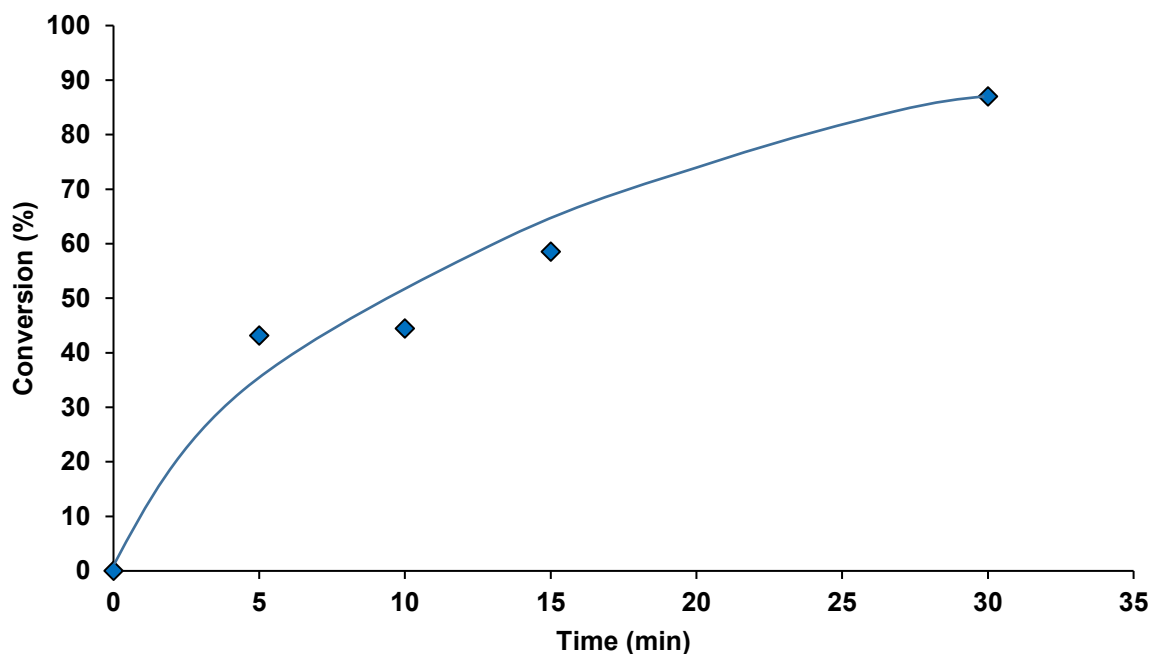


**Figure 3-4** Conversion of benzyl alcohol (◆) in 5 ml water using a AuPd/TiO<sub>2</sub> catalyst (20 mg, 1:1 mol), 2 bar (g) O<sub>2</sub>, 1000 rpm at 80 °C and 200 mg alcohol

Solvent can have a significant influence on alcohol oxidation and its effect was studied on the oxidation of benzyl alcohol. As can be seen from Figure 3-4, benzyl alcohol can be oxidised quite easily in the presence of water. The timescale for the reaction is quite short with 50% conversion occurring at just ca. 12 minutes. Selectivity was also high at >95% towards the desired aldehyde product. There were no traces of acid or any other undesired products. The reaction had high conversion (~87%) within the 30-minute period studied. Since water seemed to be a suitable medium for oxidation, it was then investigated to see if it played a role in the mechanism of oxidation. This was done by replacing water with deuterium oxide (D<sub>2</sub>O).

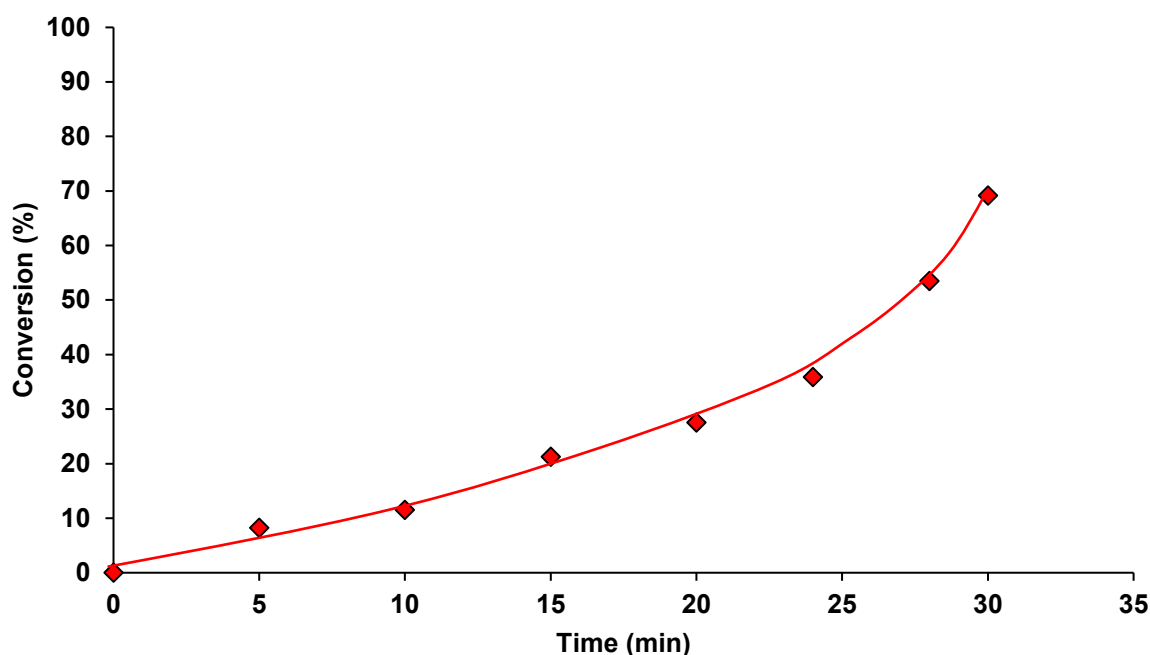


**Figure 3-5 Conversion of benzyl alcohol (♦) in 5 ml deuterium oxide using a AuPd/TiO<sub>2</sub> catalyst (20 mg, 1:1 mol), 2 bar (g) O<sub>2</sub>, 1000 rpm at 80 °C and 200 mg alcohol**

The results of this experiment can be seen in Figure 3-5 and it is clear from this graph that the reaction has indeed slowed down in the presence of heavy water. This effect is most pronounced at the beginning of the reaction where there appears to be an induction period on the graph. During the first 25 minutes, the rate of reaction is steady and conversion reaches ca. 40% compared to water, which was around 80% after the same amount of time. After 25 minutes, there appears to be a rate increase and conversion increases from 40% to just less than 80% in five minutes. This could suggest a change in reaction mechanism occurs after 25 minutes explaining the increase in the reaction rate. This may be caused by a change in the support structure, or reaction mechanism. Future work such as spectroscopic methods for surface species determination on the metal support could be carried out to determine the reason for this variation.

Previous research by Hutchings *et al.*<sup>9</sup> into benzyl alcohol oxidation has demonstrated two reaction pathways which display a large kinetic isotope effect (KIE) for the cleavage of the benzylic C-H(D) bond which is involved in the rate determining step. It was hypothesised that two principal scenarios were taking place, that (i) the KIE arises by transformation of the adsorbed benzyl alcohol into a reactive species on the catalyst surface by C-H bond cleavage, e.g.  $\text{PhCH}_2\text{O(H)-M/PhCH(OH)-M} + \text{H-M}$ , and (ii) rate limiting attack of adsorbed H-atoms or

active oxygen species directly on an adsorbed molecule of benzyl alcohol to abstract a benzylic H(D). This research proposed a new reaction mechanism which was different to what was previously accepted<sup>10</sup>.

The change was necessary to accommodate the new finding by Hutchings *et al.*, who demonstrated that a substantial proportion of PhCD<sub>3</sub> was formed, suggesting that on adsorption at the catalyst surface C-D bonds are broken and this in turn implies that dissociative chemisorption of benzyl alcohol is not wholly by O-H cleavage as suggested by Corma *et al.* as shown in Figure 3-6<sup>11</sup>.

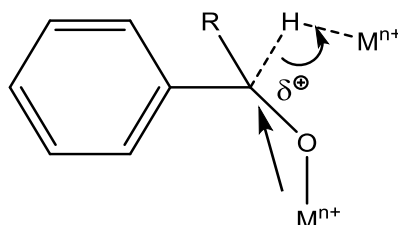


**Figure 3-6<sup>5</sup> Oxidation of benzyl alcohol with an Au catalyst as proposed by Corma *et al.*<sup>11</sup>**

It could be during this transition state that influence of the deuterated solvent is having an effect. The benzyl alcohol molecule will coordinate to the metal centre of the catalyst and undergo a metal hydride shift, the transition state will then give rise to the carbonyl product. If the deuterated water has adsorbed onto the surface, the benzyl alcohol will abstract the deuterium instead and suffer from a KIE that will slow down the reaction as can be seen again in Figure 3-5. The mass balance of the reaction remained high, suggesting some deuterated compounds were produced, but not in great quantities as these deuterated compounds would not be detected via the NMR methodology used in sample analysis.

One explanation as to why there were no deuterated products is due to the water activating the oxygen coverage of the catalyst to facilitate reaction<sup>12</sup>. As can be seen from Figure 3-7, water is adsorbing on the surface and reacting with the adsorbed oxygen species to create an activated oxygen compound that will react with the benzyl alcohol while the water is reformed. When D<sub>2</sub>O is used, the process must be slower due to the extra mass of the deuterium. The oxygen activation step should be slower due to KIE and would also explain why no products

<sup>5</sup> Copyright © 2008 WILEY-VCH Verlag GmbH & Co. KGaA, Weinheim, reproduced under license

were deuterated in this study as  $D_2O$  activates the oxygen and then reforms itself on the catalyst surface.

Hydrogen species activate oxygen,  
after it dissociates from  $H_2O$

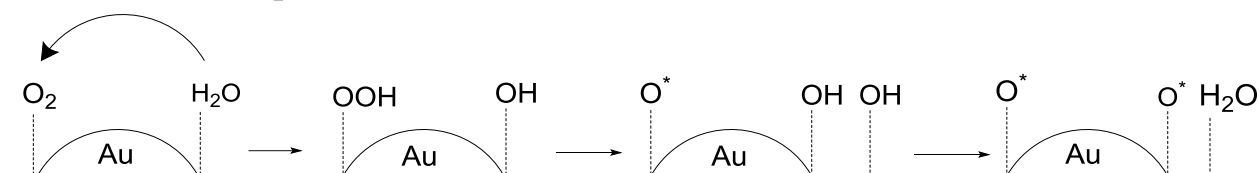


**Figure 3-7 Possible reaction mechanism for the activation of molecular oxygen by water on Au catalysts, the water is depicted as<sup>12</sup>**

Whilst the difference between water and deuterium oxide is interesting from an isotopic and mechanistic point of view, the effect of solvent was further investigated. The solvents chosen were toluene, methanol and benzene. These were chosen since they are organic solvents with good solubility of the starting material and resulting products. It was expected that conversion would be at least comparable to that of water since mass transport effects where water limits the contact time of the reactant with the catalyst may be mitigated by the improved solvation of compounds. This may not be the case and conversion was much lower than expected in all cases. Another parameter to be aware of would be oxygen solubility as this would potentially introduce mass transfer issues and would be an area to assess in future work.

For benzene, Figure 3-8, maximum conversion after 30 minutes was less than 10%, far lower than what was expected based on the water experiments. Another organic solvent was used, toluene, as demonstrated in Figure 3-9 it was also relatively poor at facilitating reaction.



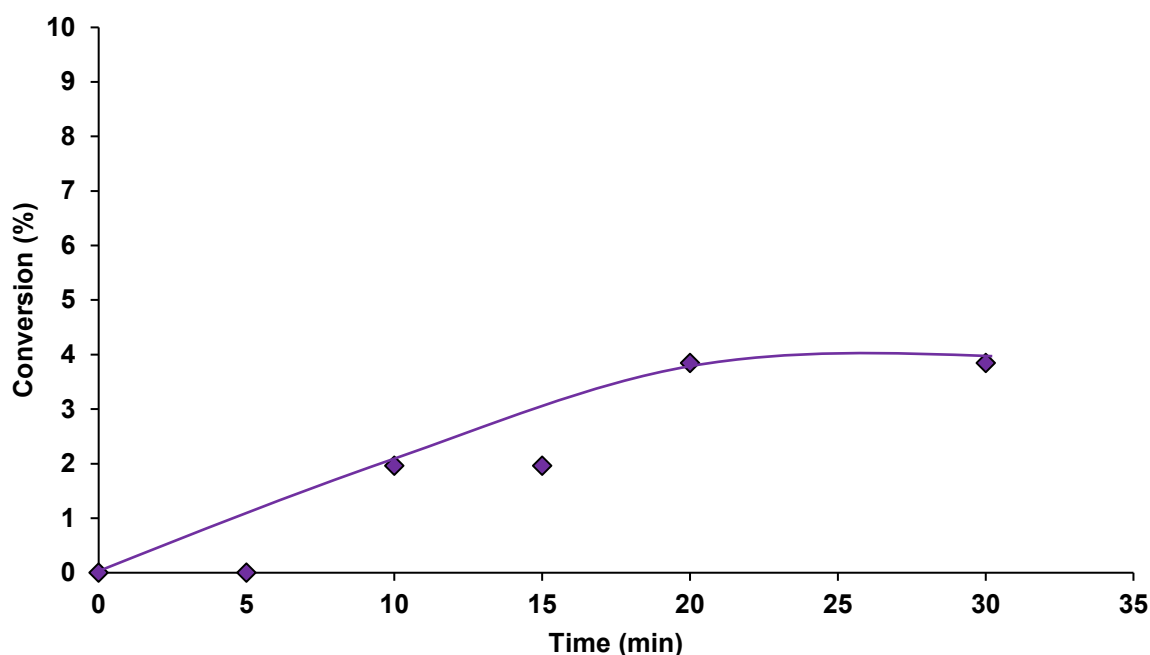


**Figure 3-8 Conversion of benzyl alcohol (◆) in 5 ml benzene using a AuPd/TiO<sub>2</sub> catalyst (20 mg, 1:1 mol), 2 bar (g) O<sub>2</sub>, 1000 rpm at 80 °C and 200 mg alcohol**

The only solvent able to achieve 10% conversion after 30 minutes was methanol, Figure 3-10. What is interesting is that even though methanol is also organic solvent, it is much more polar than toluene and benzene; it seems this polarity is needed in some form to facilitate reaction and that water seems ideally placed to provide this. Keresszegi *et al.* found in their work that in their system, water was formed as a co-product, and via ATR-IR concluded that water accumulated on the catalyst surface. This correlated positively with an increase in catalyst activity and they determined that this phenomenon was involved with the polarity of water and the alcohol substrate, benzyl alcohol<sup>13</sup>.

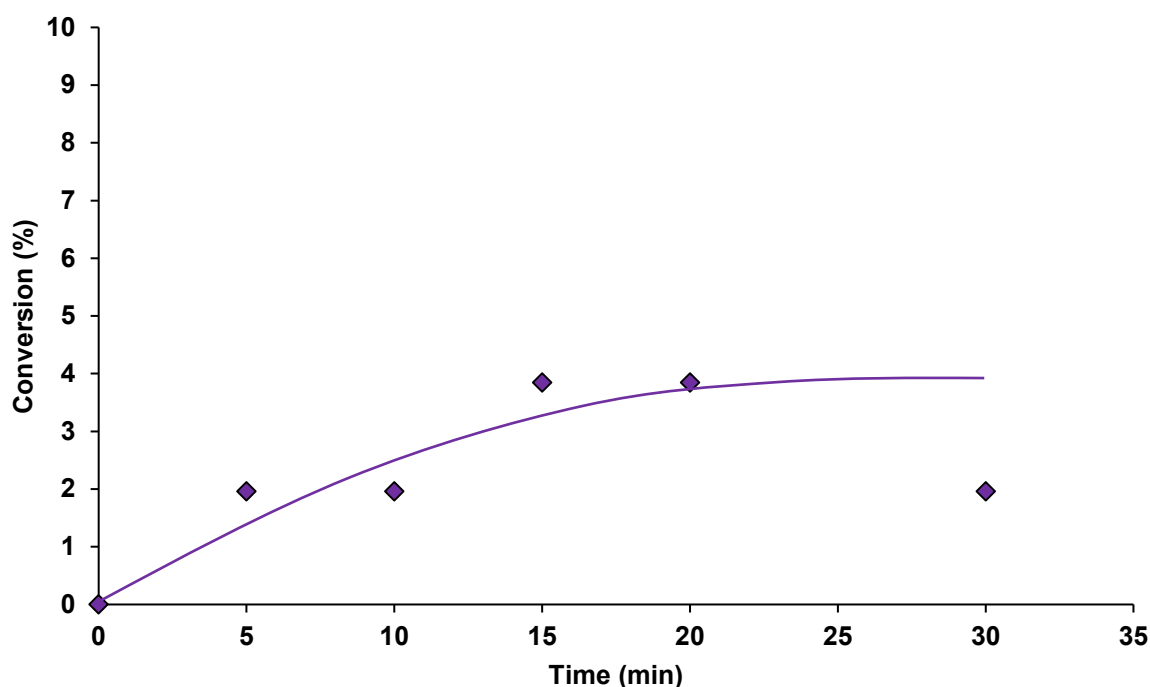


**Figure 3-9** Conversion of benzyl alcohol (◆) in 5 ml toluene using a AuPd/TiO<sub>2</sub> catalyst (20 mg, 1:1 mol), 2 bar (g) O<sub>2</sub>, 1000 rpm at 80 °C and 200 mg alcohol

Pasha *et al.*<sup>14</sup> observed rate of conversion of benzyl alcohol was fastest in acetone as well as polar solvents such as CH<sub>3</sub>CN, DMSO and DMF. Non-polar solvents such as benzene, toluene and petroleum ether did not have a rate comparable to that of the polar solvents and the reaction progressed much more slowly. Benzyl alcohol substitution was found to have minimal effect with regards to conversion to the corresponding aldehyde. Pasha *et al.*'s work used ultrasound and proposed an ionic pathway for the reaction's mechanism. Polar solvents can stabilise ionic transition states, the observed conversion rates in polar solvents would be greater than rates observed in non-polar solvents. This observation is in agreement with Mason's<sup>15</sup> review of sonochemistry in heterogeneous systems which stated reactions would progress via an ionic or radical pathway. Rahimi *et al.*<sup>16</sup> discovered in their system non-polar solvents were necessary for quick reactions between benzyl alcohol and the non-polar catalyst CuTPP, with o-xylene being the best solvent to use in this system.

As oxidation of benzyl alcohol to benzaldehyde was greater in water than toluene or benzene, this suggests benzyl alcohol oxidation is progressing with an ionic transition state which is being stabilised by the water present in the system.

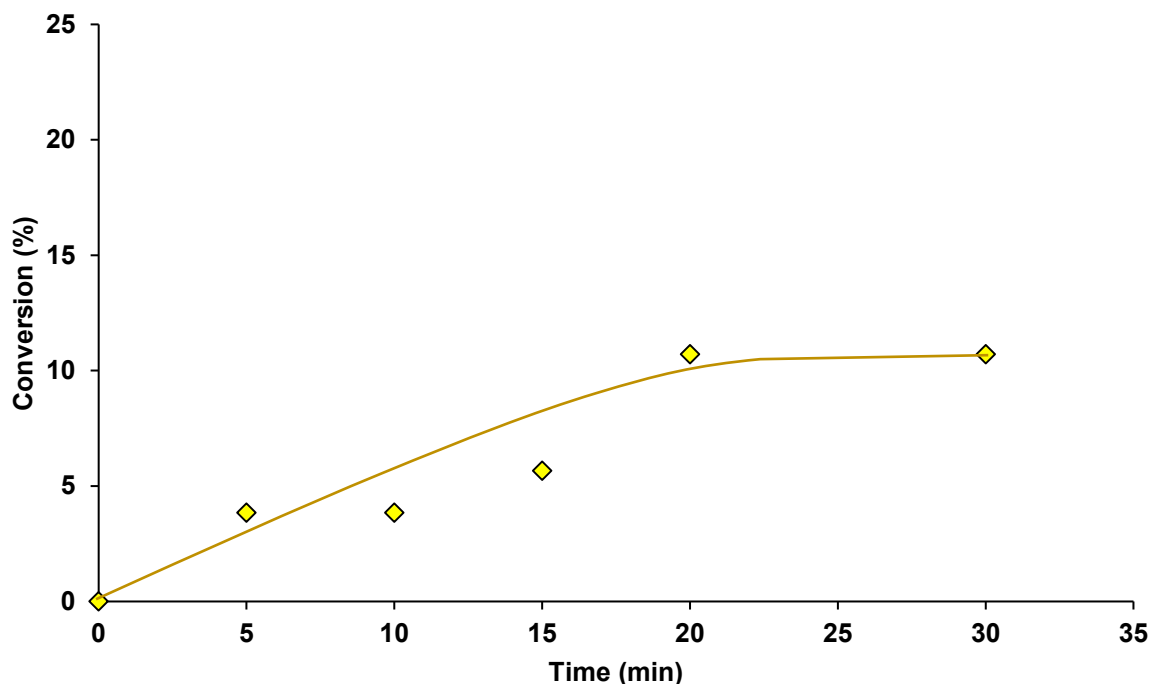


**Figure 3-10 Conversion of benzyl alcohol (◆) in 5 ml methanol using a AuPd/TiO<sub>2</sub> catalyst (20 mg, 1:1 mol), 2 bar (g) O<sub>2</sub>, 1000 rpm at 80 °C and 200 mg alcohol**

Simakov *et al.*<sup>17</sup> found whilst working with Au supported on MgO and Mg(OH)<sub>2</sub> that multiple oxidation products were possible when reacting benzyl alcohol with Au supported on MgO and Mg(OH)<sub>2</sub> catalysts, as shown in Figure 3-11. Compounds (b) and (c) are possible if benzaldehyde, (b), forms a hemiacetal and subsequently undergoes esterification with either benzyl alcohol or methanol, the solvent used in Simakov's system.

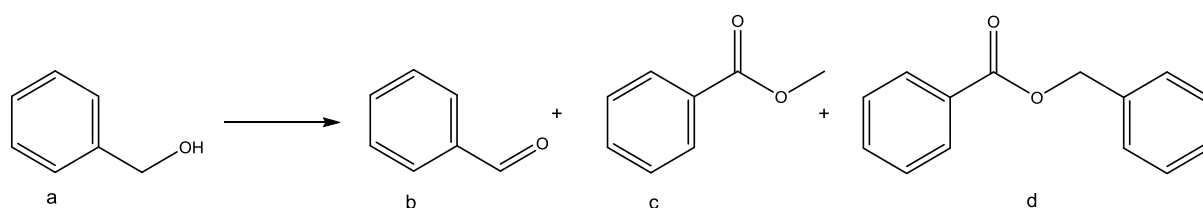


**Figure 3-11 Oxidation of benzyl alcohol (a) can give rise to the following products: benzaldehyde (b), methyl benzoate (c) and benzyl benzoate (d)<sup>17</sup>**

It is thought that the formation of the benzoate compounds occurs via the dehydrogenation of hemiacetals which are considered key intermediates to the reaction. Chaudhary *et al.*<sup>18</sup> found that when benzyl alcohol was oxidised under solvent free conditions, no benzoic acid was

detected but benzyl benzoate was observed. It was hypothesised that the reaction pathway involved either the generation of benzoic acid, which immediately reacted with benzyl alcohol over the gold catalyst to form benzyl benzoate, or that no benzoic acid was generated and it was in fact the benzyl alcohol and benzaldehyde forming the hemiacetal  $[\text{PhCH}(\text{OH})\text{OCH}_2\text{Ph}]$ .

Complicating the reaction of benzyl alcohol in toluene and benzene is the fact that these compounds can coordinate with the catalyst surface and may actively block active sites. Medlin *et al.*<sup>19</sup> found that on Pd(111) surfaces, the following reaction scheme was taking place:

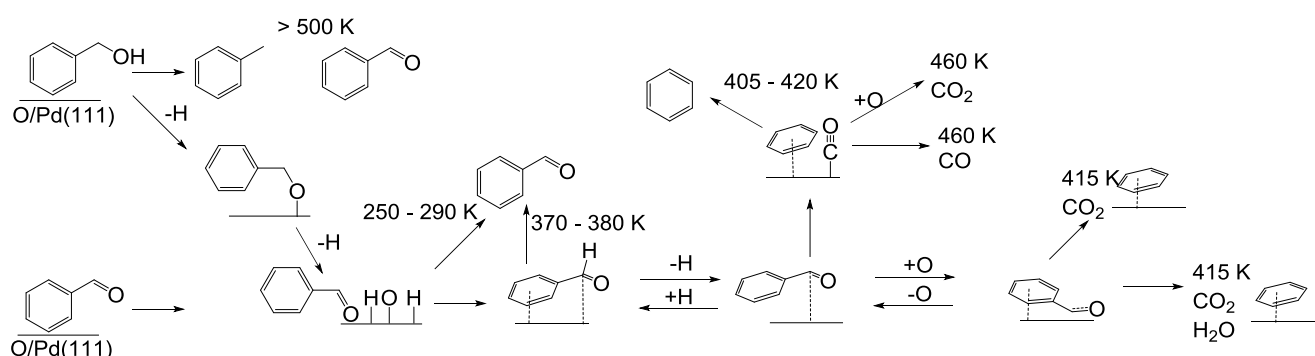


**Figure 3-12 Reaction scheme of benzyl alcohol over an oxygen pre-covered Pd(111) surface<sup>19</sup>**

Figure 3-12 shows how benzyl alcohol reacts on a Pd(111) surface. There is a mix of  $\eta^1$ -bonding whereby the lone pair on the oxygen is bonding to the metal surface. Benzyl alcohol forms an alkoxide intermediate before being converted to benzaldehyde. The benzaldehyde is weakly bound to the Pd(111) surface and is easily removed with heat treatment at around 90 °C. In the work presented in this thesis, the reaction temperature was 80 °C using AuPd alloyed catalysts. The Au within the catalyst could be lowering the thermal barrier to desorption from the catalyst surface. This lower thermal barrier may then facilitate increased conversion and selectivity observed in this study at lower temperatures compared to Medlin *et al.*<sup>19</sup>.

Furthermore, by abstracting hydrogen from benzaldehyde, there is a mix of  $\eta^1$  – bonding from the lone pair and  $\pi$  bonding from the benzene ring. This allows benzaldehyde to decarbonylate to benzene which is removed from the catalyst surface at temperatures around 147 °C and even with the hypothesis that Au is lowering the bonding energy of the adsorbed species, benzene could be getting stuck on the catalyst surface when formed during the reaction or

when used as a solvent. The same is true for toluene and it could be this reason why it and benzene act as such poor solvents for the conversion of benzyl alcohol. These solvents could also play a part in product inhibition and further studies involving toluene:water solvent mixes would need to be conducted to test this theory

Further research by Friend *et al.*<sup>20</sup> on Au(111) surfaces found that benzyl alcohol undergoes partial oxidation to form benzaldehyde, at high oxygen concentrations benzoic acid and CO<sub>2</sub> are formed whereas at lower O<sub>2</sub> coverage, benzyl benzoate is formed. As no benzoic acid or CO<sub>2</sub> was observed during oxidation of benzyl alcohol with supported Au catalysts, these products were likely not formed in great quantity. It is therefore assumed that oxygen, in O<sub>2</sub> as well as the activated O and OOH forms, coverage on the catalyst surface was such that the benzaldehyde formation pathway was maximised.

Further investigations utilizing benzene as a solvent were carried out, this time investigating what effect an increasing ratio of benzene to water had on the reaction (Figure 3-13). As can be seen from the results, there is a slight increase in conversion when the water:benzene ratio is high with regards to water. Conversion is highest at 70% with a water:benzene ratio of 1:4, however, as the ratio of benzene increases conversion begins to decrease. When the solvent is exclusively benzene, oxidation is completely inhibited. Selectivity at all solvent ratios remains high, above 95%, towards the desired aldehyde product.

As organic solvents demonstrated reduced catalyst activity compared to water, it further suggests water is playing a key role in the oxidation of benzyl alcohol to benzaldehyde. Benzene is unsuitable as a solvent for this reaction and may even be a poison if in high enough concentration. In low concentrations, benzene is enhancing the oxidation of benzyl alcohol whereas in higher concentrations, the conversion decreases.

In all cases, the ratio of benzene to catalyst is quite high and whilst poisons generally only need to be present in small quantities, the effect of the presence of benzene is phenomenologically appearing to deactivate the catalyst just like a poison<sup>21</sup>. Further research is needed to ascertain the effect benzene is having on the catalytic system.

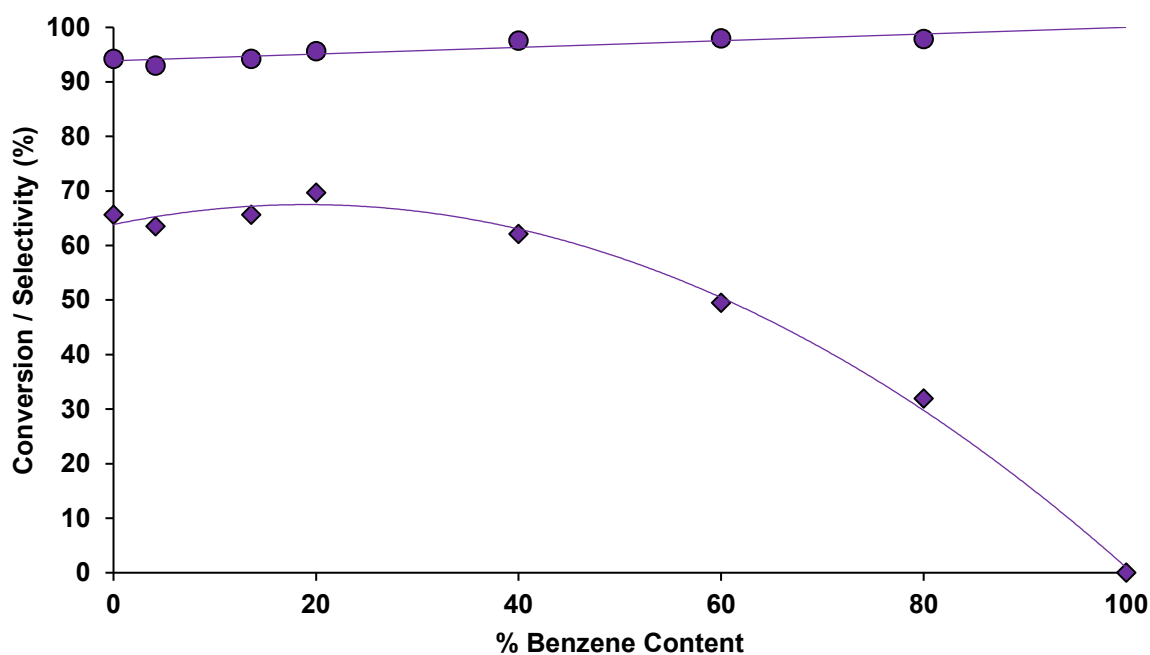


Figure 3-13 Conversion of benzyl alcohol (◆) and selectivity (●) in 5 ml benzene:water using a AuPd/TiO<sub>2</sub> catalyst (20 mg, 1:1 mol), 2 bar (g) O<sub>2</sub>, 1000 rpm at 80 °C and 200 mg alcohol for 30 minutes

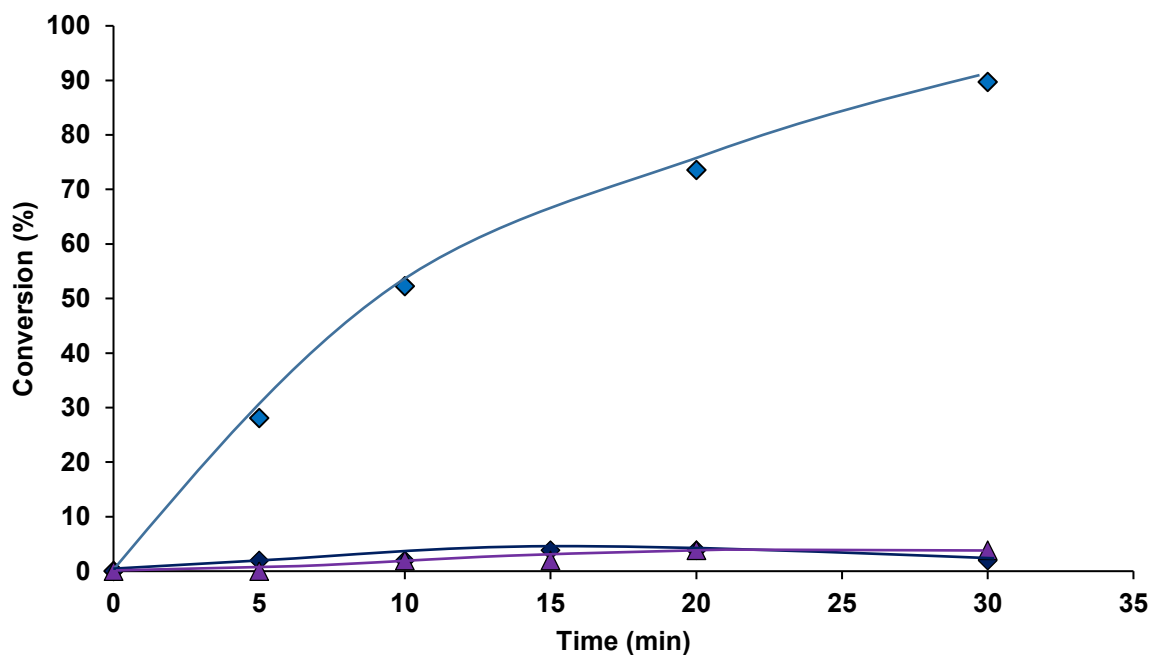
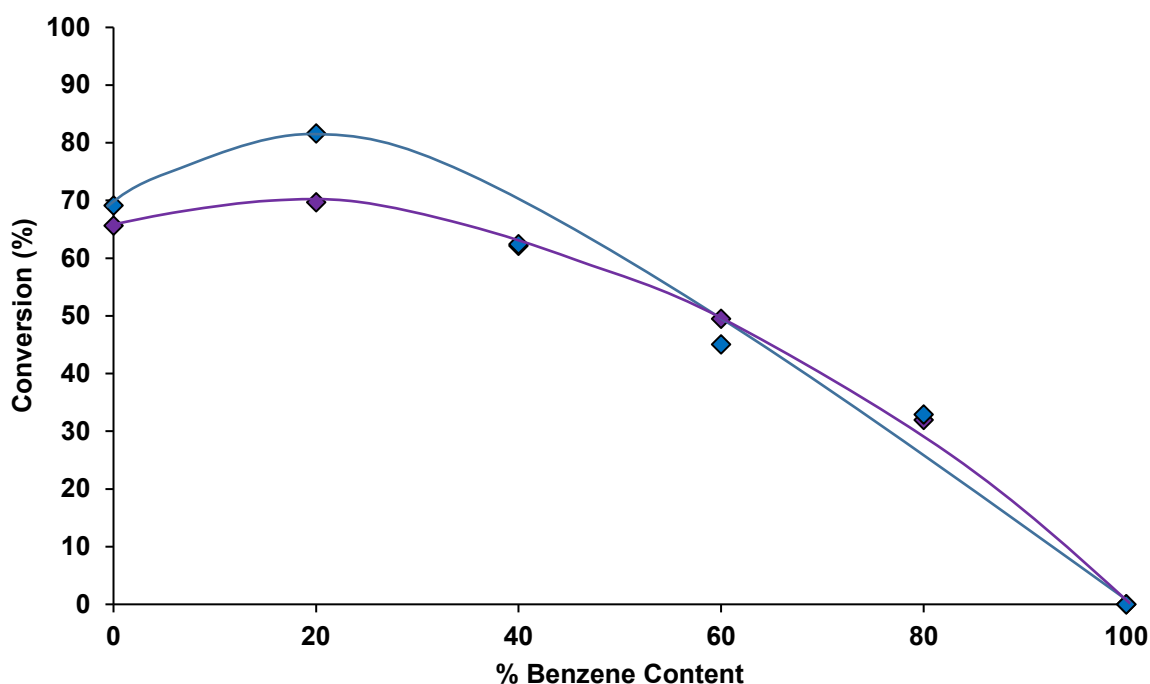


Figure 3-14 Conversion of benzyl alcohol in 5 ml solvent (water(◆)), (toluene(◆)), (benzene(◆)) using a AuPd/MgO catalyst (20 mg, 1:1 mol), 2 bar (g) O<sub>2</sub>, 1000 rpm at 80 °C and 200 mg alcohol

Figure 3-14 shows the results for the oxidation of benzyl alcohol in a variety of solvents whilst using MgO as the Au:Pd catalyst support. It is evident from this graph that water has a large effect on the oxidation of benzyl alcohol, promoting the reaction when compared to the organic solvents used which show very little activity which is analogous to the trend observed for the TiO<sub>2</sub> supported Au:Pd catalysts.

Oxygen solubility in benzene is less than that of water so one hypothesis was that increasing the benzene ratio was inhibiting the number of O<sub>2</sub> molecules that were reaching the active sites. An experiment was carried out utilising different pressures to assess if oxygen solubility was indeed a factor in reaction. The results of this experiment can be seen in Figure 3-15.

As can be seen in Figure 3-15 below, there was no significant change in conversion when the reaction was carried out at 3 bar (g) and 2 bar (g) suggesting oxygen solubility is not a factor in the rate determining step and mass transport issues were mitigated, potentially by the 1000 rpm speed of the stirrer bars. This leads further credence to the theory that aromatic solvents are inhibitory factors in the oxidation of benzyl alcohol. With the increased pressure, lower selectivity would have been anticipated based on work by Friend *et al.*<sup>20</sup> demonstrating cross coupling being possible. This was not seen however, suggesting that either the oxygen concentration on the surface of the catalyst was not great enough or that this pathway was inhibited.



**Figure 3-15** Conversion of benzyl alcohol at 2 bar (g) O<sub>2</sub> (◆) and 3 bar (g) O<sub>2</sub> (◆) in 5 ml benzene using a AuPd/TiO<sub>2</sub> catalyst (20 mg, 1:1 mol), 1000 rpm at 80 °C and 200 mg alcohol for 30 minutes

In conclusion, water plays a key role in the oxidation of benzyl alcohol, increasing conversion after 30 minutes when compared to that of organic solvents such as toluene and benzene which may poison the catalyst by having a large thermal barrier to desorption. There also appears to be no mass transport limitations due to the different O<sub>2</sub> solubility in benzene and water but further reactions of varying stirrer speed are needed to confirm the eradication of mass transport effects.

### 3.3.2. Effect of AuPd Ratio

The ratio of Au to Pd was investigated to see if this influenced the oxidation reaction. It is known that there is a synergistic effect between the Au and Pd whereby the Au promotes the oxidising ability of the palladium<sup>3</sup>. The AuPd ratio was investigated to ascertain if there is an optimal Au:Pd ratio for this synergy as most previous studies have only used a 1:1 molar ratio AuPd catalyst when prepared via sol immobilisation.



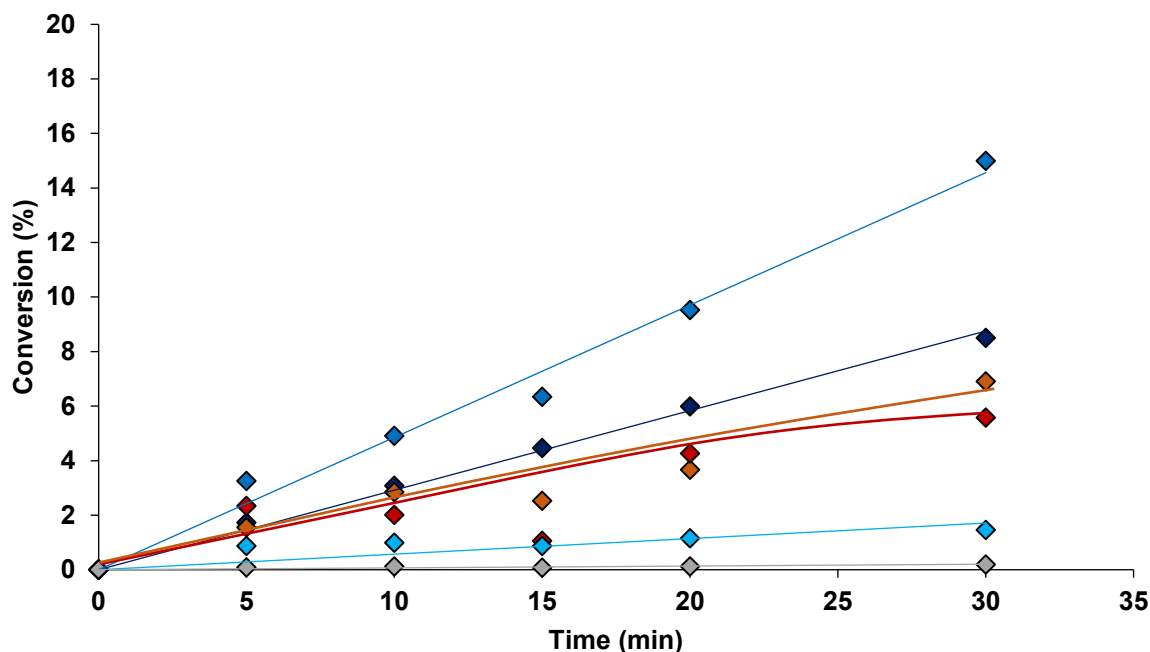


**Figure 3-16** Conversion of benzyl alcohol using a AuPd/TiO<sub>2</sub> catalyst (20 mg), 2 bar (g) O<sub>2</sub>, 1000 rpm at 80 °C and 1 g alcohol with Au:Pd ratios of 1:1 (◆), 1:2 (◆), 1:9 (◆), 0.5:9.5 (◆), 1:0 (◆), 9:1 (◆), 9.5:0.5 (◆)

As can be seen from Figure 3-16, changing the Au:Pd ratio influences the oxidation of benzyl alcohol. The most active catalyst for benzyl alcohol oxidation is the 1:2 Au to Pd ratio which effects a conversion of roughly 15% after 30 minutes whereas the standard 1:1 ratio catalyst has a conversion of 10% after 30 minutes. The 1:9 and 0.5:9.5 have similar conversion to the 1:1 catalyst, with the palladium rich catalyst being slightly lower in activity than the previous two. The least active catalysts are the gold rich catalysts which is in keeping with the idea that monometallic gold catalysts are not very active for oxidation systems such as the one used in this study<sup>22</sup>. Monometallic gold catalysts are able to catalyse certain systems very well, such as low temperature CO oxidation<sup>23</sup> and so must not be discounted prematurely.

This trend is somewhat supported by previous work by Enache *et al.*<sup>22</sup> who found Au-rich catalysts were less active than their Pd-rich equivalents. The reaction conditions in this work were much harsher than reaction conditions employed in this thesis as well as utilising a solvent in the reaction, the high TOF (h<sup>-1</sup>) values for the Pd rich catalysts may be explained by this demanding environment, whereas in this work, the synergistic effect is much more important at these reaction conditions.

The reason as to why metal ratio affects oxidation has not been studied in this work.

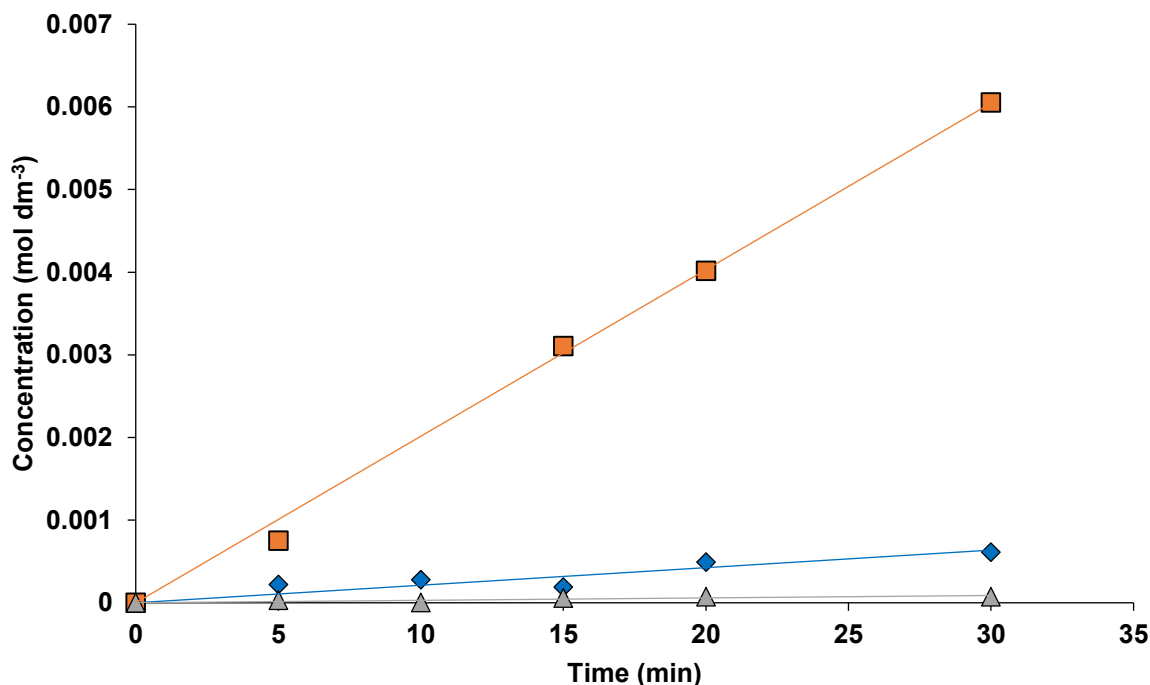


**Figure 3-17** Conversion of benzyl alcohol (◆), 4-methoxybenzyl alcohol (■), cinnamyl alcohol (◆) and 4-Fluorobenzyl alcohol (△) in 5 ml water using a AuPd/TiO<sub>2</sub> catalyst (20 mg, 0.5:9.5 mol), 2 bar (g) O<sub>2</sub>, 1000 rpm at 80 °C and 200 mg alcohol

Figure 3-17 shows that 4-methoxybenzyl alcohol is the most active substrate with the 0.5:9.5 Au: Pd catalyst, and the reasons as to why 4-methoxy benzyl alcohol is readily oxidised by supported AuPd catalysts is explored in Chapter 4 using the Hammett methodology. In the above case the conversion by catalyst is generally low apart from 4-methoxybenzyl alcohol, which is readily oxidised compared to benzyl alcohol. Interestingly, cinnamyl alcohol, which is vinylogous to benzyl alcohol, is less active but only marginally so. This could be due to the extra bulk of the molecule preventing benzyl alcohol reaching the catalyst active sites, preventing the molecule from reacting with the catalyst. However, this extra bulk is spatially distant to the -OH group and so electronic effects may also be inhibiting the reaction rate. Cinnamyl alcohol's -OH group is influenced by the alcohol's benzene ring as it's a conjugated system but the C=C bond may affect the stability of reaction intermediaries such that it is less readily oxidised compared with its non-conjugated analogue, benzyl alcohol. 4-Fluorobenzyl alcohol is the least active of the species and displays no significant activity with this catalyst.

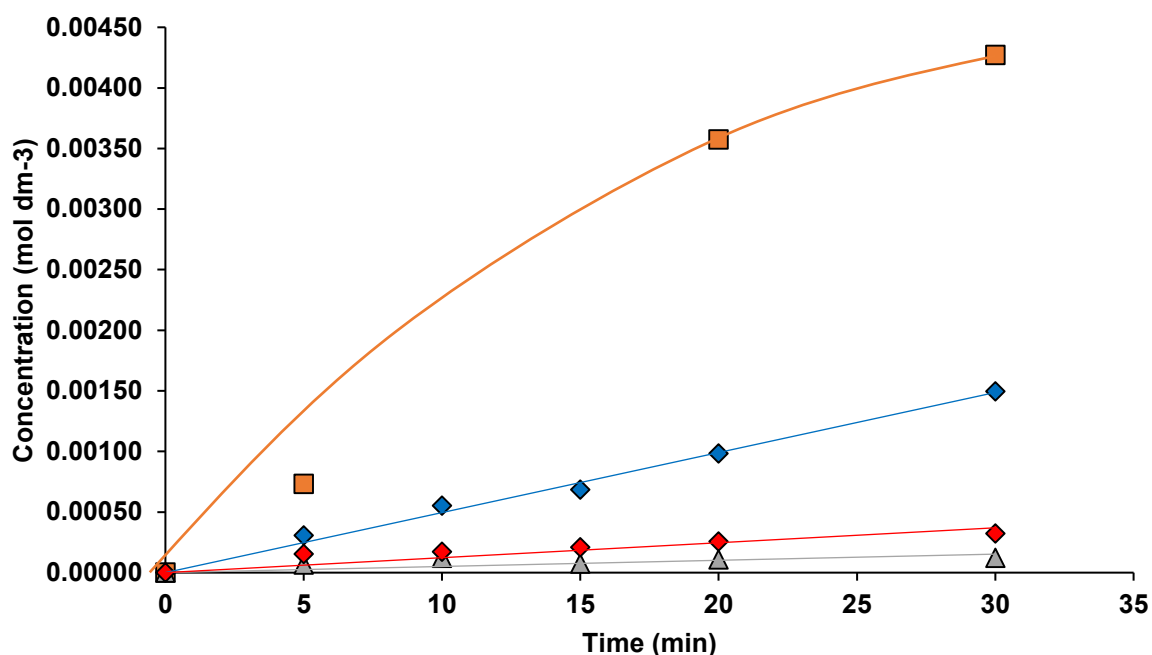
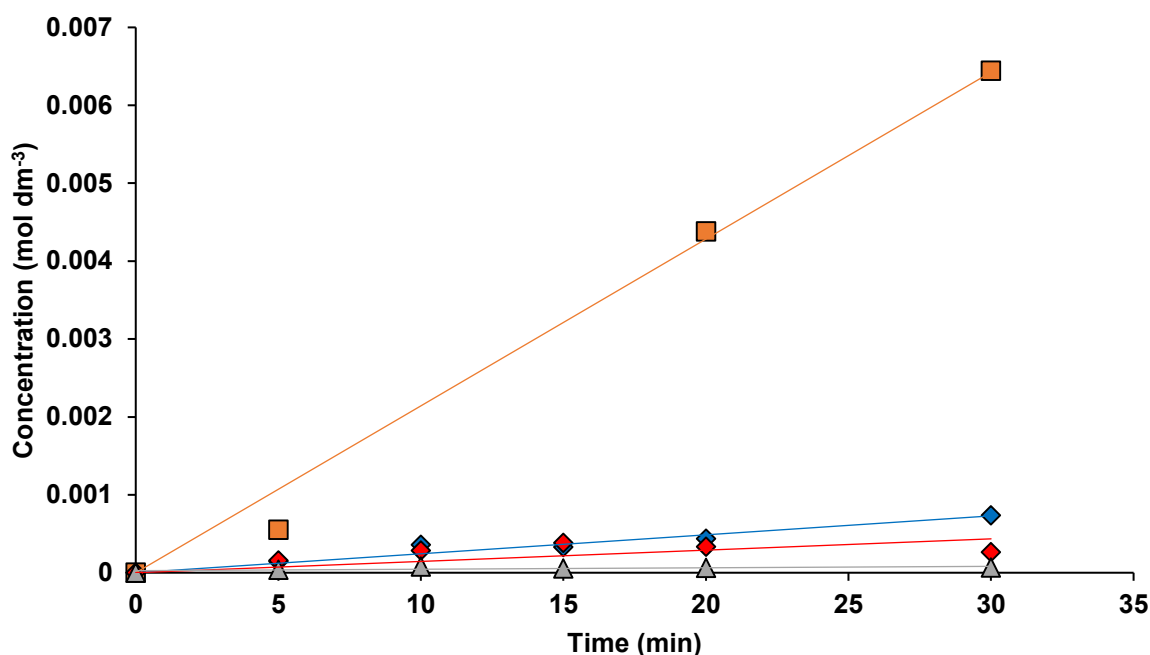


Figure 3-18 Conversion of benzyl alcohol (◆), 4-methoxybenzyl alcohol (■), cinnamyl alcohol (◆) and 4-Fluorobenzyl alcohol (△) in 5 ml water using a AuPd/TiO<sub>2</sub> catalyst (20 mg, 1:2 mol), 2 bar (g) O<sub>2</sub>, 1000 rpm at 80 °C and 200 mg alcohol

Figure 3-18 shows that for the 1:2 Au:Pd ratio, the activity of the catalyst is higher than the catalyst in Figure 3-17 with respect to benzyl alcohol but only slightly so. The activity for 4-methoxybenzyl alcohol has dropped suggesting that this is not the most optimal metal ratio for the oxidation of this molecule and a higher ratio of Pd to Au is needed for the synergistic effect to be at its greatest. It seems however, that this ratio is beneficial to benzyl alcohol oxidation. Cinnamyl alcohol has remained relatively inactive, again due to the possibility of steric effects blocking its ability to react with the catalysts active sites. 4-fluorobenzyl alcohol is still unreactive with this catalyst.



**Figure 3-19** Conversion of benzyl alcohol (◆), 4-methoxybenzyl alcohol (■), cinnamyl alcohol (◆) and 4-Fluorobenzyl alcohol (△) in 5 ml water using a AuPd/MgO catalyst (20 mg, 0.5:9.5 mol), 2 bar (g) O<sub>2</sub>, 1000 rpm at 80 °C and 200 mg alcohol

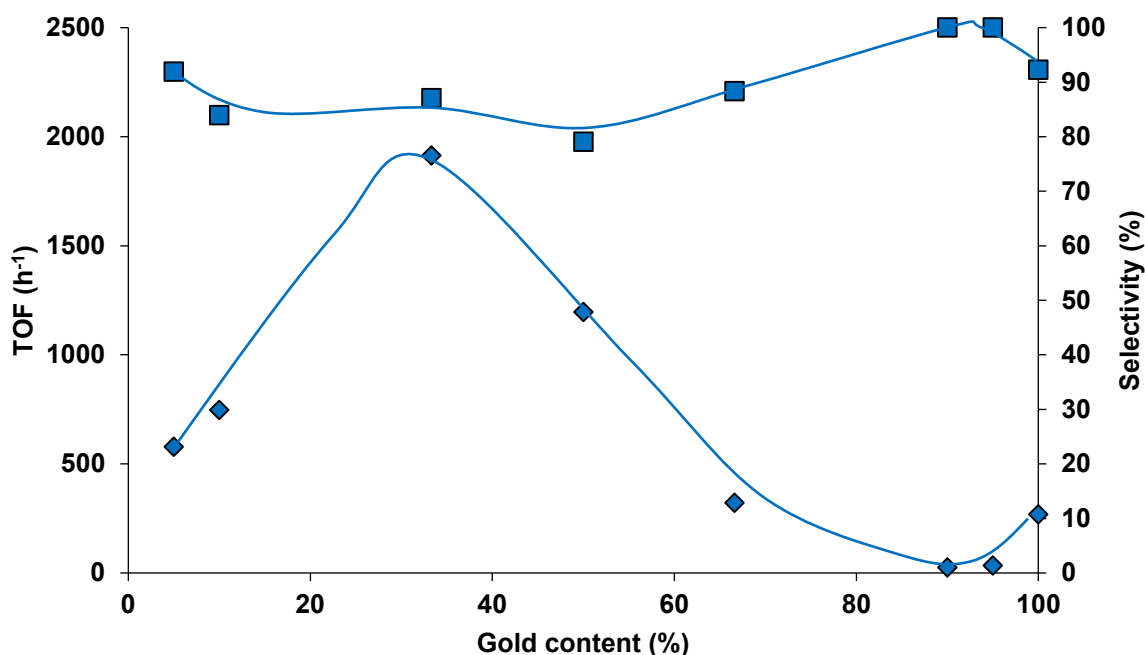
Figure 3-19 shows a 0.5:9.5 Au:Pd metal ratio and its reaction profile over the reaction timescale of 30 minutes. An Au:Pd ratio of 0.5:9.5 led to the most active catalyst observed for the oxidation of 4-methoxybenzyl alcohol, but this catalyst was not active for the remaining alcohols. What these results show is that in all cases, 4-methoxybenzyl alcohol is highly active in all ratios, the conversion varying only slightly between them. This suggests that the methoxy group is promoting the reaction more than the electronic effects of the Au:Pd catalysts, which are altered when the metal ratio is changed.

The ratio of 1:2 Au:Pd was the most active for the standard benzyl alcohol oxidation reaction, the synergistic effect between the Au and Pd is not at its greatest when the Au and Pd are equimolar within the catalyst. Au needs only to be a minor constituent of the catalyst for the promotion effect to be observed.

4-Fluorobenzyl alcohol was barely active with the AuPd catalyst with an AuPd ratio of 0.5:9.5 on TiO<sub>2</sub>, and the AuPd ratios 1:2 and 0.5:9.5 on MgO. This suggests the *para*-fluoro group was inhibiting the reaction when Au is a minor constituent of an AuPd catalyst. As we will see in chapter 4, a unimolar AuPd catalyst supported on MgO has a TOF (h<sup>-1</sup>) for 4-fluorobenzyl

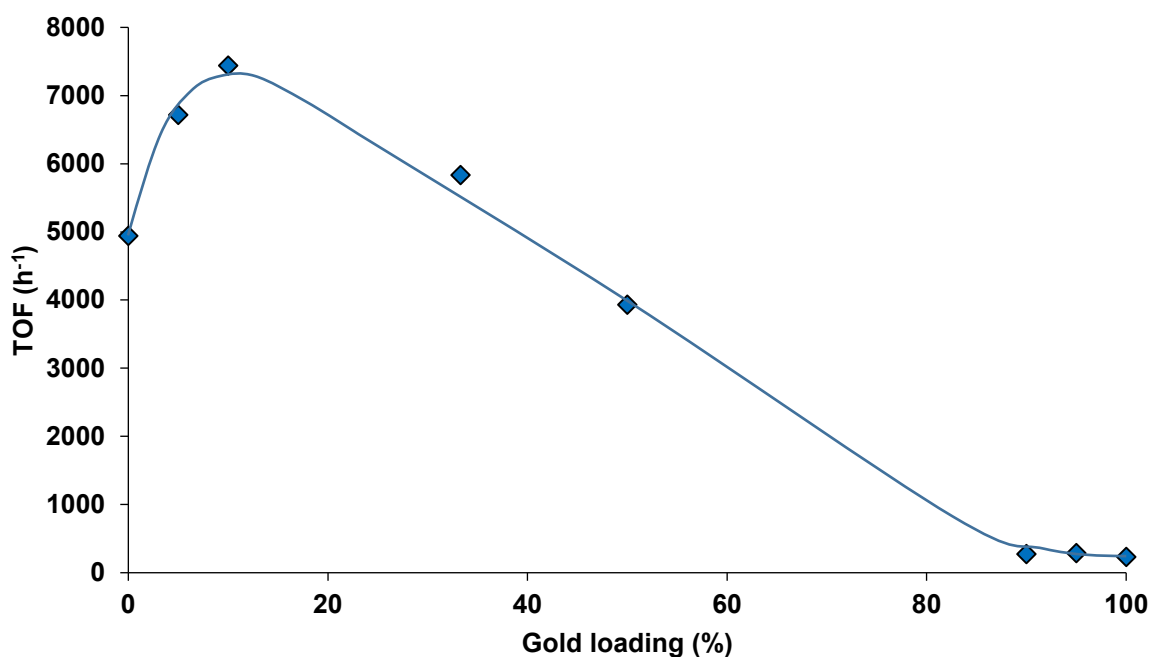
alcohol comparable to benzyl alcohol in the same system. When the support is changed to  $\text{TiO}_2$  whilst keeping the AuPd ratio unimolar, 4-fluorobenzyl alcohol has a very small TOF ( $\text{h}^{-1}$ ) value.

Examining the turn over frequency for the catalysts with each compound allowed a better overall picture to be elucidated on the effect of molar metal ratio on the oxidation of certain alcohols.



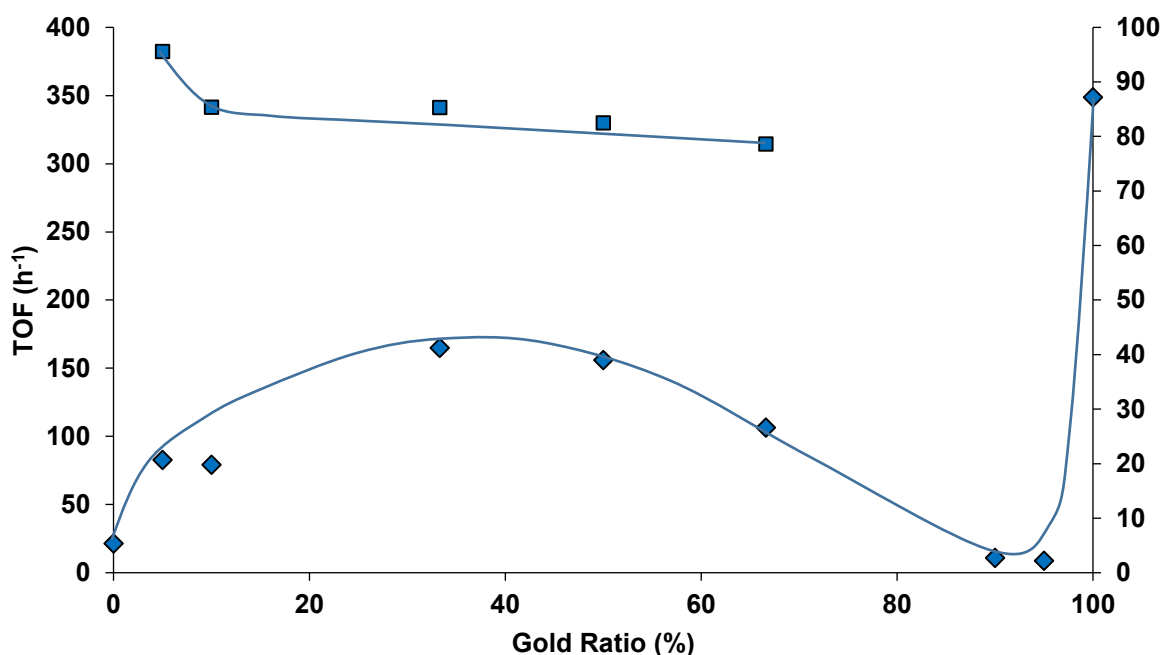
**Figure 3-20** Effect of increasing gold content on the TOF ( $\text{h}^{-1}$ ) (◆) and selectivity (■) of an AuPd/ $\text{TiO}_2$  catalyst reacting with benzyl alcohol, 2 bar (g)  $\text{O}_2$ , 1000 rpm at 80 °C and 1 g alcohol. As gold content increases, palladium content decreases whilst keeping the total number of moles of AuPd the same.

Figure 3-20 shows that the promotional properties of Au are at their maximum when the catalyst is 1/3 Au and 2/3 Pd for benzyl alcohol. The gold loading is relative to Pd, with 0% Au being Pd/ $\text{TiO}_2$  and 100% Au being Au/ $\text{TiO}_2$ . When the catalyst is all Pd, there is very little activity suggesting gold is indeed needed to achieve high activity in oxidation reactions, even though Pd is known as a good oxidation catalyst, being used in several systems<sup>24</sup>. Selectivity for the catalysts remained high through all ratios suggesting the reaction pathway is unchanged with varying Au:Pd but that the pathway is promoted when Au is present. When the catalyst is 100% gold there is little activity in the oxidation of benzyl alcohol.



**Figure 3-21** Effect of gold ratio on the TOF (h<sup>-1</sup>) (◆) and selectivity (■) of an AuPd/TiO<sub>2</sub> catalyst reacting with 4-methoxybenzyl alcohol, 2 bar (g) O<sub>2</sub>, 1000 rpm at 80 °C and 1 g alcohol.

Similarly, Figure 3-21 shows the activity of a range of catalysts with varying gold loading on TiO<sub>2</sub>, relative to Pd, with Pd/TiO<sub>2</sub> being 0% gold loading and Au/TiO<sub>2</sub> being 100% gold loading. A catalyst comprising only of Pd has a high activity but this activity can be promoted by the addition of small amounts of Au into the catalytic system. In this case, the highest activity was recorded when the catalyst contained around 10% gold with additional gold loading not having as great an activity suggesting that the gold is inhibiting reaction with increasing presence. When the catalyst was 100% Au there was little activity for oxidation, again showing that Au is only effective in small quantities in the catalyst. In all cases, selectivity towards the desired aldehyde product was >95% suggesting a similar reaction pathway for the catalysts was in effect but the electronics of the catalyst played an important part in promoting the reaction.



**Figure 3-22** Effect of gold ratio on the TOF ( $\text{h}^{-1}$ ) (◆) and selectivity (■) of an AuPd/TiO<sub>2</sub> catalyst reacting with 4-fluorobenzyl alcohol, 2 bar (g) O<sub>2</sub>, 1000 rpm at 80 °C and 1 g alcohol

Finally, Figure 3-22 shows the activity of the catalysts with 4-fluorobenzyl alcohol. In all cases, TOF ( $\text{h}^{-1}$ ) was  $< 200 \text{ h}^{-1}$  and so the catalysts were not very active for this system. It did however display the same trend as the other catalysts with the promotion effect observed with the highest activity seen with the 1:2 Au: Pd catalyst but this was only marginally more active than the standard 1:1 catalyst. Selectivity was  $> 80\%$  for all catalysts with this system producing up to 20% 4-fluorobenzoic acid, much more than any other system. Whilst activity was low, it seemed this system could over-oxidise the desired aldehyde product to the unwanted acid product.

### 3.4. Summary

In this chapter, the oxidation of benzyl alcohol has been discussed and how the effects of solvent and AuPd ratio affects the oxidation and selectivity of this reaction. Previous work has mostly been carried out under solvent free conditions<sup>3, 25, 26</sup> but it is now clear to see that the presence of water has a promoting effect on this reaction, Figure 3-4. It was also observed that organic solvents such as benzene, toluene and methanol could influence the reaction but in these instances, the affect was an inhibitory one, rather than a promotion one. This would

suggest that water has a unique role to play in benzyl alcohol oxidation and a possible mechanism for this was proposed in Figure 3-7. Selectivity was high to the desired benzaldehyde product in all cases and a reason for this was proposed in Figure 3-12 whereby benzene and toluene derivatives became “stuck” on the catalyst surface. Consequently, the benzene and toluene derivatives on the catalyst surface may inhibit the oxidation pathways in the system, inhibiting benzyl alcohol oxidation when in excess and preventing over oxidation when present in trace amounts.

AuPd ratio was investigated and it was found that Au rich catalysts were not as active for the oxidation of benzyl alcohol compared to the catalysts with 1:1 and 1:2 AuPd ratio. XPS and TEM analysis of these catalysts suggest that the nanoparticles were alloying and not displaying core shell morphology as some other catalyst preparation methods can produce<sup>27</sup>.

Having investigated reaction parameters such as solvent and metal ratio of the Au and Pd nanoparticles, attention was turned to investigating if substitution on the benzene ring in benzyl alcohol affected the rate of oxidation of these substituted benzyl alcohols over supported AuPd catalysts supported on metal oxides. If AuPd catalysts can readily oxidise substituted benzyl alcohols at the same, or similar, rate to unsubstituted benzyl alcohol with high selectivity, an alternative route to substituted benzaldehydes may be viable which would be advantageous to synthetic chemists.



## Chapter 3 References

1. Pillai UR, Sahle-Demessie E. Oxidation of alcohols over  $\text{Fe}^{3+}$ /montmorillonite-K10 using hydrogen peroxide. *Applied Catalysis A: General* 2003, **245**(1): 103-109.
2. Pagliaro M, Campestrini S, Ciriminna R. Ru-based oxidation catalysis. *Chemical Society Reviews* 2005, **34**(10): 837-845.
3. Enache DI, Edwards JK, Landon P, Solsona-Espriu B, Carley AF, Herzing AA, Watanabe M, Kiely CJ, Knight DW, Hutchings GJ. Solvent-Free Oxidation of Primary Alcohols to Aldehydes Using Au-Pd/TiO<sub>2</sub> Catalysts. *Science* 2006, **311**(5759): 362-365.
4. Pritchard J, Kesavan L, Piccinini M, He Q, Tiruvalam R, Dimitratos N, Lopez-Sanchez JA, Carley AF, Edwards JK, Kiely CJ, Hutchings GJ. Direct Synthesis of Hydrogen Peroxide and Benzyl Alcohol Oxidation Using Au-Pd Catalysts Prepared by Sol Immobilization. *Langmuir* 2010.
5. Dimitratos N, Lopez-sanchez J, Morgan D, Carley A, Prati L, Hutchings G. Solvent free liquid phase oxidation of benzyl alcohol using Au supported catalysts prepared using a sol immobilization technique. *Catalysis Today* 2007, **122**(3-4): 317-324.
6. Dimitratos N, Lopez-Sanchez JA, Morgan D, Carley AF, Tiruvalam R, Kiely CJ, Bethell D, Hutchings GJ. Solvent-free oxidation of benzyl alcohol using Au-Pd catalysts prepared by sol immobilisation. *Phys Chem Chem Phys* 2009, **11**(25): 5142-5153.
7. Villa A, Wang D, Su DS, Prati L. Gold Sols as Catalysts for Glycerol Oxidation: The Role of Stabilizer. *ChemCatChem* 2009, **1**(4): 510-514.
8. Lopez-Sanchez JA, Dimitratos N, Hammond C, Brett GL, Kesavan L, White S, Miedziak P, Tiruvalam R, Jenkins RL, Carley AF, Knight D, Kiely CJ, Hutchings GJ. Facile removal of stabilizer-ligands from supported gold nanoparticles. *Nat Chem* 2011, **3**(7): 551-556.

9. Meenakshisundaram S, Nowicka E, Miedziak PJ, Brett GL, Jenkins RL, Dimitratos N, Taylor SH, Knight DW, Bethell D, Hutchings GJ. Oxidation of alcohols using supported gold and gold-palladium nanoparticles. *Faraday Discussions* 2010, **145**: 341-356.
10. Lopez-Sanchez JA, Dimitratos N, Miedziak P, Ntainjua E, Edwards JK, Morgan D, Carley AF, Tiruvalam R, Kiely CJ, Hutchings GJ. Au-Pd supported nanocrystals prepared by a sol immobilisation technique as catalysts for selective chemical synthesis. *Physical Chemistry Chemical Physics* 2008, **10**(14): 1921-1930.
11. Abad A, Corma A, García H. Catalyst Parameters Determining Activity and Selectivity of Supported Gold Nanoparticles for the Aerobic Oxidation of Alcohols: The Molecular Reaction Mechanism. *Chemistry – A European Journal* 2008, **14**(1): 212-222.
12. Yang X, Wang X, Liang C, Su W, Wang C, Feng Z, Li C, Qiu J. Aerobic oxidation of alcohols over Au/TiO<sub>2</sub>: An insight on the promotion effect of water on the catalytic activity of Au/TiO<sub>2</sub>. *Catalysis Communications* 2008, **9**(13): 2278-2281.
13. Keresszegi C, Ferri D, Mallat T, Baiker A. On the role of CO formation during the aerobic oxidation of alcohols on Pd/Al<sub>2</sub>O<sub>3</sub>: an in situ attenuated total reflection infrared study. *Journal of Catalysis* 2005, **234**(1): 64-75.
14. Naik R, Nizam A, Siddekha A, Pasha MA. An efficient sonochemical oxidation of benzyl alcohols into benzaldehydes by FeCl<sub>3</sub>/HNO<sub>3</sub> in acetone. *Ultrasonics Sonochemistry* 2011, **18**(5): 1124-1127.
15. Mason TJ. Ultrasound in synthetic organic chemistry. *Chemical Society Reviews* 1997, **26**(6): 443-451.
16. Rahimi R, Gholamrezapor E, Naimi-Jamal MR. Oxidation of benzyl alcohols to the corresponding carbonyl compounds catalyzed by copper (II) meso-tetra phenyl porphyrin as cytochrome P-450 model reaction. *Inorganic Chemistry Communications* 2011, **14**(10): 1561-1568.

17. Estrada M, Costa VV, Beloshapkin S, Fuentes S, Stoyanov E, Gusevskaya EV, Simakov A. Aerobic oxidation of benzyl alcohol in methanol solutions over Au nanoparticles:  $\text{Mg}(\text{OH})_2$  vs  $\text{MgO}$  as the support. *Applied Catalysis A: General* 2014, **473**(0): 96-103.
18. Choudhary V, Dumbre D. Supported Nano-Gold Catalysts for Epoxidation of Styrene and Oxidation of Benzyl Alcohol to Benzaldehyde. *Topics in Catalysis* 2009, **52**(12): 1677-1687.
19. Williams RM, Medlin JW. Benzyl Alcohol Oxidation on Pd(111): Aromatic Binding Effects on Alcohol Reactivity. *Langmuir* 2014, **30**(16): 4642-4653.
20. Rodríguez-Reyes JCF, Friend CM, Madix RJ. Origin of the selectivity in the gold-mediated oxidation of benzyl alcohol. *Surface Science* 2012, **606**(15–16): 1129-1134.
21. Choudhary VR, Samanta C. Role of chloride or bromide anions and protons for promoting the selective oxidation of  $\text{H}_2$  by  $\text{O}_2$  to  $\text{H}_2\text{O}_2$  over supported Pd catalysts in an aqueous medium. *Journal of Catalysis* 2006, **238**(1): 28-38.
22. Enache DI, Barker D, Edwards JK, Taylor SH, Knight DW, Carley AF, Hutchings GJ. Solvent-free oxidation of benzyl alcohol using titania-supported gold–palladium catalysts: Effect of Au–Pd ratio on catalytic performance. *Catalysis Today* 2007, **122**(3–4): 407-411.
23. Taketoshi A, Haruta M. Size- and Structure-specificity in Catalysis by Gold Clusters. *Chemistry Letters* 2014, **43**(4): 380-387.
24. Yan Y, Chen Y, Jia X, Yang Y. Palladium nanoparticles supported on organosilane-functionalized carbon nanotube for solvent-free aerobic oxidation of benzyl alcohol. *Applied Catalysis B: Environmental* 2014, **156–157**(0): 385-397.

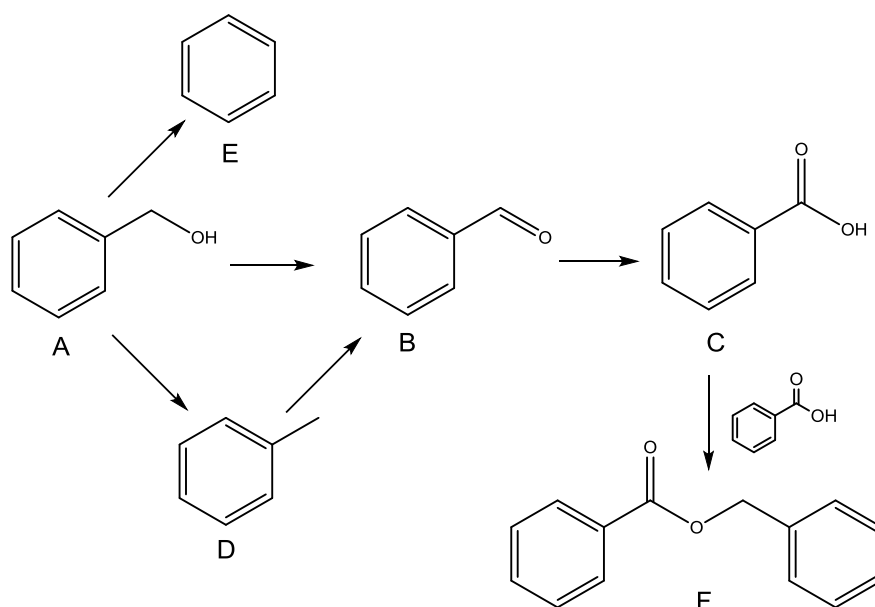
25. Dimitratos N, Lopez-Sanchez JA, Morgan D, Carley AF, Tiruvalam R, Kiely CJ, Bethell D, Hutchings GJ. Solvent-free oxidation of benzyl alcohol using Au–Pd catalysts prepared by sol immobilisation. *Physical Chemistry Chemical Physics* 2009, **11**(25): 5142.
26. Dimitratos N, Lopez-Sanchez JA, Morgan D, Carley A, Prati L, Hutchings GJ. Solvent free liquid phase oxidation of benzyl alcohol using Au supported catalysts prepared using a sol immobilization technique. *Catalysis Today* 2007, **122**(3–4): 317-324.
27. Abad A, Almela C, Corma A, García H. Unique gold chemoselectivity for the aerobic oxidation of allylic alcohols. *Chemical Communications* 2006(30): 3178-3180.

# Chapter 4

## 4. Effect of substituent groups on the oxidation of benzyl alcohol

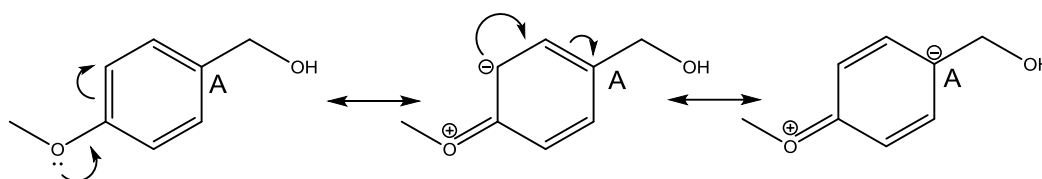
### 4.1. Introduction

The oxidation of alcohols is an important chemical and industrial process as it is a source of many fine and commodity chemicals. The products of alcohol oxidation act as starting materials for a wide variety of products such as perfumes, cosmetics and chemical reagents. Traditionally, chemicals such as aldehydes and ketones have been sourced from a diminishing supply of crude oil and petrochemicals with around 5% of worldwide crude oil consumption going towards chemical production<sup>1</sup>. As the availability of global crude oil supply diminishes, a new source of traditionally petroleum-derived compounds is needed. One area that is of interest and which can provide an alternative source of aldehydes, ketones and alcohols is biomass, which has been described as a renewable source of energy and a route to chemicals akin to current compounds derived from crude oil<sup>2</sup>.



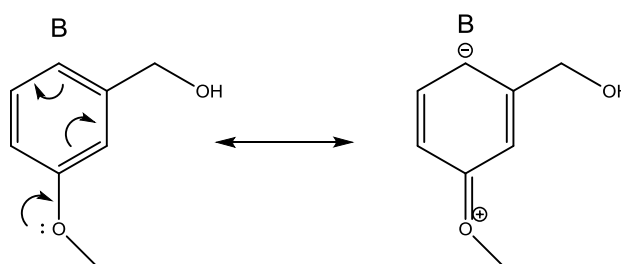
**Scheme 4-1** Reaction scheme of benzyl alcohol under solvent free conditions<sup>3</sup>. Benzyl Alcohol (A), Benzaldehyde (B), Benzoic Acid (C), Toluene (D), Benzene (E), Benzyl Benzoate (F)

Biomass, such as lignin, contains many compounds that resemble benzyl alcohol, which are bonded together with many different kind of chemical linkages, a proportion of which include methoxy groups<sup>4</sup>. Benzyl alcohol has been used as a model compound for testing supported metal catalysts for oxidation reactions, the possible products from benzyl alcohol oxidation are shown in Scheme 4-1. This reaction has been compared to the oxidation of methoxy-substituted benzyl alcohols as well as halogenated benzyl alcohols in water. This is an attempt to understand how the electronic structures of such benzyl alcohols affect the rate of reaction.



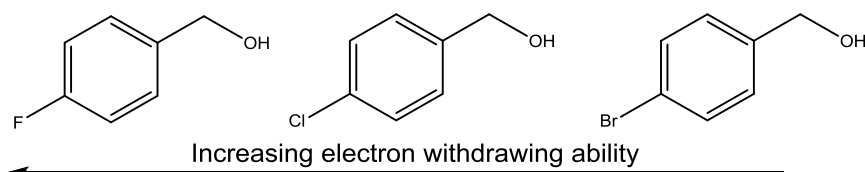
**Scheme 4-2** Resonance structures of a methoxy substituted benzyl alcohol showing charge distribution during resonance and how a negative charge is created in position A. This is typical for an electron-donating group in the *para*- position.

Electron donating groups influence the molecule depending on what position on the ring they're substituted. As can be seen in Scheme 4-2, an electron-donating group such as a methoxy substituent, when placed on the para position, results in resonance that creates a negative charge at position A on the benzene ring. This will destabilise any negative charge at the benzylic position and stabilise positive charge at the benzylic position. Compare this with Scheme 4-3 where a *meta*- substituted group results in a resonance structure where the negative charge appears in position B, *ortho*- position relative to the alcohol group.



**Scheme 4-3** Resonance structures of a methoxy substituted benzyl alcohol showing charge distribution during resonance. This is typical for an electron-donating group in the *meta*- position.

This electron donating effect by the methoxy groups were contrasted with *para*- substituted halogen groups, to see how electron withdrawing groups compare with their donating counterparts, as can be seen in Scheme 4-4, as you move down group VII, the electronegativity of the halogens decreases. The resultant perturbation to electron density lessens as you approach bromine, with electron density less concentrated towards the *para*-halogen group and more diffuse.



**Scheme 4-4 – Comparison of electronegativity of the halogen group, substituted at the *para*-position**

It could be thought then, that a *para*- substituted methoxy group will stabilise a formal positive charge at the benzylic position, a *meta*- substituted group will not have this effect and a halide will destabilise a formal negative charge at the benzylic position as it draws electron density away from this part of the molecule.

## 4.2. Methoxy group substitution in the *para*- position

Figure 4-1 shows how the addition of methoxy groups to the benzene ring within benzyl alcohol affects conversion to the corresponding methoxy containing aldehyde using an AuPd catalyst supported on MgO. When a methoxy group is added to the *para*- position in benzyl alcohol forming *para*-methoxybenzyl alcohol, conversion to *para*-methoxybenzaldehyde is greatest within the series reported in the diagram. Figure 4-2 shows how the rate of conversion increases from  $6.91 \times 10^{-4} \text{ mol s}^{-1}$  for benzyl alcohol oxidation to  $1.21 \times 10^{-3} \text{ mol s}^{-1}$  for oxidation of *para*-methoxybenzyl alcohol. Selectivity remains high (> 95%) towards the 4-methoxy substituted benzaldehyde. The addition of further methoxy groups in the *meta*- position does not have this promotion affect but decreases the rate of reaction (Figure 4-2), selectivity to the poly-substituted benzaldehyde remained high (> 95%) with no over-oxidation towards the poly-substituted benzoic acid product.

This could be due to the conflicting nature of the two resonance structures that are possible with poly-substituted benzyl alcohols; greater conjugation is possible for the intermediate for the 4-methoxybenzyl alcohol than there is for the 3-methoxybenzyl alcohol. Furthermore, steric factors could be playing a role in slowing down the rate of reaction. Methoxy groups are somewhat bulky and could be inhibiting the molecule from bonding to the catalyst surface.

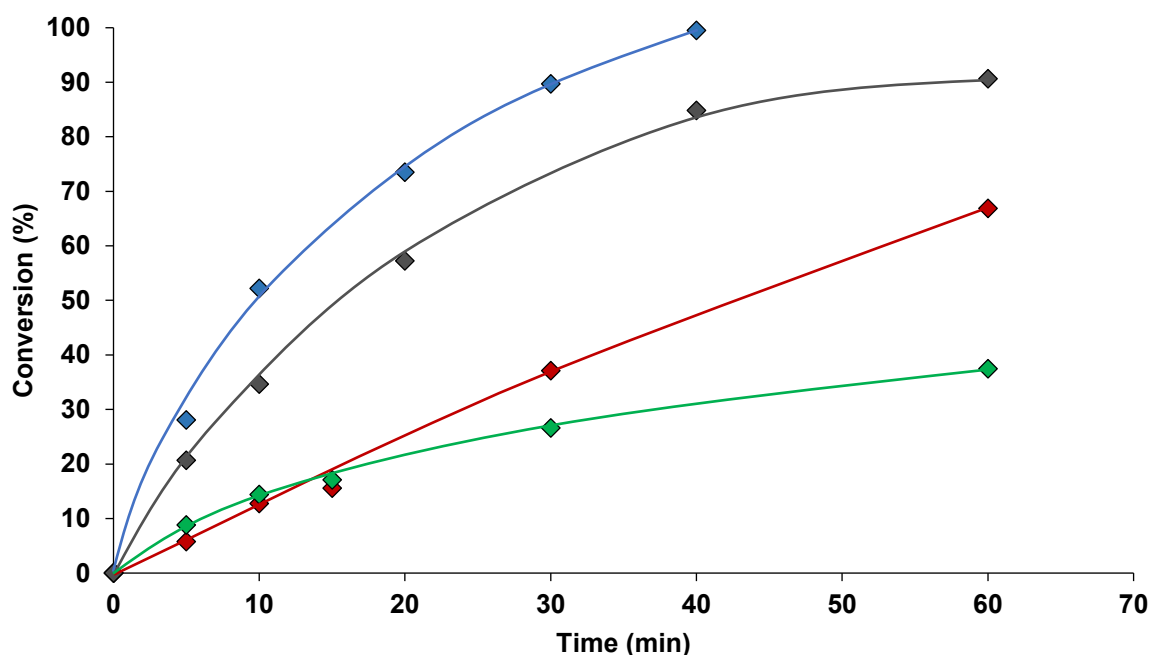


**Figure 4-1** Effect of methoxy substituent groups on the oxidation of benzyl alcohol (◆), 3,4,5-trimethoxybenzyl alcohol (◆), 3,4-dimethoxybenzyl alcohol (◆) and 4-methoxybenzyl alcohol (◆) using a AuPd/MgO catalyst (20 mg, 1:1 mol), 2 bar (g) O<sub>2</sub>, 1000 rpm at 80 °C and 200 mg alcohol in 5 ml water

Soni *et al.*<sup>5</sup> found the same trend as displayed in Figure 4-2 whereby the rate of reaction for meta-methoxybenzyl alcohol was lower than that of para-methoxybenzyl alcohol. Interestingly, this group did not investigate the bi-substituted derivative of 3,5-dimethoxybenzyl alcohol therefore, a comparison cannot be made to this group's work.



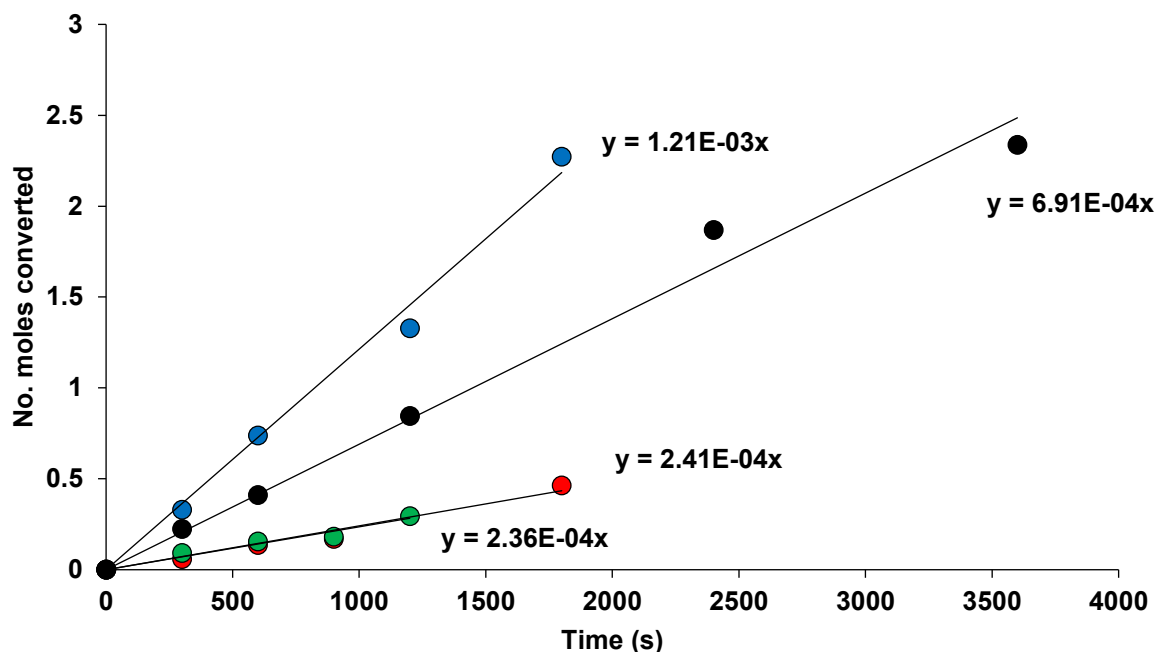


Figure 4-2 Calculation of reaction rate for the oxidation of benzyl alcohol (●), 3,4,5-trimethoxybenzyl alcohol (●), 3,4-dimethoxybenzyl alcohol (●) and 4-methoxybenzyl alcohol (●) using a 1%AuPd/MgO catalyst (20 mg, 1:1 mol), 2 bar (g) O<sub>2</sub>, 1000 rpm at 80 °C and 200 mg alcohol in 5 ml water

### 4.3. Halide group substitution in the *para*- position

Figure 4-3 depicts how the addition of a halide group at the *para*- position results in less conversion when compared to the non-substituted benzyl alcohol. The rate of reaction compared to benzyl alcohol (Figure 4-4) decreases from  $6.91 \times 10^{-4} \text{ mol s}^{-1}$  to  $1.02 \times 10^{-4} \text{ mol s}^{-1}$  for 4-chlorobenzyl alcohol which is the most active out of the three halogenated derivatives of benzyl alcohol. Soni *et al.*<sup>5</sup> found that *para*-fluorobenzyl alcohol displayed the greatest rate of oxidation in a series of halogenated benzyl alcohols however, this was carried out with morpholinium chlorochromate (MCC) in DMSO. The reaction in MCC was found to be first order with respect to the alcohol and with  $[\text{H}^+]$  which was provided by toluene-*p*-sulfonic acid.

In the work represented within this thesis, reactions were carried out in water which contains  $[\text{H}_3\text{O}]^+$  ions. These ions may promote the reaction in a different pathway, resulting in a different mechanism in halogenated benzyl alcohol oxidation.

The highly electronegative fluorine group and the less electronegative bromine group are both low in reactivity. Chlorine, being intermediate in electronegativity between fluorine and bromine, may be inducing an electron density perturbation away from the target alcohol group and size in a way which is not detrimental to oxidation. Bromine is a large functional group and may be blocking access to the catalytic active sites via steric inhibition. The Au to Pd molar ratio in the catalyst seems to be less important for halogenated 4-fluorobenzyl alcohol than it is for benzyl alcohol (Figure 4-5).

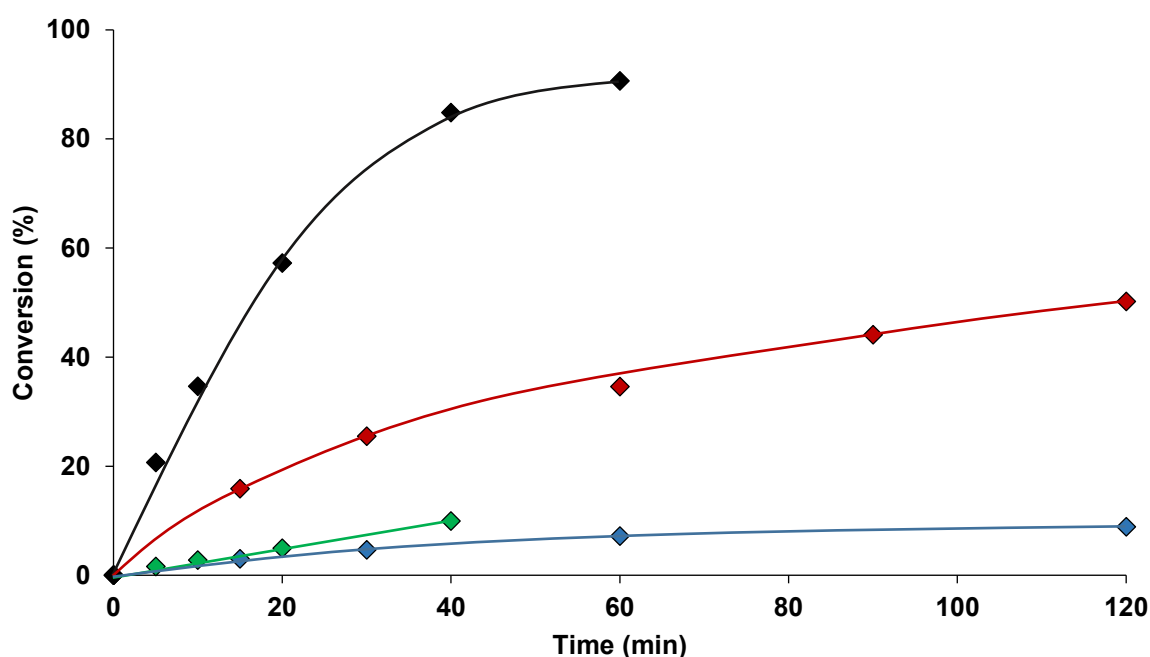


**Figure 4-3** Time on line study for the oxidation of benzyl alcohol (◆), 4-fluorobenzyl alcohol (◆), 4-chlorobenzyl alcohol (◆) and 4-bromobenzyl alcohol (◆) using a 1%AuPd/MgO catalyst (20 mg, 1:1 mol), 2 bar (g) O<sub>2</sub>, 1000 rpm at 80 °C and 200 mg alcohol in 5 ml water

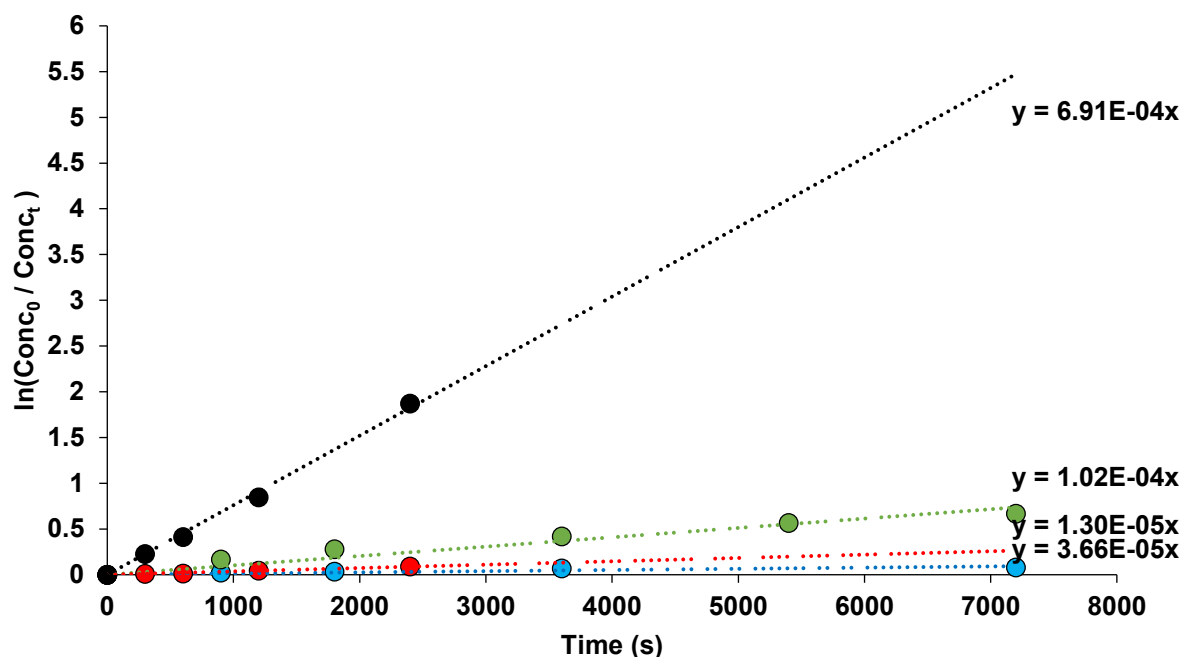


Figure 4-4 Graph of  $\ln(\text{Conc}_{\text{time}=0} / \text{Conc}_{\text{time}=t})$  of benzyl alcohol (●), 4-fluorobenzyl alcohol (●), 4-chlorobenzyl alcohol (●) and 4-bromobenzyl alcohol (●) over a 1% AuPd/MgO catalyst (20 mg, 1:1 mol), 2 bar (g)  $\text{O}_2$ , 1000rpm at 80 °C and 0.2 g alcohol and 5ml water

Figure 4-4 shows the rate of reaction in the form of  $\ln \frac{\text{Conc}_{\text{time}=0}}{\text{Conc}_{\text{time}=t}}$  and shows how the rate of reaction has decreased when a halogen group is added to the *para*- position of benzyl alcohol.

#### 4.4. Effect of Au:Pd ratio and support on the oxidation of 4-Methoxybenzyl alcohol and 4-Fluorobenzyl alcohol

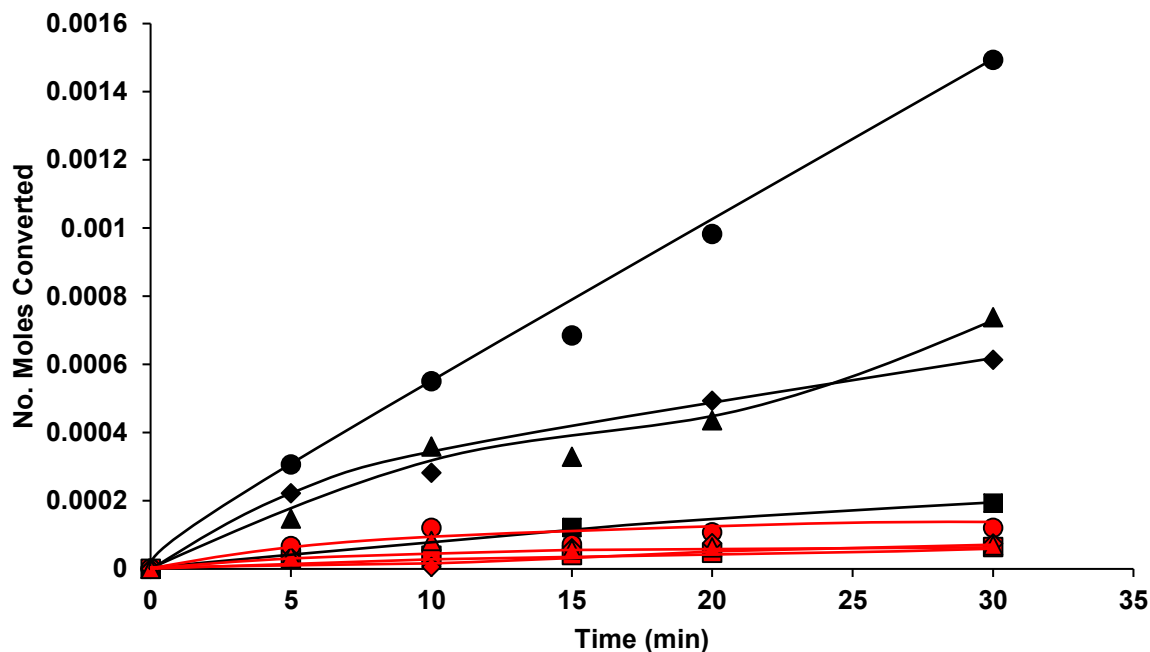


Figure 4-5 Time online study of the effect of gold loading for benzyl alcohol (black) and 4-fluorobenzyl alcohol (red) on 2:1 mol (■), 1:2 mol (●) 0.5:9.5 mol (◆) and 1:9 mol (▲) over a 1%AuPd/MgO catalyst (20 mg), 2 bar (g) O<sub>2</sub>, 1000rpm at 80 °C and 0.2 g alcohol and 5ml water

As can be seen from the above graph (Figure 4-5), the molar ratio of AuPd is most important for benzyl alcohol, with a less pronounced affect for 4-fluorobenzyl alcohol.

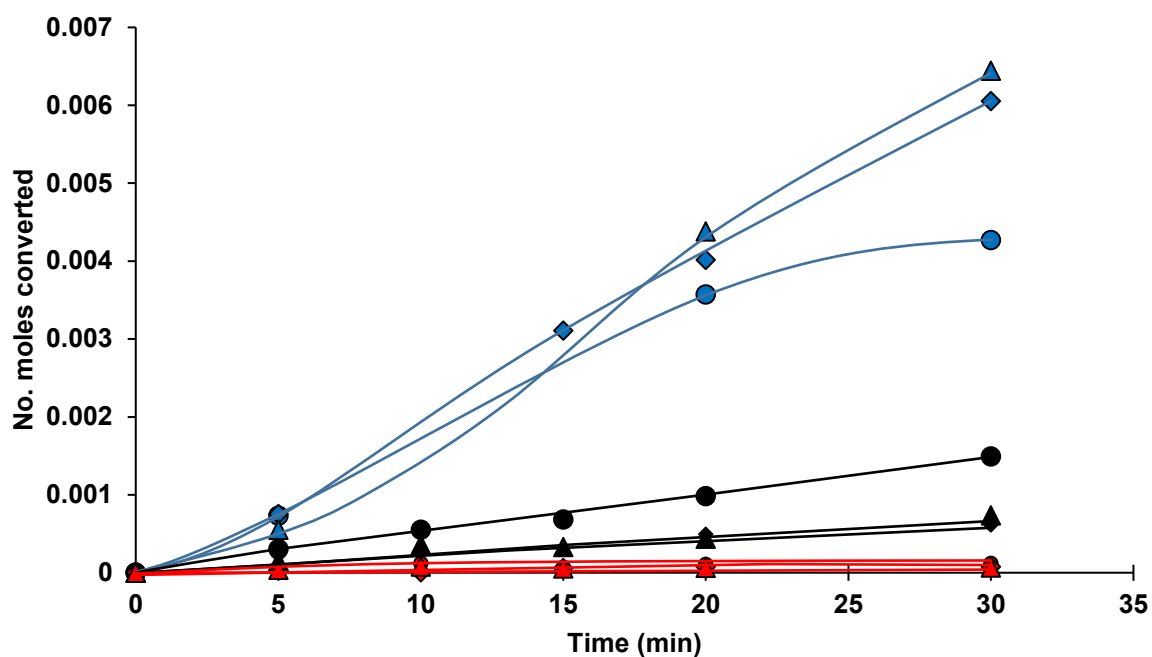


Figure 4-6 Time online study of the effect of gold loading for benzyl alcohol (black) and 4-fluorobenzyl alcohol (red) and 4-methoxybenzyl alcohol (blue) on 2:1 mol (■), 1:2 mol (●) 0.5:9.5 mol (◆) and 1:9 mol (▲) over a 1%AuPd/MgO catalyst (20 mg), 2 bar (g) O<sub>2</sub>, 1000rpm at 80 °C and 0.2 g alcohol and 5ml water

Comparing this further with 4-methoxybenzyl alcohol (Figure 4-6), it seems that it is only benzyl alcohol which is affected by the change in AuPd ratio, as both other molecules show similar activity for all metal ratios for the supported AuPd catalysts<sup>6</sup>.

## 4.5. Overall comparison/Hammett plot

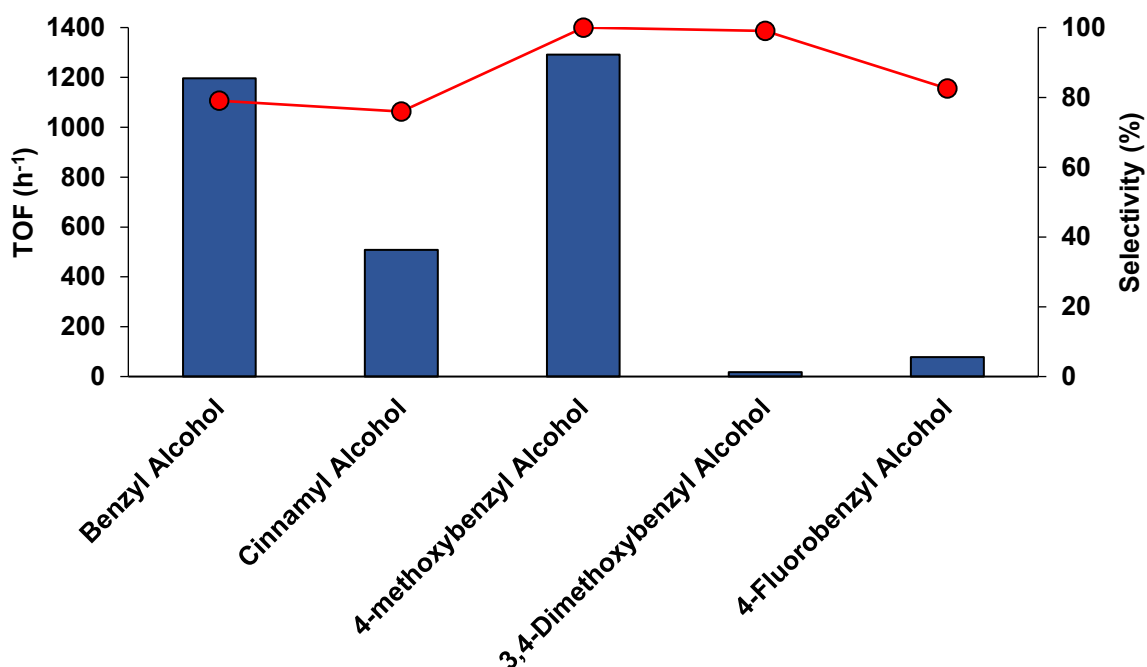
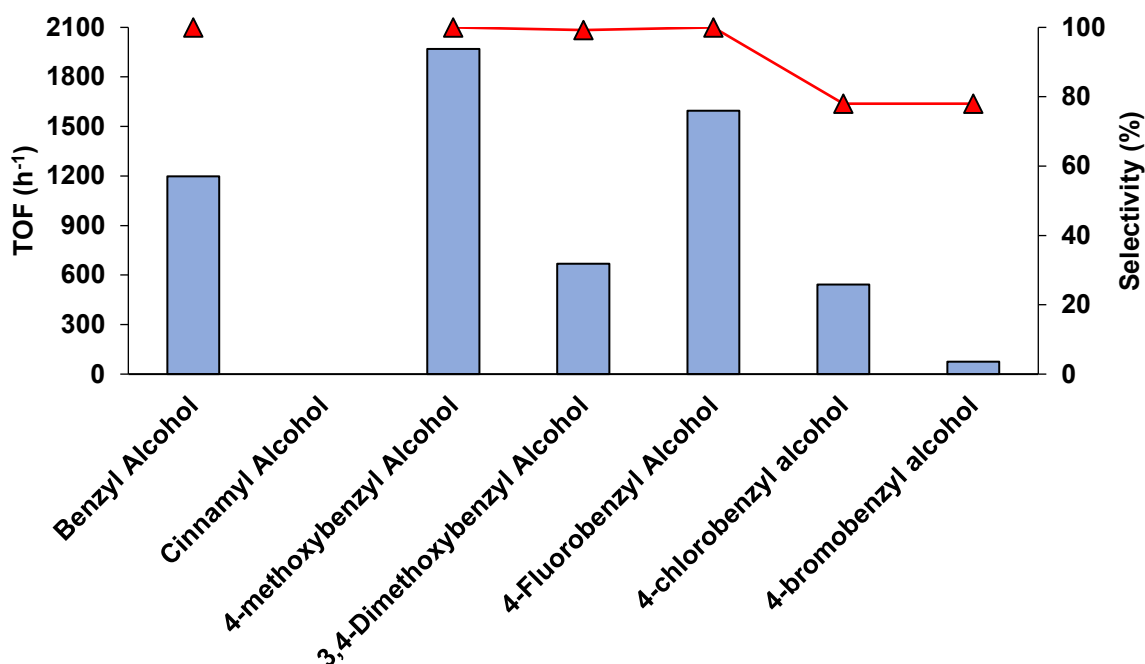


Figure 4-7 TOF ( $\text{h}^{-1}$ ) (■) and selectivity to corresponding aldehyde (●) of a selection of alcohols over a 1%AuPd (20 mg, 1:1 mol) supported catalyst on  $\text{TiO}_2$  (20 mg), 2 bar (g)  $\text{O}_2$ , 1000rpm at 80 °C and 0.2 g alcohol and 5ml water

Figure 4-7 shows the turn over frequency (TOF ( $\text{h}^{-1}$ )) of a 1%AuPd (1:1 mol) supported on  $\text{TiO}_2$ . From the results, benzyl alcohol and 4-methoxybenzyl alcohol have similar TOF ( $\text{h}^{-1}$ ) values of about 1200. Cinnamyl alcohol has a much lower TOF ( $\text{h}^{-1}$ ) compared to that of benzyl alcohol. This may be due to the bulk of the molecule compared to that of benzyl alcohol since both cinnamyl alcohol and benzyl alcohol are structurally similar in terms of shape.



**Figure 4-8** TOF ( $\text{h}^{-1}$ ) (■) and selectivity to corresponding aldehyde (▲) of a selection of alcohols over a 1%AuPd (20 mg, 1:1 mol) supported catalyst on MgO (20 mg), 2 bar (g)  $\text{O}_2$ , 1000rpm at 80 °C and 0.2 g alcohol and 5ml water

Figure 4-8 shows the turn over frequency (TOF ( $\text{h}^{-1}$ )) for several substituted compounds whilst using AuPd catalyst supported on MgO. Benzyl alcohol has a TOF ( $\text{h}^{-1}$ ) of 1200  $\text{h}^{-1}$  but 4-methoxybenzyl alcohol has a TOF ( $\text{h}^{-1}$ ) of 1970  $\text{h}^{-1}$  which is a marked improvement compared to benzyl alcohol. Of note is the large increase in TOF ( $\text{h}^{-1}$ ) for 4-fluorobenzyl alcohol using AuPd supported on MgO compared to the same reaction using an AuPd catalyst supported on  $\text{TiO}_2$ .

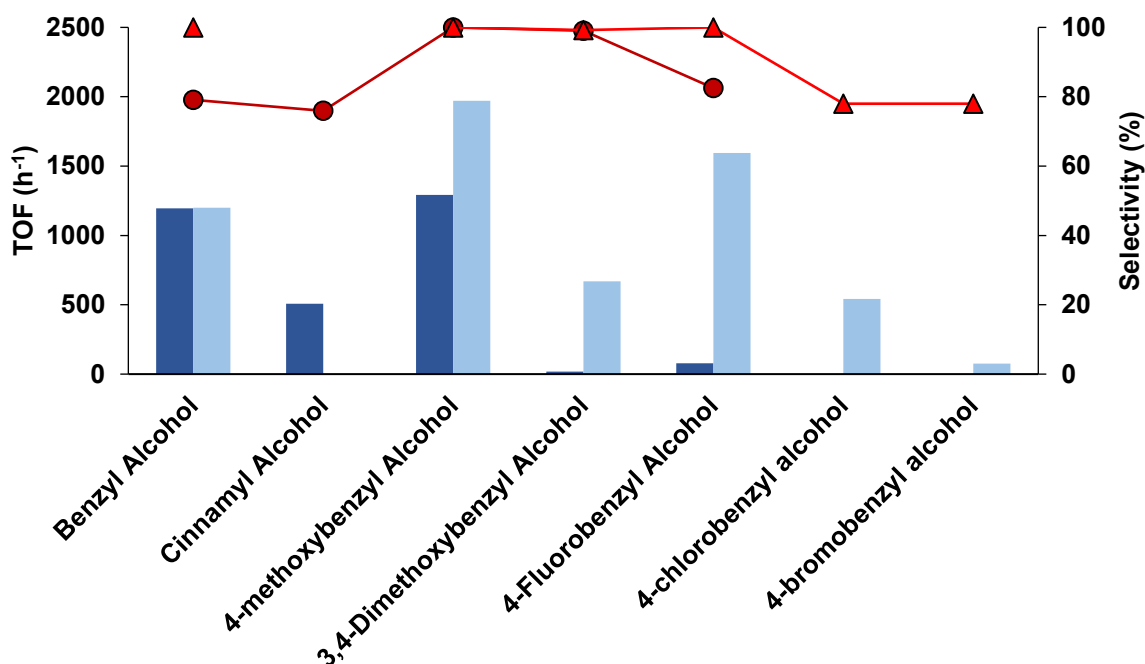


Figure 4-9 TOF (h<sup>-1</sup>) (TiO<sub>2</sub> ■ , MgO ■) and selectivity to corresponding aldehyde (TiO<sub>2</sub> ● , MgO ▲) of a selection of alcohols over a 1%AuPd (1:1 mol) supported catalyst on MgO and TiO<sub>2</sub> (20 mg), 2 bar (g) O<sub>2</sub>, 1000rpm at 80 °C and 0.2 g alcohol and 5ml water

Figure 4-9 consolidates the data from Figure 4-7 and Figure 4-8 to better highlight the difference observed in TOF (h<sup>-1</sup>) between AuPd supported on TiO<sub>2</sub> and AuPd supported on MgO. It is evident that AuPd on MgO is much more active when compared to the same catalyst supported on TiO<sub>2</sub> for most alcohols used in this study. The only alcohol to show comparable TOF (h<sup>-1</sup>) between the two metal-oxide supports is benzyl alcohol. This highlights that the electronic configuration of the substituted benzyl alcohols can interact with the metal supports in such a way as to affect the observed TOF (h<sup>-1</sup>) for the catalyst.

The interaction of the substituted benzyl alcohol has on the metal oxide support is not directly investigated in this study, instead, work is focused on how substitution on the benzene ring of benzyl alcohol affects the observed reaction activity. This is carried out on the AuPd catalyst supported on MgO via a Hammett plot.



## 4.6. Hammett Plot

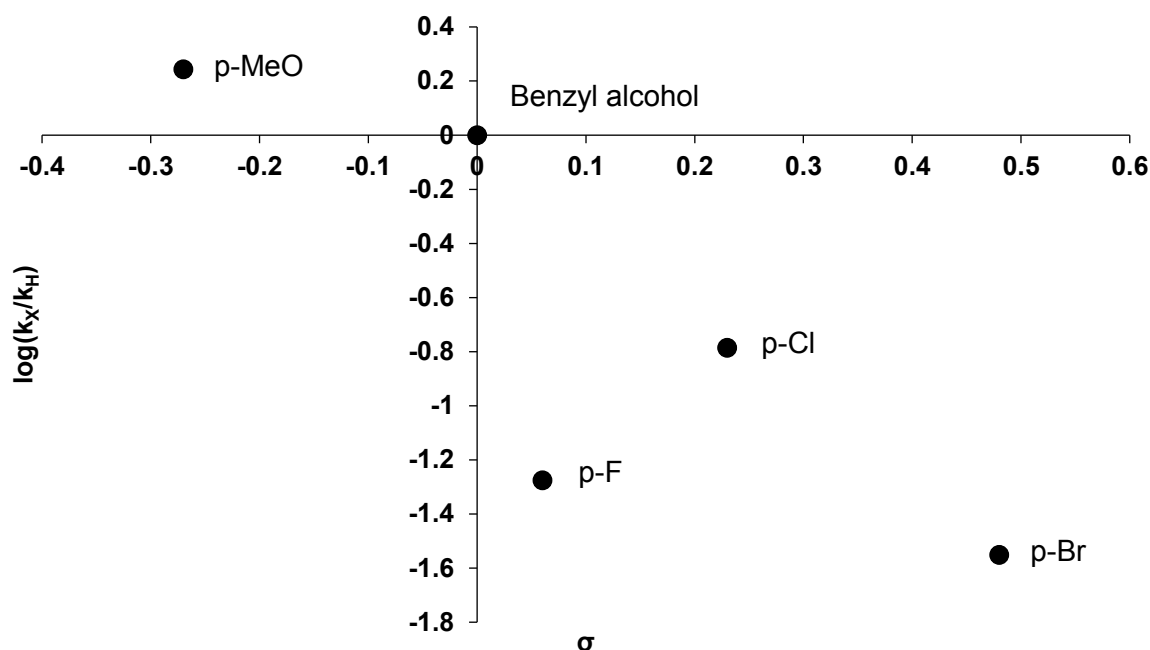
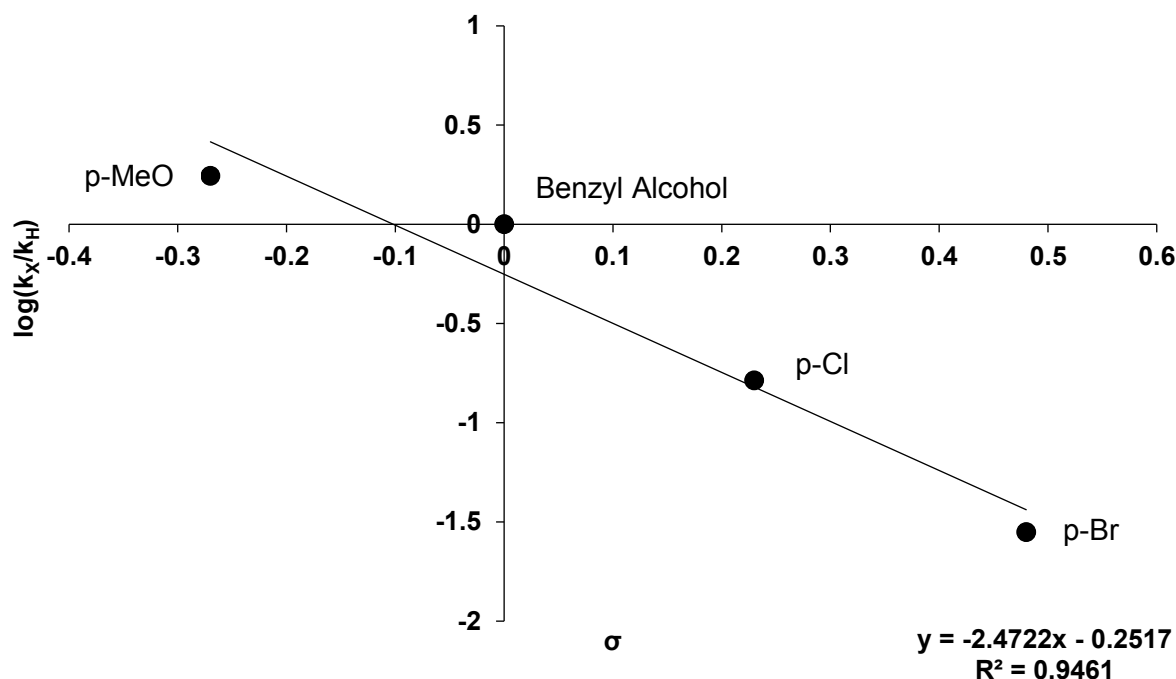


Figure 4-10 Hammett plot of benzyl alcohol, 4-methoxybenzyl alcohol, 4-fluorobenzyl alcohol, 4-chlorobenzyl alcohol and 4-fluorobenzyl alcohol using 1:1 AuPd catalyst supported on MgO (20 mg), 2 bar (g) O<sub>2</sub>, 1000rpm at 80 °C and 0.2 g alcohol and 5ml water

Figure 4-10 shows the Hammett study of a range of *p*-X-benzyl alcohol derivatives. The Hammett substituent constants were obtained from literature<sup>7</sup>. *para*-Fluorobenzyl alcohol does not seem to fit the trend displayed by the other substituted benzyl alcohol compounds. Reasons for such a deviation have not been uncovered and will be a topic of further research. The *para*-fluorobenzyl alcohol data point has been omitted from the final graph to produce Figure 4-11. As can be seen from Figure 4-11, the Hammett study has produced a  $\rho$  value of -2.47 by using the  $\sigma^-$  values. There was no correlation with  $\sigma^+$  values which rules out any reaction via radical intermediaries.

These results are in keeping with work by Baiker and co-workers<sup>8</sup> who found a similar trend in substituted benzyl alcohols with organically modified ruthenium-hydroxyapatite complexes. Relating this to gold, a  $\rho < 0$  value was also obtained by Christensen *et al.*<sup>9</sup>. These observations, coupled with the results of this study, seem to suggest a common mechanism for benzyl alcohol oxidation using Au and Ru complexes allowing a comparison to be made between the results obtained in this study and theory presented in literature. This also seems

to extend to the alloyed AuPd catalysts in this study, and suggests the mechanism is independent of oxygen coverage which varied greatly between the Au and Ru complexes.



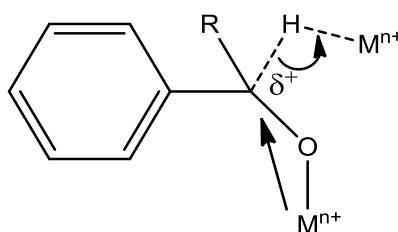
**Figure 4-11 modified from Figure 4-10, Hammett plot of selected benzyl alcohol derivatives plotted against  $\sigma$ . Conditions are the same as Figure 4-11.**

The Hammett plot (Figure 4-11) suggests that benzyl alcohol and its derivatives undergo reaction via generation of a cation in the benzylic position and oxidation proceeds via  $\beta$ -hydride elimination. Christensen *et al.*<sup>10</sup> probed this reaction further using the kinetic isotope effect (KIE). The determined kinetic isotope effect ( $k_H/k_D$ ) was found to be 2.8–2.9, indicating that breakage of the bond to the neighbouring hydrogen atom takes place in the rate-determining step. This KIE was less than that of a fully bond broken transition state suggesting that the transition state is being stabilised by the supported Au-oxo species on the catalyst.

It has been postulated by Guzman *et al.*<sup>11</sup> that a mechanism involving two Au species exists in supported gold catalysts, these being  $Au^0$  and  $Au^+$  and further elucidation by Corma *et al.*<sup>12</sup> have found that, at least in CO oxidation by supported gold catalysts, that there exists  $\eta^1$ -superoxide and peroxide species at one electron deficient sites. These species may be the stabilising factor for a partially bond broken transition state. Furthermore, Corma *et al.*<sup>13</sup> later described a possible mechanism for the reaction (Figure 4-12) using Au/npCeO<sub>2</sub> catalysts.

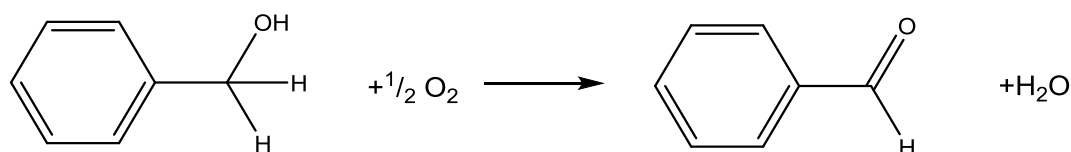
This was elucidated by utilising both the Hammett methodology and the Kinetic Isotope Effect as mentioned earlier which led them to believe that the breakage of the benzylic C-H bond is faster than the formation of the C=O bond and the C-OH bond builds up a partial positive charge in the transition state. Interestingly, while Corma *et al.* investigated the macroscopic kinetic effects, they found that the number of moles of benzaldehyde produced was double that of the number of moles of O<sub>2</sub> consumed. This correlates with

Figure 4-13 as only one oxygen atom is required to oxidise one molecule of benzyl alcohol.



**Figure 4-12<sup>6</sup> Proposed mechanism by Corma *et al.* for the H-abstraction step of aerobic alcohol oxidation over supported gold catalysts<sup>13</sup>.**

Further macroscopic investigations found the reaction was independent of oxygen pressure as Corma *et al.*<sup>13</sup> varied the reaction pressure from 0 to 3.5 atm and found the rate to be zero order with respect to oxygen, this was also discovered to be the case in work by Mizuno *et al.*<sup>14</sup> on work with Ru/Al<sub>2</sub>O<sub>3</sub> catalysts. This seems to suggest that the re-oxidation of the metal hydride by molecular oxygen proceeds quickly and is not the rate determining step.



**Figure 4-13 Reaction stoichiometry for the oxidation of benzyl alcohol to benzaldehyde using a supported Au catalyst on CeO<sub>2</sub><sup>13</sup>.**

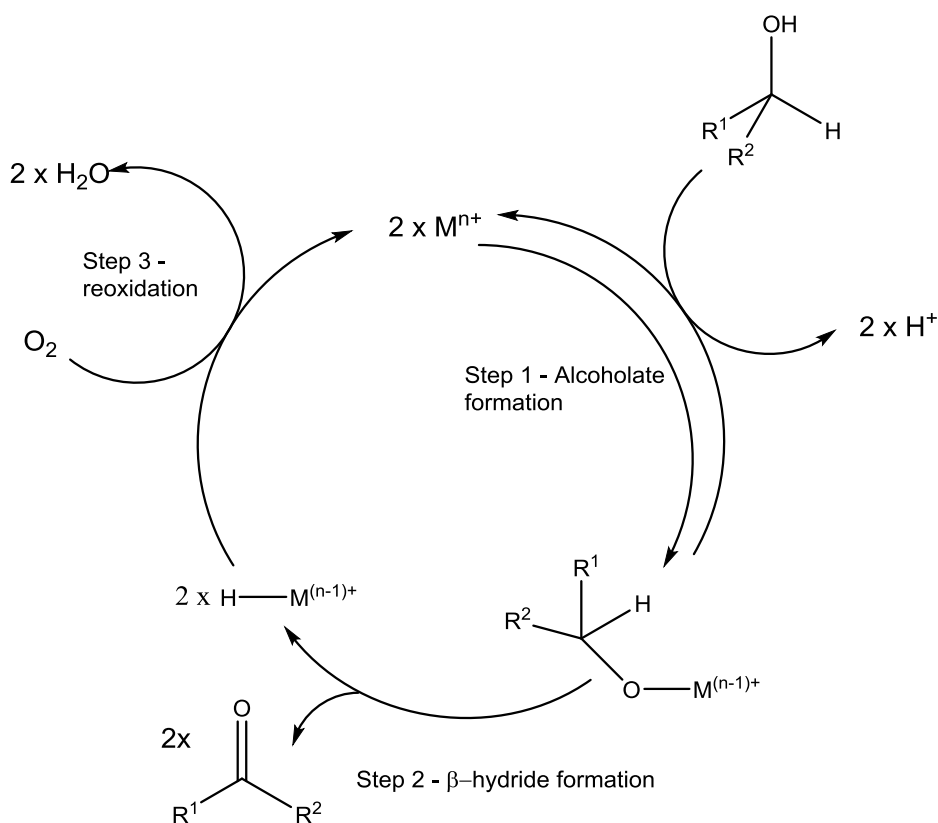
Combining what Corma *et al.* found with the work by Mizuno *et al.*, a general reaction scheme can be elucidated for the aerobic oxidation of substituted benzyl alcohol over AuPd catalysts

<sup>6</sup> Figure 4-12 Reproduced under license from John Wiley and Sons

since the same mechanism was present in both studies with similar catalysts, namely Au/npCeO<sub>2</sub> and Ru/Al<sub>2</sub>O<sub>3</sub>.

For the reaction scheme elucidated in

Scheme 4-5, step 1 is the generation of an alcoholate formation in which the hydrogen of the OH group is substituted for a metal, this alcoholate is in equilibrium with the free alcohol species. The second step is when the metal-alcoholate species undergoes a  $\beta$ -hydride elimination to give rise to the carbonyl product and a metal hydride intermediate. The metal hydride is then reoxidised by molecular oxygen which is postulated to occur via molecular oxygen insertion into the Au-hydride bond. This Au-hydride species is surprisingly stable. The third and final step is the reoxidation of the metal hydride by oxygen to form water while recovering the initial metal site.



**Scheme 4-5 Potential mechanistic scheme for the oxidation of alcohols over supported AuPd catalysts<sup>13, 14</sup>**

Work by Andrews *et al.*<sup>15</sup> has shown via matrix-isolation and DFT studies that AuH<sub>2</sub><sup>-</sup> species exhibit high energy and reactivity properties that allow it to participate in oxidation reactions.

Furthermore, the negative charge on the hydride stabilises the species and facilitates charge transfer from the support to the metal cluster<sup>16</sup>. As such, metal-support interactions become a very important consideration to make since the support must be able to stabilise the Au-hydride species and Au<sup>3+</sup> species that are generated during the catalytic reaction cycle, along with facilitating oxygen activation to re-oxidise the metal-hydride species.

It was noted by d'Itri *et al.*<sup>17</sup> that oxygen was able to adsorb into vacant sites on the npCeO<sub>2</sub> surface through *in situ* Raman spectroscopy. It was found that the O-O stretching frequency of 1135-1127 cm<sup>-1</sup> and 877-831 cm<sup>-1</sup> were due to the adsorbed oxygen interacting with one- and two-electron defects on the npCeO<sub>2</sub> surface to form the superoxides O<sub>2</sub><sup>-</sup> and O<sub>2</sub><sup>2-</sup> species respectively, findings that echo Corma *et al.*'s work. Further work is necessary to understand if these species were also present in the AuPd supported catalysts in this study, and would be of future interest.

Metal-support interactions are not only important in their ability to stabilise the active species that exist on the AuPd surface but they can actively alter the product selectivity. An example of this phenomenon is MgO and ZnO as supports which can suppress one reaction pathway for the solventless oxidation of benzyl alcohol<sup>18</sup>. In this study, Hutchings *et al.* studied a range of supports including TiO<sub>2</sub>, MgO, ZnO, Nb<sub>2</sub>O<sub>3</sub> and activated carbon.

It was found that the MgO and ZnO catalysts in the study were the least reactive in the solventless reaction but their selectivity profile was different to the remaining three supports. These three supports, TiO<sub>2</sub>, Nb<sub>2</sub>O<sub>3</sub> and activated carbon, produced toluene as a major by-product of reaction by catalysing a disproportionation reaction pathway as opposed to the  $\beta$ -hydride elimination pathway discussed earlier. Conversely, MgO and ZnO suppressed disproportionation and promoted an exclusive selectivity to benzaldehyde.

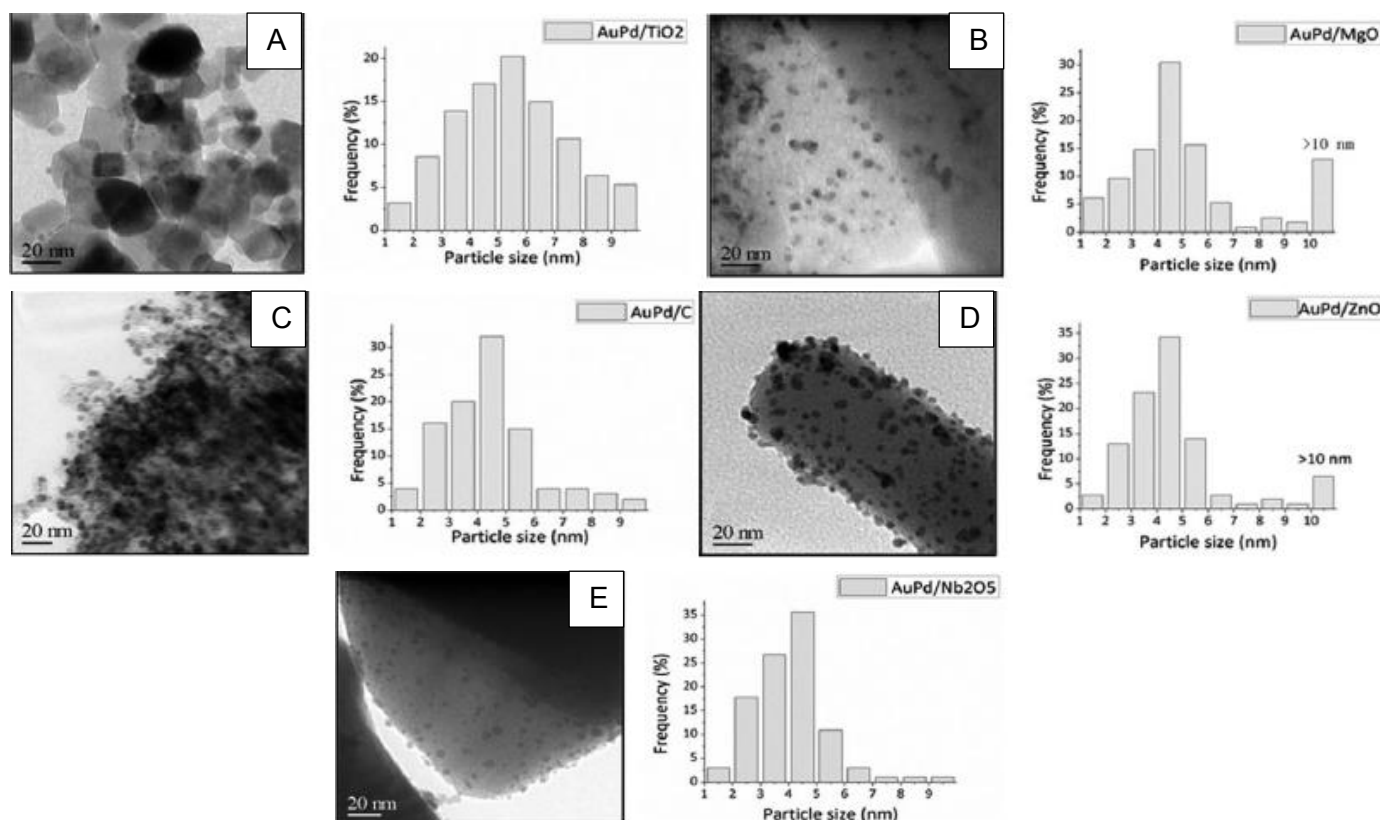
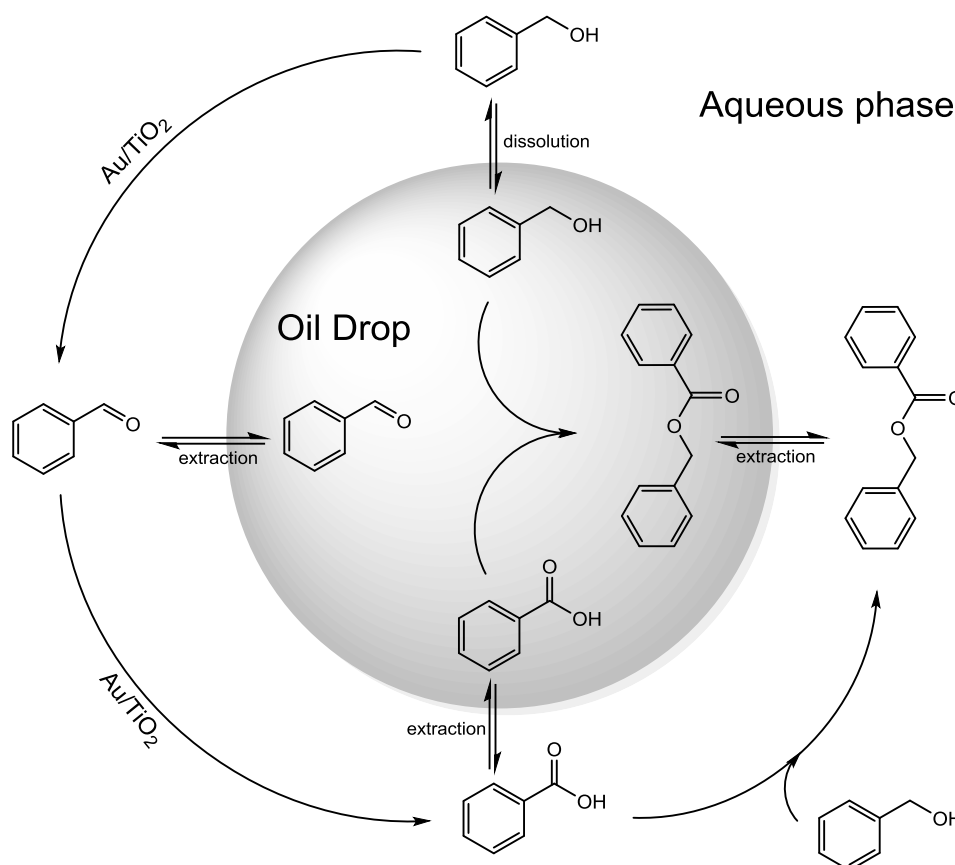


**Figure 4-14<sup>7</sup>** Particle-size distribution data determined from bright field TEM micrographs for supported AuPd catalysts, A) 1%AuPd/TiO<sub>2</sub>, B) 1%AuPd/MgO, C) 1%AuPd/C, D) 1%AuPd/ZnO and E) 1%AuPd/Nb<sub>2</sub>O<sub>5</sub><sup>18</sup>

Microscopy studies of these catalysts revealed no structurally significant differences so it was hypothesised that the acidity/basicity of the support played a key part in the reaction mechanism since the supports exhibited such effects. This was confirmed by the small addition of NaOH (aq) to the reaction mixture of benzyl alcohol with Au/TiO<sub>2</sub> which suppressed toluene formation in this system. The generation of toluene involves the cleavage of the C-O bond of benzyl alcohol, possibly in step 2 of Scheme 4-5 involves generation of a carbocation in a pathway that is catalysed in acidic environments. This relates to the catalytic system for AuPd/MgO catalysts used in this study as these catalysts exhibited the same effect. The presence of water did not interfere with the unique properties observed whilst using MgO as support for AuPd nanoparticles. AuPd/MgO can promote the oxidation of benzyl alcohol to benzaldehyde whilst suppressing disproportionation into toluene. Furthermore, the study found that Au sites on the catalyst surface do not catalyse the disproportionation reaction but that it was the addition of Pd that switched on this pathway.

<sup>7</sup> Figure 4-14 reproduced under license from the Royal Society of Chemistry

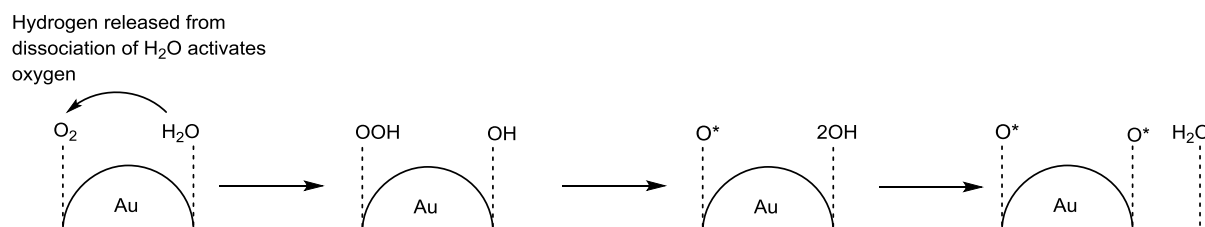
How water affects the oxidation of substituted benzyl alcohols is of interest since they are not completely miscible in a system using water as a solvent. Work by Qui *et al.*<sup>19</sup> has gone some way to explain the role of water and its ability to activate molecular oxygen, facilitating the reaction. Qui *et al.* found the system to be quad-phasic, consisting of vapour (molecular O<sub>2</sub>), organic phase, aqueous phase, and solid catalyst. The solid phase, the catalyst, is dispersed in the reaction medium by rapid stirring while the reactants are dispersed in the reaction medium as shown in Scheme 4-6. The products and reactants would be transferred from different phases via dissolution, diffusion and extraction, while the oil drops would be homogeneously dispersed.



**Scheme 4-6** Proposed reaction scheme for benzyl alcohol oil droplets suspended in an aqueous phase<sup>19</sup>

The interface between the organic and aqueous phases in the micro-droplets favour the mass transfer of reactants and products. The number of micro-droplets increases when water

content is increased, resulting in more organic-aqueous interfaces available for reaction. A possible mechanism for the activation of oxygen from this work is given in Scheme 4-7.



**Scheme 4-7 Possible reaction mechanism for the activation of molecular oxygen by water on Au catalysts<sup>19</sup>**

Further studies by Bongiorno *et al.*<sup>20</sup>, who used first principles investigations to explore a significant enhancement in the binding and activation energies of  $\text{O}_2$  occurring when it co-adsorbed with water on small Au clusters supported on MgO (100). There existed a partial proton sharing or transfer resulting in the hydroxyl-like intermediates. Hu *et al.*<sup>21</sup> discovered  $\text{O}_2$  would not adsorb on Ti(110) surfaces unless water was present and this effect was apparent for oxygen over a long range; oxygen's adsorption energy was unchanged but oxygen coverage was affected by the amount of water adsorbed. It was hypothesised by Hu *et al.* that the oxygen coverage was the limiting factor in the reaction and that water coverage could remove this bottleneck. Further investigation of this effect on MgO surface found that water did not have sufficient adsorption energy on the Au/MgO interface, and the system mainly depended on the formation of  $\text{CO-O}_2$  complexes at the interface.

This was further confirmed by Hammer *et al.*<sup>22</sup> who noted that Au-MgO interfaces exhibited a small cavity between the Au and MgO which resembled enzyme active sites and this would go some way to explain how previous groups have observed Michaelis-Menten type kinetics in their work and why this reaction system can produce a linear Lineweaver-Burke plot. Furthermore, the selectivity observed in the reaction to almost exclusively benzaldehyde may be a result of this phenomenon. Hammer *et al.*<sup>23</sup> also managed to model and confirm the existence of  $\text{CO-O}_2$  complexes observed by Hu *et al.*<sup>21</sup>. They found  $\text{O}_2$  capture and the  $\text{CO} \cdot \text{O}_2$  intermediate was greatest at the edge of the Au/MgO interface and this reactivity, coupled with the attraction between  $\text{CO} \cdot \text{O}_2$  and MgO, helps stabilise the reaction's transition state.



Finally, Hammer *et al.* tried to explain why molecular oxygen has such a high reactivity when adsorbed on to gold. They speculate that this is due to the adsorption energy being very low and so oxygen bonding to Au clusters is facile and can easily lend itself to the reacting complex. This was juxtaposed by investigating more traditional, “active” transition metals such as Pt which can easily dissociate O<sub>2</sub> but also bind it strongly and so the bound adsorbates must overcome energy barriers to overcome resulting in reaction rates that are only significant at higher temperatures. Au meanwhile, appears to loosely bind the reaction species and so they can adsorb, react and desorb at lower temperatures when compared to other catalysts.

## Chapter 4 References

1. Donaldson TL, Culberson OL. An industry model of commodity chemicals from renewable resources. *Energy* 1984, **9**(8): 693-707.
2. Chheda JN, Huber GW, Dumesic JA. Liquid-Phase Catalytic Processing of Biomass-Derived Oxygenated Hydrocarbons to Fuels and Chemicals. *Angewandte Chemie International Edition* 2007, **46**(38): 7164-7183.
3. Dimitratos N, Lopez-sanchez J, Morgan D, Carley A, Prati L, Hutchings G. Solvent free liquid phase oxidation of benzyl alcohol using Au supported catalysts prepared using a sol immobilization technique. *Catalysis Today* 2007, **122**(3-4): 317-324.
4. Sedai B, Díaz-Urrutia C, Baker RT, Wu R, Silks LAP, Hanson SK. Aerobic Oxidation of  $\beta$ -1 Lignin Model Compounds with Copper and Oxovanadium Catalysts. *ACS Catalysis* 2013, **3**(12): 3111-3122.
5. Soni N, Tiwari V, Sharma V. Correlation analysis of reactivity in the oxidation of substituted benzyl alcohols by morpholinium chlorochromate. *Indian Journal of Chemistry Section a-Inorganic Bio-Inorganic Physical Theoretical & Analytical Chemistry* 2008, **47**(5): 669-676.
6. Kesavan L, Tiruvalam R, Rahim MHA, bin Saiman MI, Enache DI, Jenkins RL, Dimitratos N, Lopez-Sanchez JA, Taylor SH, Knight DW, Kiely CJ, Hutchings GJ. Solvent-Free Oxidation of Primary Carbon-Hydrogen Bonds in Toluene Using Au-Pd Alloy Nanoparticles. *Science* 2011, **331**(6014): 195-199.
7. Hansch C, Leo A, Taft RW. A Survey of Hammett Ssubstituent Constants and Resonance and Field Parameters. *Chemical Reviews* 1991, **91**(2): 165-195.
8. Opre Z, Ferri D, Krumeich F, Mallat T, Baiker A. Aerobic oxidation of alcohols by organically modified ruthenium hydroxyapatite. *Journal of Catalysis* 2006, **241**(2): 287-295.

9. Fristrup P, Johansen L, Christensen C. Mechanistic Investigation of the Gold-catalyzed Aerobic Oxidation of Alcohols. *Catalysis Letters* 2008, **120**(3-4): 184-190.
10. Fristrup P, Bahn Johansen L, Hviid Christensen C. Mechanistic investigation of the gold-catalyzed aerobic oxidation of aldehydes: added insight from Hammett studies and isotopic labelling experiments. *Chemical Communications* 2008(24): 2750-2752.
11. Guzman J, Gates BC. Catalysis by Supported Gold: Correlation between Catalytic Activity for CO Oxidation and Oxidation States of Gold. *Journal of the American Chemical Society* 2004, **126**(9): 2672-2673.
12. Guzman J, Carrettin S, Fierro-Gonzalez JC, Hao Y, Gates BC, Corma A. CO Oxidation Catalyzed by Supported Gold: Cooperation between Gold and Nanocrystalline Rare-Earth Supports Forms Reactive Surface Superoxide and Peroxide Species. *Angewandte Chemie International Edition* 2005, **44**(30): 4778-4781.
13. Abad A, Corma A, García H. Catalyst Parameters Determining Activity and Selectivity of Supported Gold Nanoparticles for the Aerobic Oxidation of Alcohols: The Molecular Reaction Mechanism. *Chemistry – A European Journal* 2008, **14**(1): 212-222.
14. Yamaguchi K, Mizuno N. Scope, Kinetics, and Mechanistic Aspects of Aerobic Oxidations Catalyzed by Ruthenium Supported on Alumina. *Chemistry – A European Journal* 2003, **9**(18): 4353-4361.
15. Wang X, Andrews L. Gold Is Noble but Gold Hydride Anions Are Stable. *Angewandte Chemie International Edition* 2003, **42**(42): 5201-5206.
16. Sanchez A, Abbet S, Heiz U, Schneider WD, Häkkinen H, Barnett RN, Landman U. When Gold Is Not Noble: Nanoscale Gold Catalysts. *The Journal of Physical Chemistry A* 1999, **103**(48): 9573-9578.

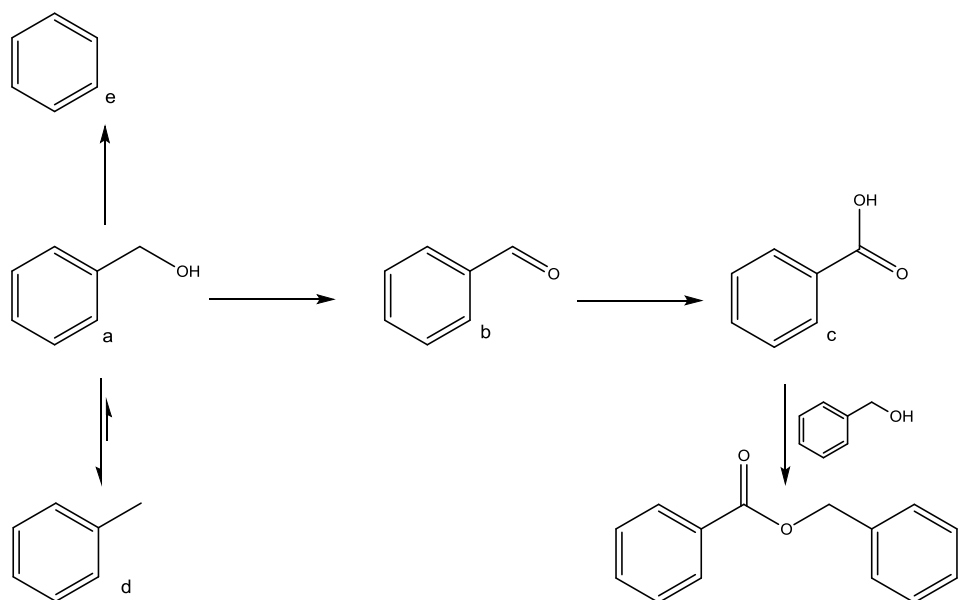
17. Pushkarev VV, Kovalchuk VI, d'Itri JL. Probing Defect Sites on the CeO<sub>2</sub> Surface with Dioxygen. *The Journal of Physical Chemistry B* 2004, **108**(17): 5341-5348.
18. Sankar M, Nowicka E, Tiruvalam R, He Q, Taylor SH, Kiely CJ, Bethell D, Knight DW, Hutchings GJ. Controlling the Duality of the Mechanism in Liquid-Phase Oxidation of Benzyl Alcohol Catalysed by Supported Au–Pd Nanoparticles. *Chemistry – A European Journal* 2011, **17**(23): 6524-6532.
19. Yang X, Wang X, Liang C, Su W, Wang C, Feng Z, Li C, Qiu J. Aerobic oxidation of alcohols over Au/TiO<sub>2</sub>: An insight on the promotion effect of water on the catalytic activity of Au/TiO<sub>2</sub>. *Catalysis Communications* 2008, **9**(13): 2278-2281.
20. Bongiorno A, Landman U. Water-Enhanced Catalysis of CO Oxidation on Free and Supported Gold Nanoclusters. *Physical Review Letters* 2005, **95**(10): 106102.
21. Liu LM, McAllister B, Ye HQ, Hu P. Identifying an O<sub>2</sub> Supply Pathway in CO Oxidation on Au/TiO<sub>2</sub>(110): A Density Functional Theory Study on the Intrinsic Role of Water. *Journal of the American Chemical Society* 2006, **128**(12): 4017-4022.
22. Molina LM, Hammer B. Active Role of Oxide Support during CO Oxidation at Au/MgO. *Physical Review Letters* 2003, **90**(20): 206102.
23. Molina LM, Hammer B. Theoretical study of CO oxidation on Au nanoparticles supported by MgO(100). *Physical Review B* 2004, **69**(15): 155424.

# Chapter 5

## 5. Cinnamyl Alcohol Oxidation

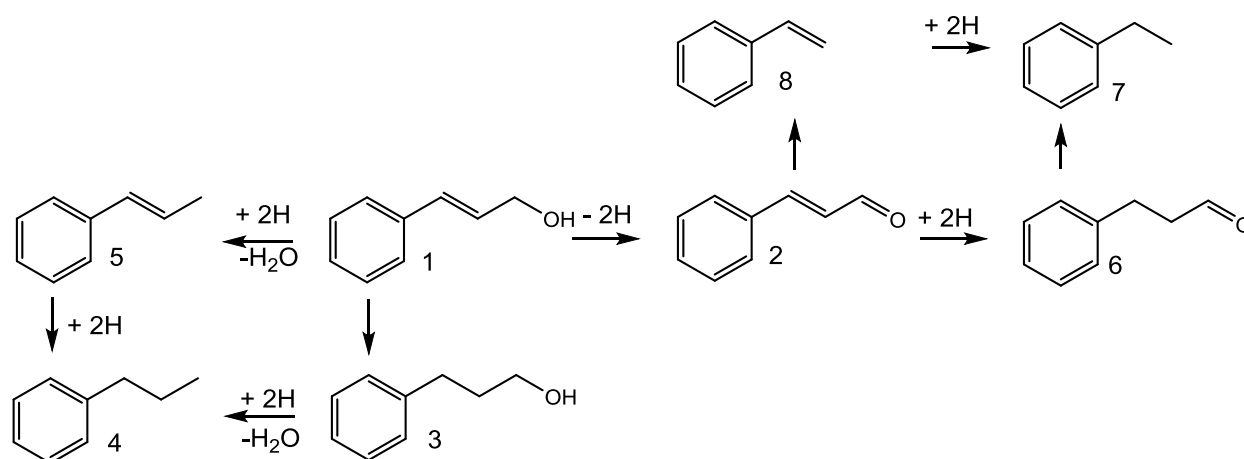
### 5.1. Introduction

Benzyl alcohol oxidation is a standard test for the oxidation potential of supported gold catalysts on metal oxides<sup>1</sup>. Building upon work in chapter 3, it was investigated whether cinnamyl alcohol would display similar results to benzyl alcohol oxidation with supported Au and Au:Pd catalysts on metal oxides. Cinnamyl alcohol is vinylogous<sup>2</sup> to benzyl alcohol, differing in structure only by the addition of a double bond between the terminal OH group and benzene ring. Cinnamyl alcohol was expected to display similar catalytic oxidation activity using Au and Au:Pd supported on metal oxides to that of benzyl alcohol. Cinnamaldehyde is used extensively in the perfume industry and is a useful precursor molecule.



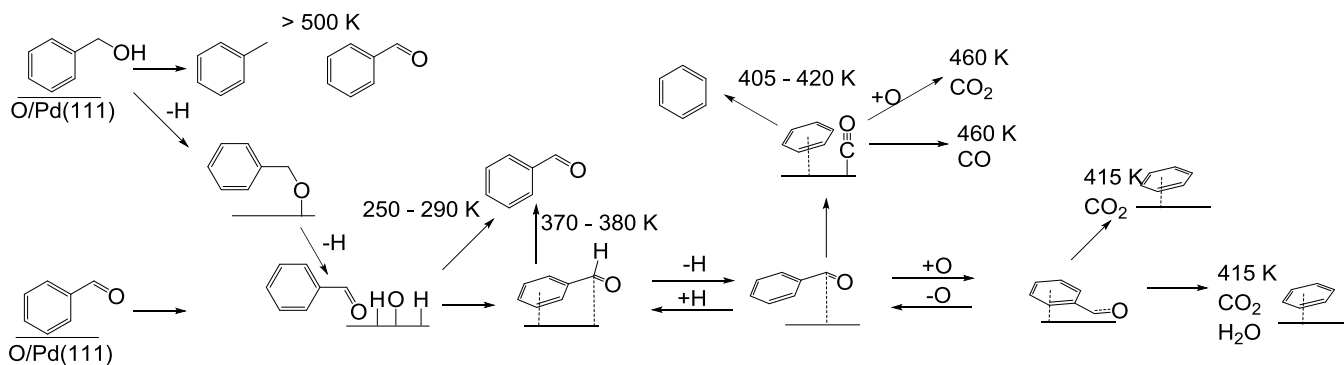
**Figure 5-1** General reaction scheme of benzyl alcohol using Au:Pd bimetallic catalysts on activated carbon, 0.05 g catalyst, 120 °C, O<sub>2</sub> (150 psi), 6 h. Benzyl alcohol (a), benzaldehyde (b), benzoic acid (c), toluene (d), benzene (e) and benzyl benzoate (f)<sup>3</sup>

Figure 5-1 shows the general reaction scheme for benzyl alcohol when oxidised by an Au:Pd bimetallic catalyst supported on activated carbon. This reaction scheme can be compared to the reaction scheme for cinnamyl alcohol oxidation; previous studies have demonstrated a possible oxidation pathway depicted in Figure 5-2<sup>4</sup>, utilising a Pd catalyst supported on Al<sub>2</sub>O<sub>3</sub>. Comparing Figure 5-1 and Figure 5-2, cinnamyl alcohol has two more potential oxidation products compared to benzyl alcohol, but also shares some vinylogous product structures. These include both alcohols being oxidised to their corresponding aldehyde and the formation of vinylogous styrene molecules. Cinnamyl alcohol does not seem to undergo over-oxidation to the corresponding acidic moiety to form cinnamic acid, the potential formation of a benzoate product is prevented. Cinnamyl alcohol contains a double bond which provides an additional reaction centre compared to that of benzyl alcohol, allowing additional products to form when compared to benzyl alcohol.



**Figure 5-2** General reaction scheme of cinnamyl alcohol (1 g) in toluene (30 ml), at 65 °C using a Pd/Al<sub>2</sub>O<sub>3</sub> catalyst (0.10 g, 5 wt.%). Cinnamyl alcohol (1), cinnamaldehyde (2), 3-phenyl-1-propanol(3), propylbenzene (4), *trans*-β-methylstyrene (5), 3-phenylpropanal (6), ethylbenzene (7), styrene (8)<sup>4</sup>

The product of interest in this study is the aldehyde moiety with both reaction schemes being similar in nature in that the alcohol undergoes direct oxidation to the corresponding aldehyde. It was investigated how well this reaction step occurred under the reaction conditions described in this chapter. No double bond isomerisation was observed during these reactions which is also true for previous work with this molecule<sup>5</sup>.



**Figure 5-3 Reaction scheme of benzyl alcohol over an oxygen pre-covered Pd(111) surface<sup>6</sup>**

This is indicative of the high reactivity of the C=C bond with bimetallic catalysts supported on metal oxides due to cinnamyl alcohol's ability to undergo multiple bonding interactions with metallic catalysts. Whereas benzyl alcohol bonds to the metal centres via its C=O bond as shown in Figure 5-3<sup>6</sup>, cinnamyl alcohol has the ability to bond simultaneously to metal centres via its O-H bond and C=C bond as depicted in Figure 5-4. The distance between the centres of the two Pd cores was determined by EXAFS to be ca. 2.76 Å and is consistent with the distance between the centre of the C=C bond and the O-H bond of the alcohol group in cinnamyl alcohol (ca. 2.80 Å) calculated by PM3 MOPAC<sup>7</sup>.

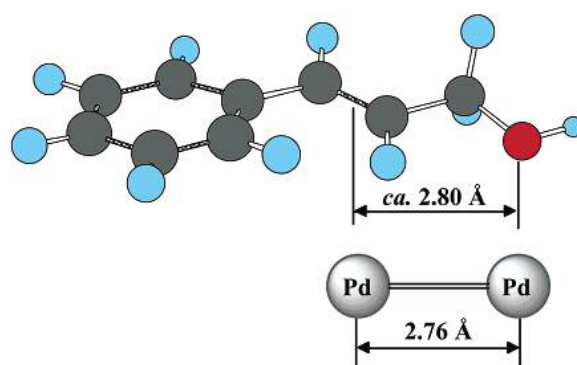


**Figure 5-4 Schematic representation of cinnamyl alcohol interacting with Pd-Pd paired site supported on hydroxyapatite<sup>7</sup>**

The distance between the two Pd cores mentioned above is analogous to the distance between Au:Pd bimetallic cores demonstrated in work by Baiker *et al.*<sup>8</sup> which determined the size distribution of Au:Pd bimetallic particles prepared by a colloidal preparation route to be between 2.4 nm and 3.7 nm with the distance between metal centres being ca. 2.6 – 2.8 Å.

This was calculated using EXAFS and is highlighted in Figure 5-5. Baiker *et al.* also demonstrated that as the nanoparticle size increased, the reactivity decreased. The researchers exposed the metal catalysts to high temperature  $H_2$  treatment for 5 hours and redid the EXAFS experiments. The nanoparticles had increased in size and conversion had markedly decreased, however, selectivity remained high. As nanoparticles grow, the number of surface atoms available to react decreases which would lead to a general reduction in activity and not one so dramatic; It was thought that further reduction of the constituent Pd present in the nanoparticles by  $H_2$  treatment would create a closed shell structure which would counteract the promotion effect that gold has on Au:Pd catalysts by preventing it from being involved in reactions. Consequently, Baiker *et al.* conclude that reactions with Au:Pd nanoparticles and substrates may occur mainly at gold atoms or at the interface between the gold and palladium interface within the bimetallic particles.

Baiker *et al.* also conducted XANES analysis on Au:Pd bimetallic catalysts, work which is complemented by Miller *et al.*'s<sup>9</sup> work using XANES. Miller *et al.* showed that smaller Au nanoparticles have increased reactivity due to their increased d electron density when compared to bulk Au. This increase in density is coupled with a narrowed d band which is shifted closer to the Fermi level, facilitating electronic configuration changes in reacting molecules and increasing the metal clusters' reactivity.

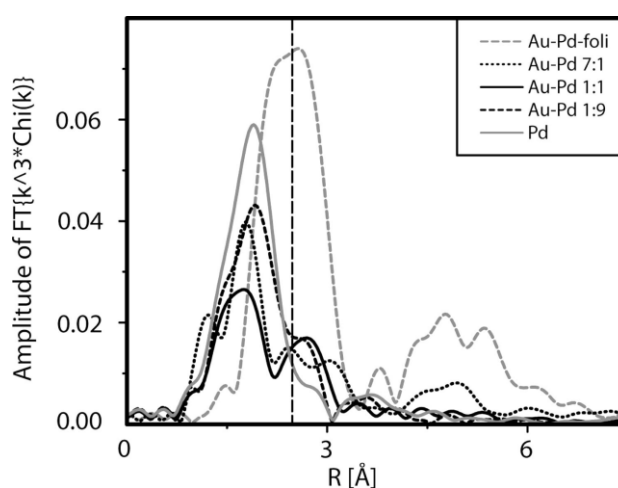


**Figure 5-5<sup>8</sup>**  $k_3$ -weighted magnitude of FT EXAFS signals for various Au:Pd ratio bimetallic particles<sup>8</sup>

<sup>8</sup> Reprinted (adapted) with permission from reference 8. Copyright 2009 American Chemical Society.



This conclusion supports work by Baiker *et al.* who found that the electronic configurations of Au and Pd were altered upon mixing the two elements. This mixing resulted in a shift to lower binding energies, a conclusion which was supported by XPS analysis of Au core levels with increasing Pd content. Au XANES indicated a decrease in d holes in the Au 5d valence band, resulting in an increase in density compared to bulk Au and the valence band had been shifted closer to the Fermi level. When bands are shifted closer to the Fermi level, the metal can conduct electrons easier due to the low barrier of energy for the electronic transition. If the band gap between the Fermi level and the d band increased, this would give the metal nanoparticles a more insulator like characteristic and would lower their reactivity.

Whilst the above research considers the electronic structures of the metal nanoparticles, these electronic changes do not seem to be influenced by the nature of the support. In the next section, the effect of support is investigated to see if the support can have a demonstrable effect on the activity of nanoparticles.

## 5.2. Effect of support

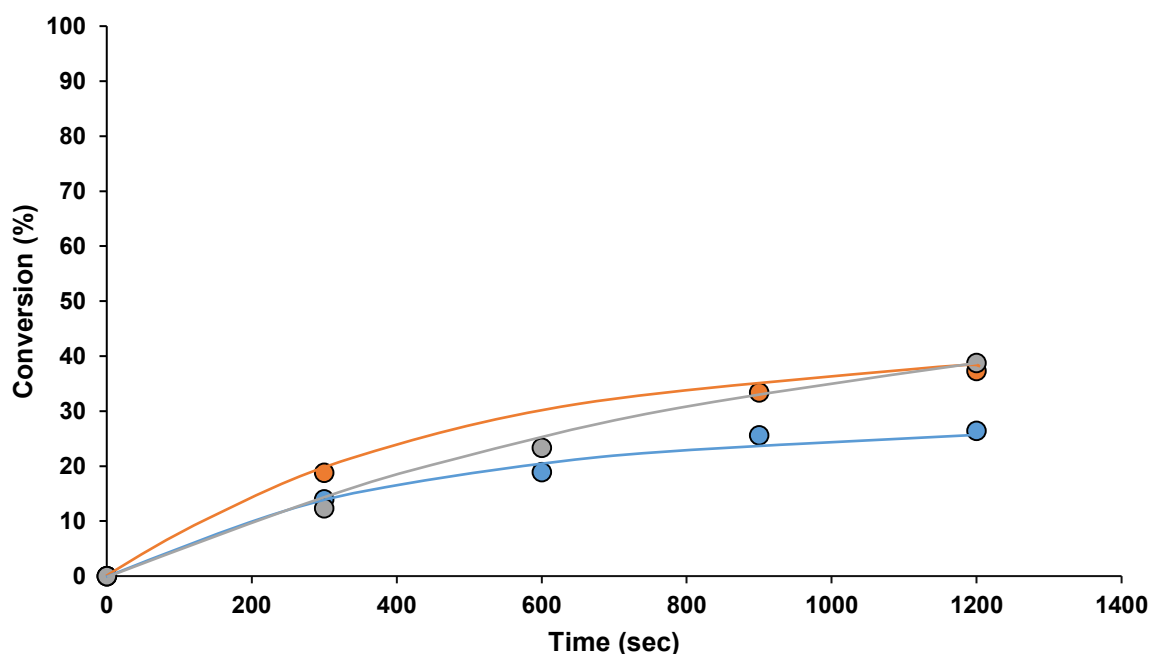


**Figure 5-6** Graph to show how conversion is influenced by the type of support used in a metal oxide supported catalyst, 20 mg of 1%AuPd supported on a metal oxide was used as a catalyst in the oxidation of 1 g cinnamyl alcohol at 120 °C at 2 bar (g) O<sub>2</sub> ZnO (●), Graphite (●) and TiO<sub>2</sub> (●)

As can be seen from Figure 5-6, the support material of the catalyst can influence the reaction. Graphite and  $\text{TiO}_2$  supports have similar activity to each other, whereas  $\text{ZnO}$  support is not as active as the other two. The selectivity between supports is also comparable to each other. As can be seen from Figure 5-7, Figure 5-8, and Figure 5-11, cinnamaldehyde is the major oxidation product for all three supports with other products being formed as minor products. For graphite, cinnamaldehyde is the major product but this support is less selective when compared to the other supports. When graphite is used as a support, phenyl propanol is produced in greater quantities compared to the other supports investigated where it is only present as a minor product.

Research by Choudhary *et al.*<sup>10</sup> indicated that the support material can have an influence on the nanoparticles immobilised onto the support. The researchers tested supported Au catalysts on a range of supports with benzyl alcohol and found that  $\text{U}_2\text{O}_3$  was the best performing support relative to the other supports in the study, achieving high conversion and selectivity. This catalyst was followed by  $\text{Au/MgO}$ ,  $\text{Au/Al}_2\text{O}_3$  and  $\text{Au/ZrO}_2$  which also demonstrated high activity. Whilst all were highly active, the selectivity profiles for each of the catalysts were different, depending on the support. In all cases, the major oxidative product was the aldehyde variant of the starting alcohol.

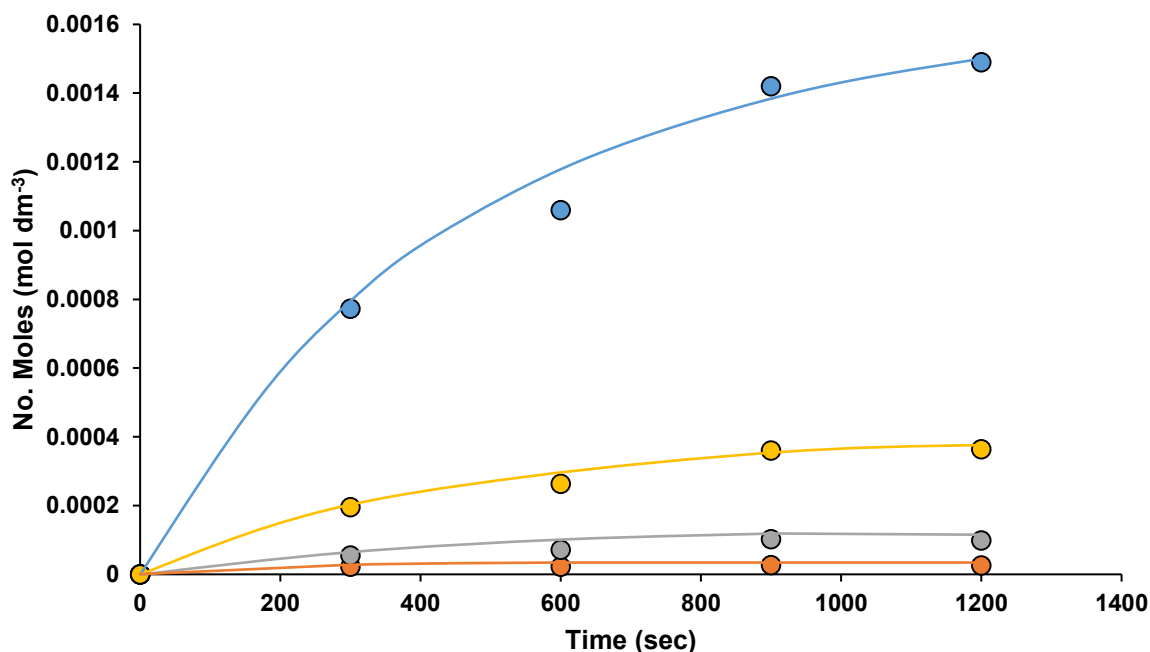
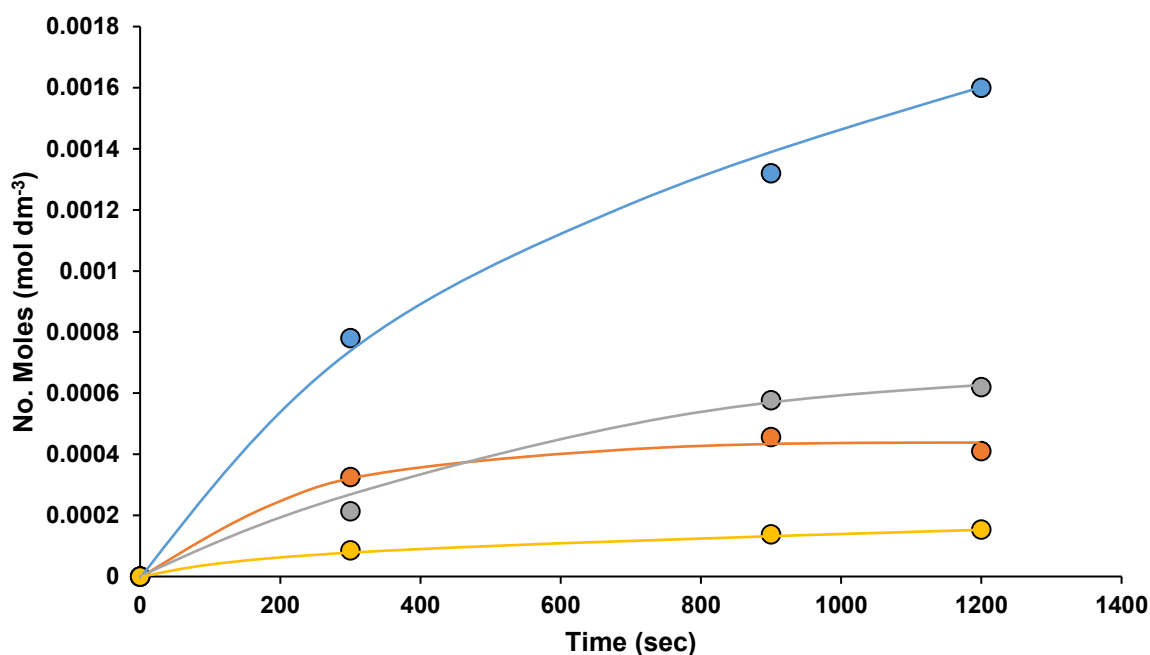


**Figure 5-7** Graph to show product distribution for 20 mg of a 1%AuPd catalyst supported on ZnO catalyst in the oxidation of 1 g cinnamyl alcohol at 120 °C at 2 bar (g) O<sub>2</sub> cinnamaldehyde (●), Benzaldehyde (○), methyl styrene (◐), phenyl propanol (●)

Figure 5-7 shows that cinnamyl alcohol, when reacted with Au: Pd supported on ZnO, the major oxidative product is the aldehyde analogue of the starting alcohol. As the aldehyde was the major product, and cinnamyl alcohol is vinylogous to benzyl alcohol, any explanation for support interactions with Au, Pd and Au: Pd should be directly relatable to cinnamyl alcohol.

As previously mentioned, work by Choudhary *et al.*<sup>10</sup> does not explain the possible origin of the support effects in their systems. Work by Suo *et al.*<sup>11</sup> demonstrated Au on Uranium oxide, both UO<sub>3</sub> and U<sub>3</sub>O<sub>8</sub>, were highly active catalysts for water-gas shift reactions. This was due to Uranium oxides exhibiting a physical influence on the WGS reaction depending on the oxidation state of the Uranium oxide, the structure of which could vary between microporous and mesoporous. When in the microporous state the corresponding pore sizes within the catalyst structure were smaller making the transportation of reactant molecules towards the catalyst active sites more difficult. Conversely, in the mesoporous state the reactant molecules were more easily able to be transported to the active sites of the catalyst, resulting in a catalyst with higher activity for the oxidation of alcohol.

Whilst this work may not directly link to the choice of supports presented in this research, it is highlighted to demonstrate that support effects may not always be electronic in nature but structural. The fact that activity was increased due to increasing pore size is a good way to demonstrate that physical properties of catalyst design should be considered at an early stage as they can be an unintended barrier to reaction. In this research, the supports used were graphite, ZnO and TiO<sub>2</sub>. None of these supports should be considered in terms of microporous and mesoporous pore sizes but they may have other physical attributes that influence the reactivity of cinnamyl alcohol.



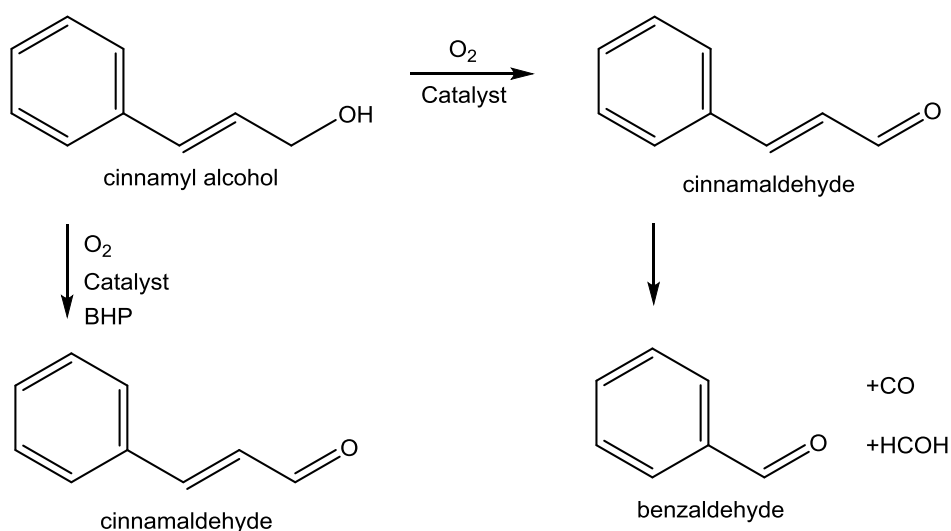
**Figure 5-8** Graph to show product distribution for 20 mg of a 1% AuPd catalyst supported on graphite catalyst in the oxidation of 1 g cinnamyl alcohol at 120 °C at 2 bar (g) O<sub>2</sub>  
cinnamaldehyde (●), Benzaldehyde (●), methyl styrene (●), phenyl propanol (●)

Figure 5-8 shows the selectivity obtained from the oxidation of cinnamyl alcohol using a 1% AuPd catalyst supported on graphite catalyst. As can be seen from the graph, the major product is cinnamaldehyde (Figure 5-2) however, selectivity towards cinnamaldehyde for the graphite support is not as high compared to the selectivity obtained from TiO<sub>2</sub> even though their activity is approximately the same (Figure 5-6). Additionally, the graphite support produced a lot more benzaldehyde when compared to ZnO and TiO<sub>2</sub> supports in which benzaldehyde was detected in trace amounts.

For benzaldehyde to be produced from cinnamyl alcohol, cleavage of the carbon-carbon double bond needs to occur. Work by Rossi *et al.*<sup>12</sup> suggested this can occur via different reaction mechanisms involving either a *cis*-diol intermediate, epoxidation or a radical-chain oxidation pathway. Cleavage of carbon-carbon double bonds within molecules is its own area of interest as this reaction adds additional functionalities to molecules derived from renewable sources, converting them into valuable precursor products<sup>13</sup>.

Cinnamyl alcohol, unlike benzyl alcohol, readily undergoes autoxidation to produce epoxy cinnamyl alcohol and cinnamaldehyde<sup>14</sup> to the extent that a sample open to the air would contain only 36% of the starting amount of cinnamyl alcohol. To mitigate this, the reactions were performed and then immediately analysed to prevent any additional drift in analysis of the product mixture. To further prevent autoxidation the product mixture was placed into airtight GC vials and the starting material was kept in the fridge in an opaque bottle. Blank reactions, whereby cinnamyl alcohol is exposed to the reaction conditions of the study but without catalyst present, would help determine the level of autoxidation occurring and is an aspect that will be tested in future work.

Returning to the possible mechanism for benzaldehyde production, Rossi *et al.*<sup>12</sup> concluded that benzaldehyde was produced via a radical pathway. When the radical trap BHP (2,6-di-*tert*-butyl-4-methylphenol) was added to cinnamyl alcohol in reaction conditions, selectivity greatly shifted to cinnamaldehyde (~97%) whereas conversion decreased from 99% to 70%. Benzaldehyde is stable to radical oxidation<sup>15</sup> and so no further oxidation would occur beyond this point. Because of this research, the following reaction scheme was proposed for the formation of benzaldehyde when reacted with AuAg nanotubes.



**Figure 5-9** Reaction scheme for the reaction of cinnamyl alcohol with an AuAg nanotube catalyst<sup>12</sup>

As benzaldehyde was a notable product with AuPd supported on graphite, a radical pathway may be in operation for this catalyst but not when ZnO or TiO<sub>2</sub> is used as a support. As no initiator was used for these reactions, the radical mechanism would have begun with either a trace amount of an initiator present in the starting compound (cinnamyl alcohol may have contained hydroperoxide species) or the Au within the AuPd catalyst may have directly activated the oxygen used in the experiments<sup>16</sup>. This would have been present in all reactions with the varying support, addition of a radical trap would help elucidate the extent of a radical mechanism within the catalytic system.

Ionita *et al.*<sup>17</sup> found Au supported catalysts are able to directly activate molecular oxygen and produce oxygen containing radicals which are able to react with adsorbed species on the catalyst surface. Ionita's team proposed that molecular oxygen adsorbs onto the surface of the gold catalyst to form the active catalyst structure. This superoxide-type species then abstracts a hydrogen atom from the incoming ligand, in this case an allylic alcohol, creating a free radical. Ionita *et al.* were able to successfully trap this radical with DMPO and their findings were consistent with other research that featured radical exchange reactions<sup>18</sup>.

The surface chemistry of graphite may also play a role in the increased occurrence of benzaldehyde formation. Rodríguez-Ramos *et al.*<sup>19</sup> studied the surface chemistry of HSAG (High Surface Area Graphite) and found many different oxygen containing functional groups on its surface. Rodríguez-Ramos found aromatic compounds interacted differently to HSAG

depending on the surface chemistry of the support, when the support was de-functionalised aromatic compounds did not readily adsorb onto the graphite's surface. It was thought that pores and discontinuities within the support were the dominant energetic sites and so adsorption would occur in these areas of the support, however, aromatic compounds did not seem to interact at these sites. When the graphite support had surface functionalisation, adsorption would preferentially occur on the surface which is readily accessible to the molecules. Surface oxygen species prevented aromatic alcohols from interacting with edge sites on the HSAG. Rodríguez-Ramos concluded the affinity of aromatic compounds towards graphite was greatest on the basal plane due to specific interaction between the aromatic ring and C-C  $\pi$  electrons.

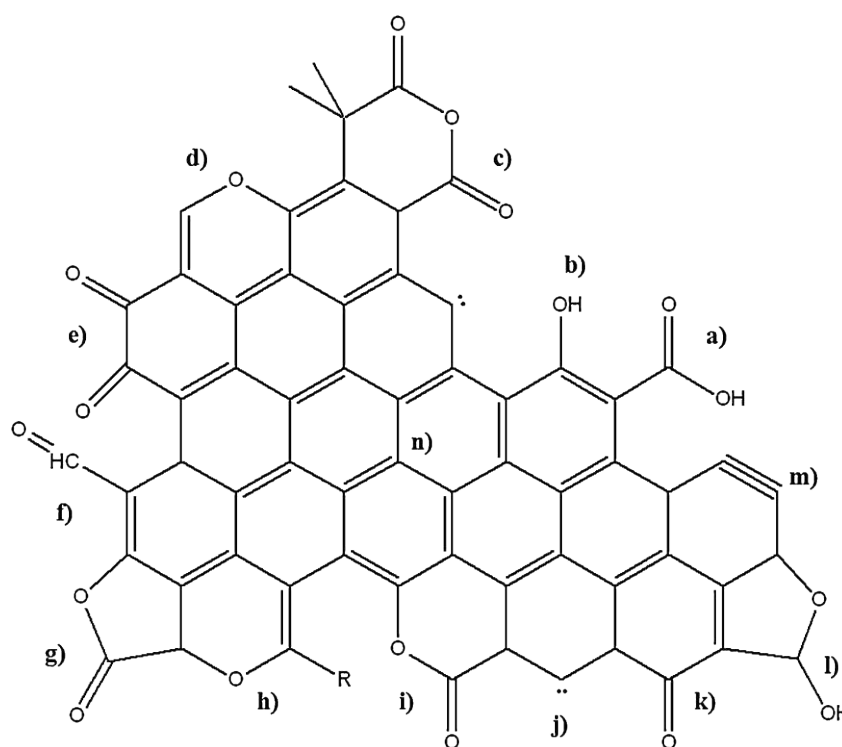


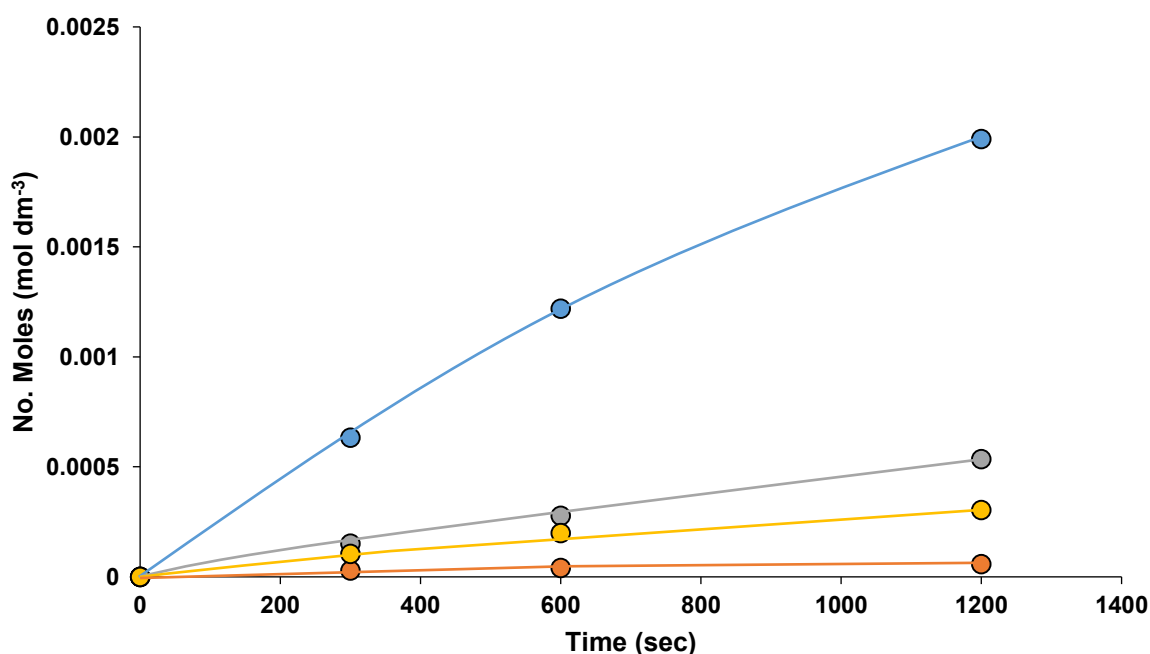
**Figure 5-10 – Oxygen containing species generally present on carbon surfaces and their decomposition products via TPD: (a) carboxylic acid, (b) phenol, (c) carboxylic anhydride, (d) ether, (e) quinone, (f) aldehyde, (g) lactone, (h) chromene, (i) pyrone, (j) carbene like species, (k) carbonyl, (l) lactol, (m) carbene like species and (n)  $\pi$  electron density on carbon basal plane<sup>20, 9</sup>**

A review by Serp *et al.*<sup>20</sup> highlighted the typical heteroatoms that are present on carbon supports such as graphite, which are oxygen, hydrogen, nitrogen, boron, sulphur and

<sup>9</sup> Reprinted from Coordination Chemistry Reviews, Vol 308, Serp *et al.*, Coordination Chemistry on Carbon Surfaces, 236-345, Copyright 2016, with permission from Elsevier

phosphorus. These heteroatoms are chemisorbed onto the carbon surface which contributes to the complex chemistry of carbon supports. This could be a possible reason as to why the graphite supported AuPd catalyst had a different selectivity profile when compared to  $\text{TiO}_2$  and  $\text{ZnO}$  supports. These have less surface heteroatoms chemisorbed to the surface. Oxygen confers a hydrophilic and cation exchange property to the carbon support whereas nitrogen containing carbon supports show an enhanced anion exchange properties and evidence of redox reaction activity. Combining both oxygen and nitrogen onto the surface leads to additional properties for the carbon support<sup>21</sup>. Whilst the surface heteroatoms resemble conventional organic molecules, as shown in Figure 5-10, it is not easily predicted how these surface atoms will interact with each other much less the incoming reaction substrates.

This research was not concerned with identifying the potential surface heteroatoms on the graphite support used but this may be an area of further study to complement the existing literature which is available for Au clusters supported on graphite<sup>22, 23, 24</sup>.



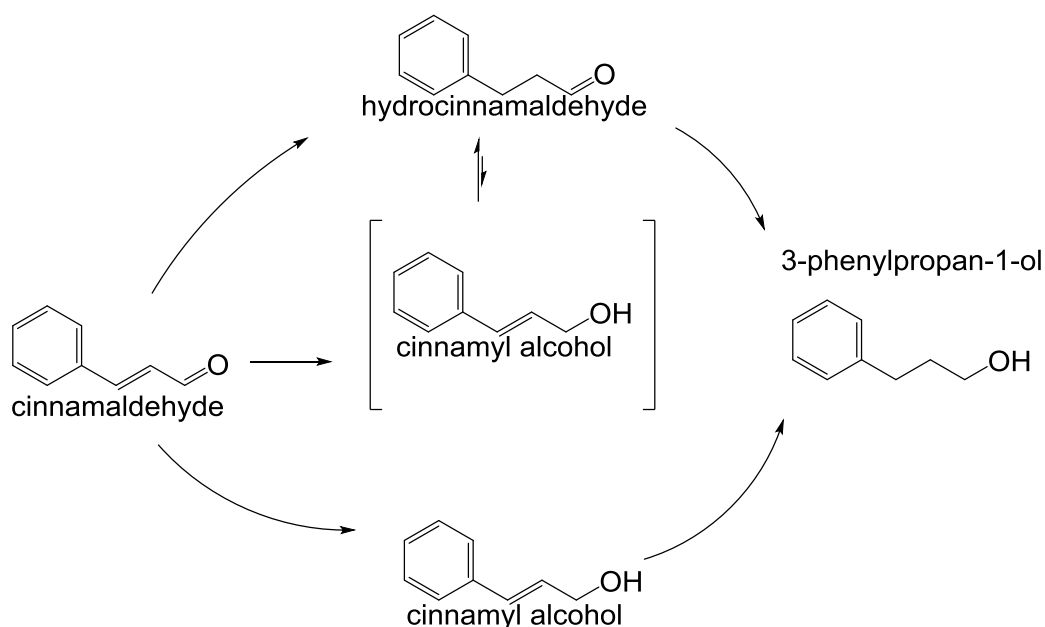
**Figure 5-11** Graph to show product distribution for 20 mg of 1%AuPd catalyst supported on  $\text{TiO}_2$  catalyst in the oxidation of 1 g cinnamyl alcohol at 120 °C at 2 bar (g)  $\text{O}_2$  cinnamaldehyde (●), Benzaldehyde (●), methyl styrene (●), phenyl propanol (●)

Figure 5-11 shows the oxidation of cinnamyl alcohol with a 1%AuPd catalyst supported on  $\text{TiO}_2$ . As can be seen from the graph, benzaldehyde formation is very low with the major



product being cinnamaldehyde. Some methyl styrene was produced along with phenyl propanol. The 1%AuPd supported on  $\text{TiO}_2$  catalyst is similar in activity to the analogous ZnO supported catalyst, however, whilst both catalysts major product was cinnamaldehyde, the minor products were present in differing ratios. For the AuPd supported on ZnO, the minor products were, in order of greatest to lowest, phenyl propanol, methyl styrene and benzaldehyde. Compare this to the AuPd on  $\text{TiO}_2$  whereby more methyl styrene was produced than phenyl propanol.

Production of methyl styrene and phenyl propanol arise from hydrogenation of either cinnamyl alcohol or cinnamaldehyde. Previous research has indicated various mechanisms to explain these hydrogenation products, such as Pietropaolo *et al.*<sup>25</sup> who studied SnPt catalysts on nylon. Pietropaolo *et al.* found four distinct pathways in this system for the hydrogenation products previously mentioned. Pietropaolo *et al.* suggested these pathways arose from new catalytic sites created on the catalyst surface from the bimetallic metals not being a homogeneous alloy, allowing a two-site structure to exist. Promotor cations can chemisorb to one metal whilst the unsaturated part of the reactant coordinates to the other metal. From previous work on AuPd nanoparticles prepared via sol-immobilisation, it is known that these catalysts form a homogeneous alloy<sup>26</sup>, therefore the two-site mechanism proposed by Pietropaolo *et al.* may not be applicable in these systems.



**Figure 5-12 Possible reaction mechanism for the hydrogenation of cinnamaldehyde to form 3-phenylpropan-1-ol<sup>27</sup>**

An alternative to the two site structure is work proposed by Webb *et al.*<sup>27</sup> where phenyl propanol is produced from the sequential hydrogenation of cinnamaldehyde to phenyl propanol via hydrocinnamaldehyde (Figure 5-12). In this work, it was discovered that after conversion of ca. 20% of cinnamaldehyde phenyl propanol formation was induced. This, the team suggested, was indicative of the catalyst surface being modified by hydrocinnamaldehyde during the initial stages of reaction. Once enough hydrocinnamaldehyde had been produced, the reaction pathway to phenyl propanol was triggered and thus was detected in the reaction mechanism.

It could therefore be surmised that as the catalysts in this study were homogeneous alloys, this latter phenomenon proposed by Webb *et al.*<sup>27</sup> may be present in the AuPd catalyst system as step sites between the two metals Au and Pd when prepared via sol-immobilisation do not exist due to their alloy nature. As AuPd catalysts are a bimetallic system, there is a known promoter effect in operation between the Au and Pd. This has been extensively studied with benzyl alcohol but it may also be influencing the hydrogenation pathway in the cinnamyl alcohol system. Previous work<sup>28</sup> on RuSn sol-gel catalysts has hypothesised that positively charged cationic sites are formed within the catalytic system which activates the C=O bond but does not affect the olefinic part of the molecule. Finally, isolated C=C bonds are more reactive than C=O bonds and is likely to be related to adsorption bond strength<sup>29</sup>. Substitution with phenyl groups decreases the reactivity of the C=C bond through steric effects. Putting this previous work together suggests the formation of phenyl propanol is via hydrogenation of cinnamaldehyde and is being promoted via cationic species on the surface of the AuPd system.

Therefore, it can be surmised that cinnamyl alcohol is oxidised to cinnamaldehyde, this cinnamaldehyde is then able to be catalytically hydrogenated to various compounds. Depending on the support material, different hydrogenation pathways are present. On the ZnO support, the hydrogenation pathway resulting in the formation of 3-phenylpropan-1-ol is the most active in the system. For the TiO<sub>2</sub> catalyst, a similar pathway is in existence but instead of hydrogenation to 3-phenylpropan-1-ol, it is further hydrogenated to *trans*- $\beta$ -methylstyrene due to the TiO<sub>2</sub> support imparting a higher reactivity in the catalytic system. This higher activity may be the result of a lower activation barrier in both the oxidative and hydrogenation pathways, resulting in a higher conversion of cinnamyl alcohol.

Finally, MgO was investigated as a support for AuPd catalysts in this study and results can be seen below in Figure 5-13. MgO was not a very active catalyst but it had the greatest selectivity to cinnamaldehyde out of all the supports tested. It also had the highest selectivity towards 3-phenylpropan-1-ol, suggesting that it is also an efficient hydrogenation catalyst. Previous work by Hutchings *et al.*<sup>30</sup> has demonstrated that AuPd catalysts supported on MgO display a unique property in their reaction mechanism when compared to other supports such as TiO<sub>2</sub>. It was discovered that two reaction pathways were in operation for the oxidation of benzyl alcohol on TiO<sub>2</sub>, these pathways were a disproportionation pathway which produces benzaldehyde and toluene, and a direct oxidation pathway, which produced benzaldehyde from molecular O<sub>2</sub>. MgO as a support can suppress the disproportionation pathway in benzyl alcohol and so no toluene is produced in this system.

MgO supported AuPd produced the least amount of *trans*- $\beta$ -methylstyrene from cinnamyl alcohol, as seen in Figure 5-13. This may indicate that AuPd/MgO doesn't have a hydrogenation pathway as mentioned above in the work by Hutchings *et al.* Hutchings' work highlighted that temperature was an important consideration in the disproportionation reaction; whereby higher temperatures promoted disproportionation. It was also found that O<sub>2</sub> promoted disproportionation as under aerobic conditions turn over numbers for disproportionation increased compared to anaerobic conditions. The temperature with the highest disproportionation turnover number was 393 K (120 °C) which is the same as this study. Consequently, the reaction conditions in this work are favouring disproportionation.

Hutchings *et al.* also discovered that under anaerobic conditions, which used helium instead of O<sub>2</sub>, disproportionation occurred which produced one molecule of benzaldehyde and one molecule of toluene over TiO<sub>2</sub> supported AuPd catalysts. There was no such reaction on MgO and ZnO supported AuPd catalysts. It was also found addition of a small amount of NaOH to the AuPd/TiO<sub>2</sub> system at the start of the reaction can result in a reduction of toluene production. This led Hutchings *et al.* to conclude that the difference in mechanism between MgO and TiO<sub>2</sub> was due to the basicity/acidity of the reaction mixture or the catalytic surface, which can play a key role in controlling catalytic pathways. The rationale was due to the generation of toluene involving cleavage of the C-O bond of benzyl alcohol via carbocation chemistry. In acidic environments C-O cleavage would be promoted whereas in basic conditions this would be inhibited. As TiO<sub>2</sub> is acidic and MgO is basic, the observed trend correlates with Hutchings *et al.*'s research and is also observed in this study. Using acidic TiO<sub>2</sub>

resulted in higher levels of *trans*- $\beta$ -methylstyrene being produced in comparison to MgO supported catalysts.

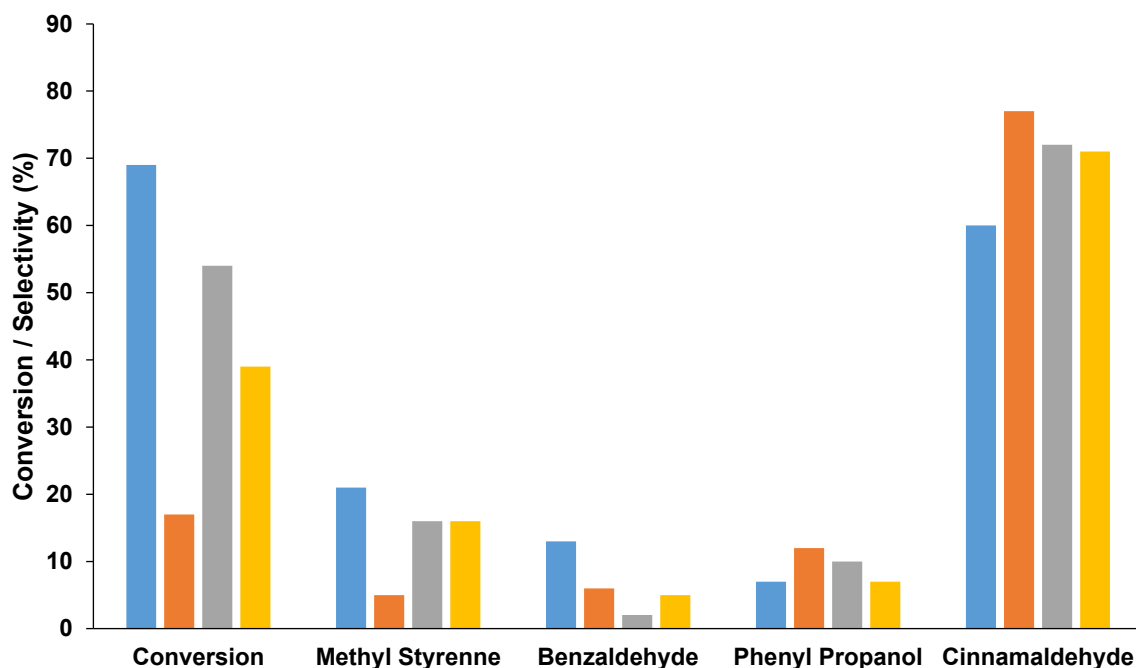


**Figure 5-13** Graph comparing different supports for the oxidation of 1 g Cinnamyl Alcohol at 120 °C, 2 bar (g) O<sub>2</sub>, with 3 g Toluene after 4 hours using 20 mg of a 1%AuPd catalyst on graphite (●), MgO (●), TiO<sub>2</sub> (●), Carbon G60 (●)

Taking all the above into consideration, the formation of *trans*- $\beta$ -methylstyrene may either be through sequential hydrogenation of cinnamaldehyde or via disproportionation as suggested by the results from the AuPd/MgO results. Further testing is required to definitively elucidate which mechanism is dominant for cinnamyl alcohol. No significant difference in electronic structure is envisioned however, the extra bulk of the molecule may introduce other factors into the catalytic system that is not in scope in this study.

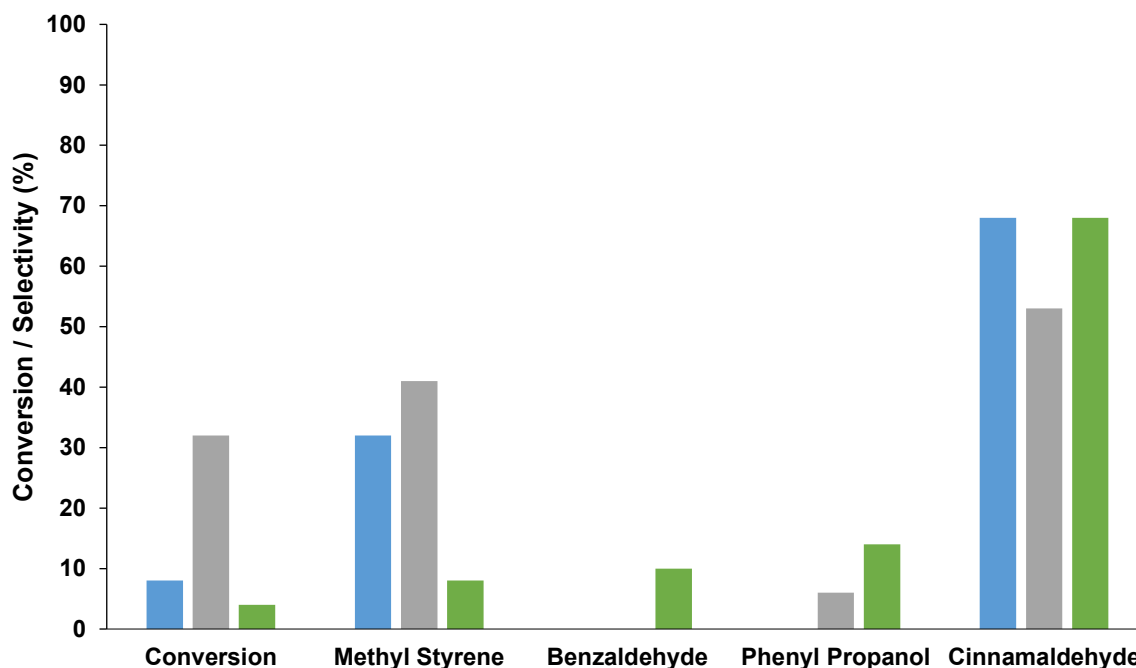


**Figure 5-14** Graph to show anaerobic conditions affect the oxidation of 1 g Cinnamyl Alcohol at 120 °C, 2 bar (g) He, 3 g toluene, 4 hours, 2 mg 1:1 Au:Pd catalyst. Graphite (●), ZnO (●), TiO<sub>2</sub> (●)

As previously mentioned, aerobic oxidation using AuPd catalysts supported on metal oxides promotes disproportionation as well as the more usual oxidation pathway. Figure 5-14 highlights the effects of carrying out the reaction of cinnamyl alcohol in helium instead of oxygen, resulting in anaerobic conditions. In this system, conversion was dramatically reduced for AuPd supported on ZnO and graphite (26% to 4% and 37% to 8% respectively). An exception to the reduction in conversion was AuPd supported on TiO<sub>2</sub>, conversion reduced from 39% under aerobic conditions to 32% in anaerobic conditions. Selectivity wasn't greatly altered, cinnamaldehyde remained the major product, closely followed by *trans*- $\beta$ -methylstyrene. Benzaldehyde production was entirely switched off under anaerobic conditions suggesting its formation is dependent on the presence of oxygen. Whilst AuPd/TiO<sub>2</sub> remained highly active for the production of cinnamaldehyde, it did not have the highest selectivity of the three supports. This was jointly shared with graphite and ZnO with selectivity towards cinnamaldehyde of 68% in each system. Notably, graphite supported AuPd catalysts resulted in no benzaldehyde or phenyl propanol but selectivity towards *trans*- $\beta$ -methyl styrene remained high. This suggests oxygen is key to produce both benzaldehyde and phenyl propanol when graphite is used as a support, hinting to the possibility that each compound is produced in a similar reaction pathway.

Another possibility to produce benzyl alcohol is via a radical mechanism which would require the activation of oxygen to initiate. Since no oxygen is available under anaerobic conditions, no radical pathway would have been initiated which supports the assumption that benzaldehyde, as well as 3-phenylpropan-1-ol, are produced via this mechanism on carbon containing supports. For non-carbonaceous supports, benzaldehyde and 3-phenylpropan-1-ol were still formed suggesting a non-radical reaction pathway present in the catalytic system.

### 5.3. Effect of temperature

Temperature is an important consideration to make when designing a catalytic system, it needs to be high enough to favour the forward reaction but low enough to minimise any waste energy put into the system. The reaction temperature in this study was 120 °C, varying this temperature to lower values (100 °C and 80 °C) lowered the conversion of the AuPd supported catalysts (Figure 5-15). This suggests 120 °C is an ideal temperature value to be running these reactions however, it would have been useful to conduct further experiments above 120 °C but this was not possible due to the equipment being used. The safe upper operating limit for the Radley's® Reactor Ready™ was 150 °C and so it was deemed the maximum safe operating temperature would be 120 °C due to the pressures involved.

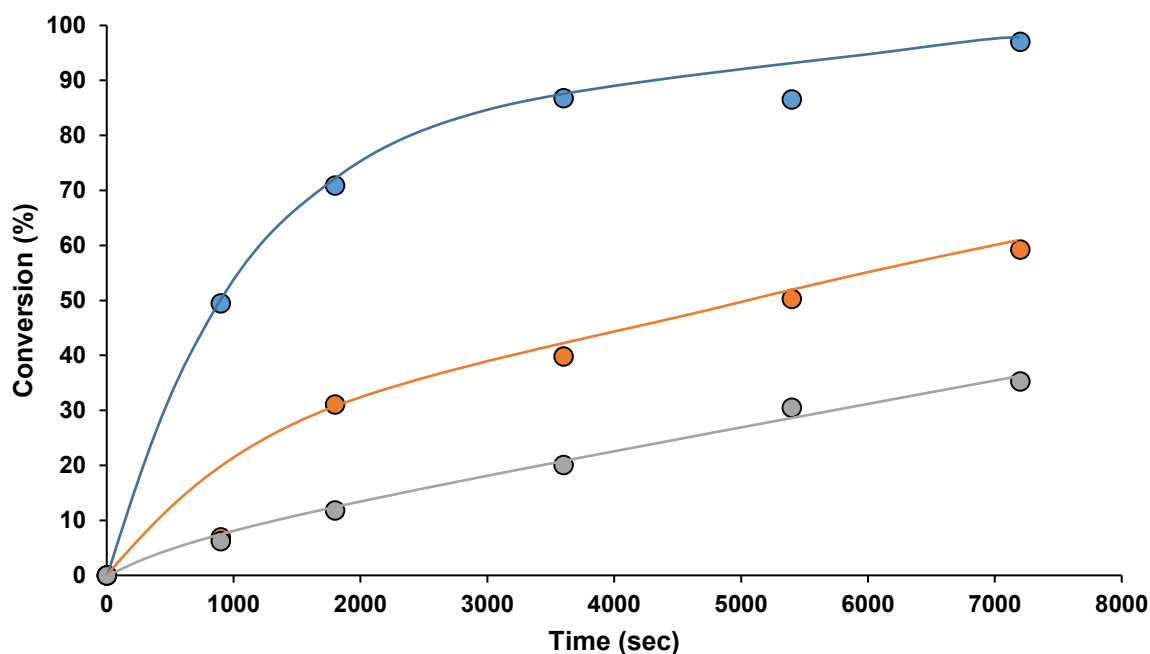


**Figure 5-15** Graph showing how temperature affects the conversion of 1 g cinnamyl alcohol in 3 g Toluene with 20 mg 1% AuPd/TiO<sub>2</sub> catalyst at 120 °C (●), 100 °C (●), 80 °C (●), 2 bar (g) O<sub>2</sub>

Hutchings *et al.*<sup>30</sup> demonstrated that higher temperatures in the oxidation of benzyl alcohol reaction promoted the disproportionation pathway displayed by AuPd catalysts supported on TiO<sub>2</sub>. AuPd catalysts supported on MgO were not used to study the effects of temperature due to the lack of disproportionation, AuPd on MgO is unique in this regard and would not have reflected the general reaction scheme of cinnamyl and benzyl alcohol over AuPd catalysts supported on metal oxides. Hutchings *et al.*'s previously mentioned research stated 120 °C was the temperature that displayed the highest amount of disproportionation and so the upper thermal limit in this study was serendipitously beneficial to the reaction rates.

As can be seen from Figure 5-15, conversion of cinnamyl alcohol at 120 °C was 97% after two hours but this reduced in line with temperature. As the temperature was lowered by 20 °C for each reaction run, conversion of the substrate lowered to ~60% and finally to ~35%. The final data point at 120 °C in Figure 5-15 may be anomalous as the preceding trend for the reaction is indicative of a either a plateau, or a slight decrease in conversion as reaction time was allowed to progress. At 100 °C, the reaction profile was linear and could suggest higher conversions could be obtained at longer reaction times. As catalysis is a trade-off between energy and time, 120 °C is still an ideal temperature even if conversion would decrease at extended reaction times as the product could be removed from the reaction mixture at maximum conversion. At 80 °C, there was again a linear reaction profile but the last data point showed a decrease in the difference between the preceding points, hinting that the rate of reaction was decreasing.

The decrease in conversion may have several explanations, the most basic being reaction rates decrease at lower temperatures due to the reduced thermal energy in the reaction system. Without this energy, the number of collisions between the reactant and active sites on the catalyst decreases; at lower temperatures, there is also a reduced number of molecules present that have the required activation energy to carry out the reaction. Whilst these two explanations apply to any system, as the AuPd/TiO<sub>2</sub> catalysts have multiple reaction pathways, the decrease in temperature may influence the various pathways in different ways, for example, shifting the equilibrium of one product from another. To test this, the selectivity would need to have been assessed during the reaction at varying temperatures. This was carried out for cinnamyl alcohol and for benzyl alcohol.

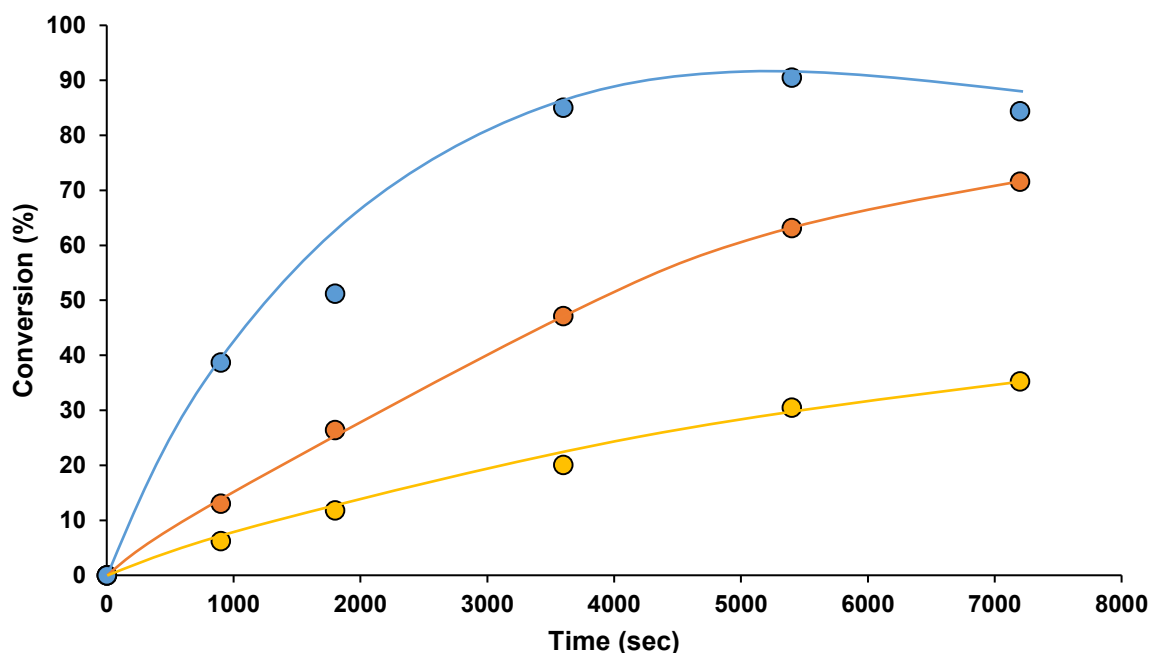


**Figure 5-16** Graph to show how temperature affects the oxidation of 1 g benzyl alcohol with a 1% (1:1 Au: Pd) AuPd/TiO<sub>2</sub> catalyst, 20 mg catalyst at 120 °C (●), 100 °C (●), and 80 °C (●) 2 bar (g) O<sub>2</sub>

Figure 5-16 shows the same reaction conditions performed for benzyl alcohol as cinnamyl alcohol and the figure shows this followed the trend as shown in Figure 5-15. For benzyl alcohol, the rate of conversion increased up to about 90 minutes after which the conversion plateaued or decreased. This may be due to the extended reaction time allowing either over-oxidation or the build-up of poisonous by-products which may have deactivated the catalyst active sites<sup>31</sup>. As these by-products build up, they will deactivate the active sites of the catalyst that are responsible for the conversion of benzyl alcohol, preventing any further reaction taking place which can result in the observed plateau.

At 100 °C, there was a linear increase in conversion as the reaction time progressed compared to 120 °C. This suggests the production of poisonous by-products which deactivate the catalyst does not occur at 100 °C. Both cinnamyl and benzyl alcohol displayed similar behaviour at this temperature. At 80 °C, the rate of conversion was at its lowest and as evident in cinnamyl alcohol oxidation, there was the beginning of a plateau after 7200 seconds.

Hermenegildo *et al.*<sup>32</sup> demonstrated deactivation of gold based catalysts was at its highest when an organic solvent was used in the catalytic system and carboxylic groups were present.



As benzyl alcohol oxidation occurred in the absence of organic solvent coupled with the fact that carboxylic acid was not detected as a reaction product, this would suggest this mechanism is not present. One possible explanation for the deactivation of the catalyst at the higher temperatures may arise from poisoning of the catalyst surface from the molecular oxygen<sup>33</sup>. Deactivation by oxygen poisoning usually manifests itself as a deviation away from the initial rate of reaction as the catalyst is deactivated and this is what appears to be happening in Figure 5-16.

An additional consideration in catalyst deactivation is the binding strength of the adsorbed by-products on the catalyst surface. On AuPd/TiO<sub>2</sub> catalysts, the bimetallic nature of the AuPd catalysts decreases the tendency of these by-products to remain on the surface. This increased desorption, whilst still contributing to the deactivation of the catalyst, contributes to a lesser degree towards the deactivation of the catalyst when compared to the monometallic catalysts<sup>34</sup>. To assess if this is the case in this system, the monometallic catalysts would need to be assessed and would be the focus of any future potential work.

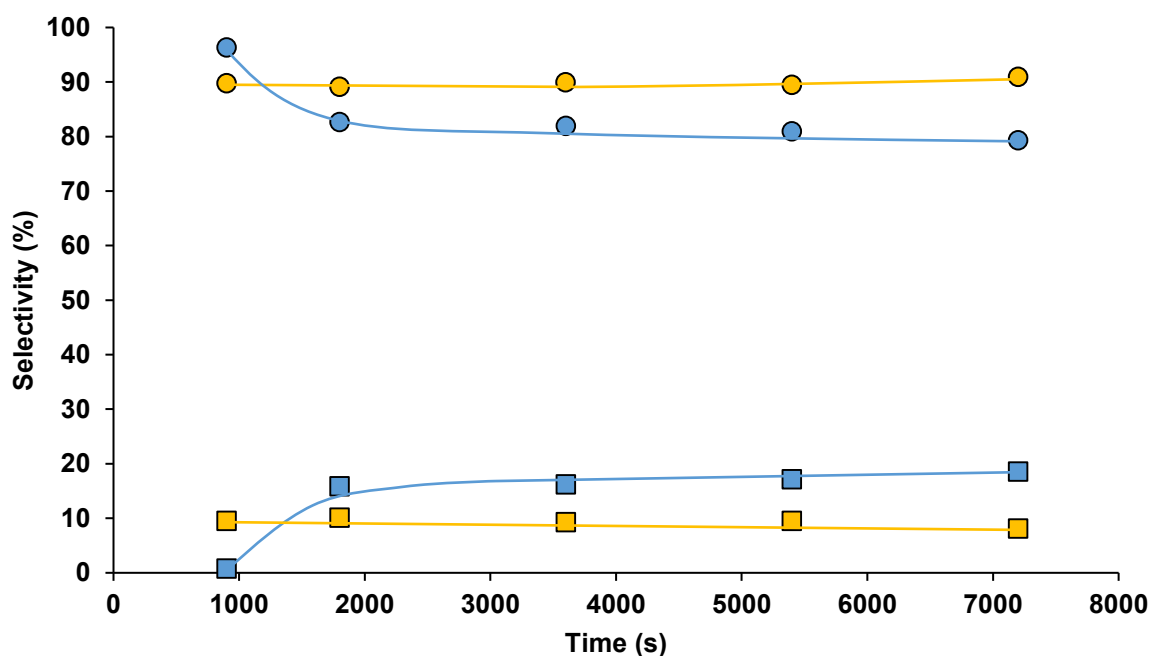
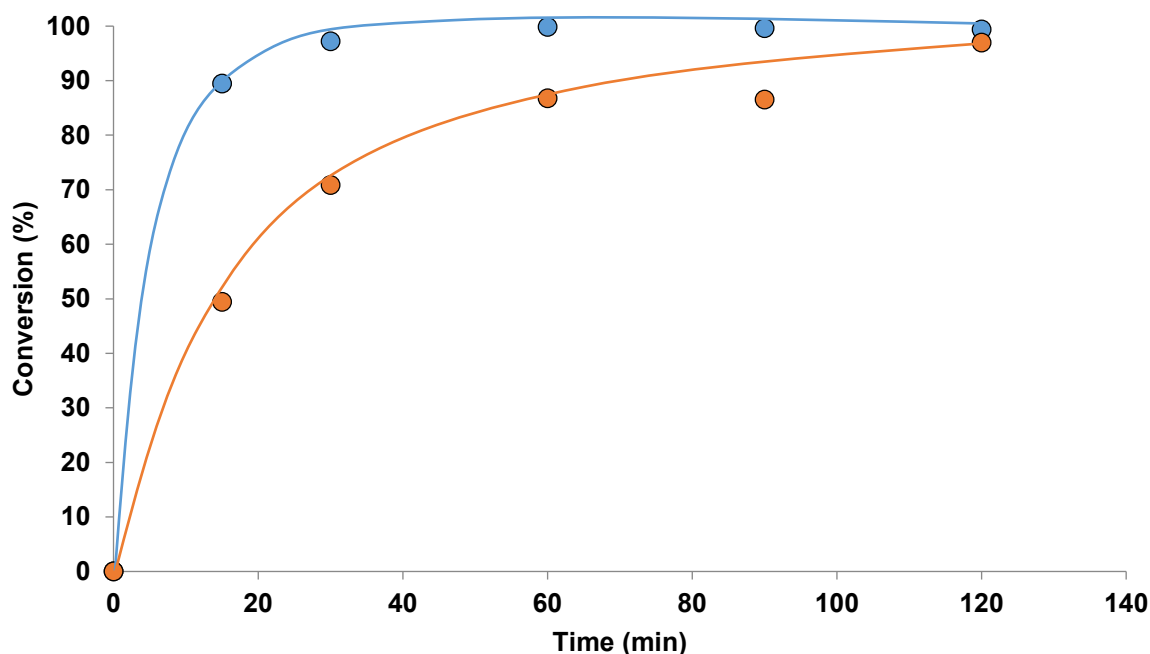


Figure 5-17 Graph to show how selectivity changes over the course of reaction at different temperatures in the reaction of Benzyl alcohol with 1%AuPd/TiO<sub>2</sub> at 100 °C and 80 °C, 20 mg 1%(1:1Au:Pd)AuPd/TiO<sub>2</sub> 100 °C Toluene(□), 100 °C Benzaldehyde (●), 80 °C Toluene (□), 80 °C benzaldehyde (●)

Concluding this investigation into the effect of temperature on benzyl alcohol oxidation, the selectivity profile of the reaction was assessed and can be seen in Figure 5-17. As can be seen from this graph, the selectivity of the reaction towards benzaldehyde was higher at 80 °C than 100 °C whereas toluene production was higher at 100 °C compared to 80 °C. As benzaldehyde is the desired product, 80 °C would be the ideal temperature to conduct this reaction to maximise advantageous product formation and minimise the side reaction that produces toluene.

#### 5.4. Effect of metal loading



**Figure 5-18 Comparison of 1 g cinnamyl alcohol oxidation with 1%AuPd/TiO<sub>2</sub> catalyst with varying Au:Pd, 1:1 (●), 1:9(●) at 120 °C, 2 bar (g) O<sub>2</sub> in 3g toluene**

As can be seen from Figure 5-18, varying the metal ratio from 1:1 molar ratio to 1:9 Au:Pd molar ratio, the initial rate of reaction was increased for the oxidation for cinnamyl alcohol. AuPd catalysts are much more active and the synergistic effect of these two metals is well known<sup>35</sup>. Only a small addition of gold is needed to enhance the oxidation of cinnamyl alcohol.

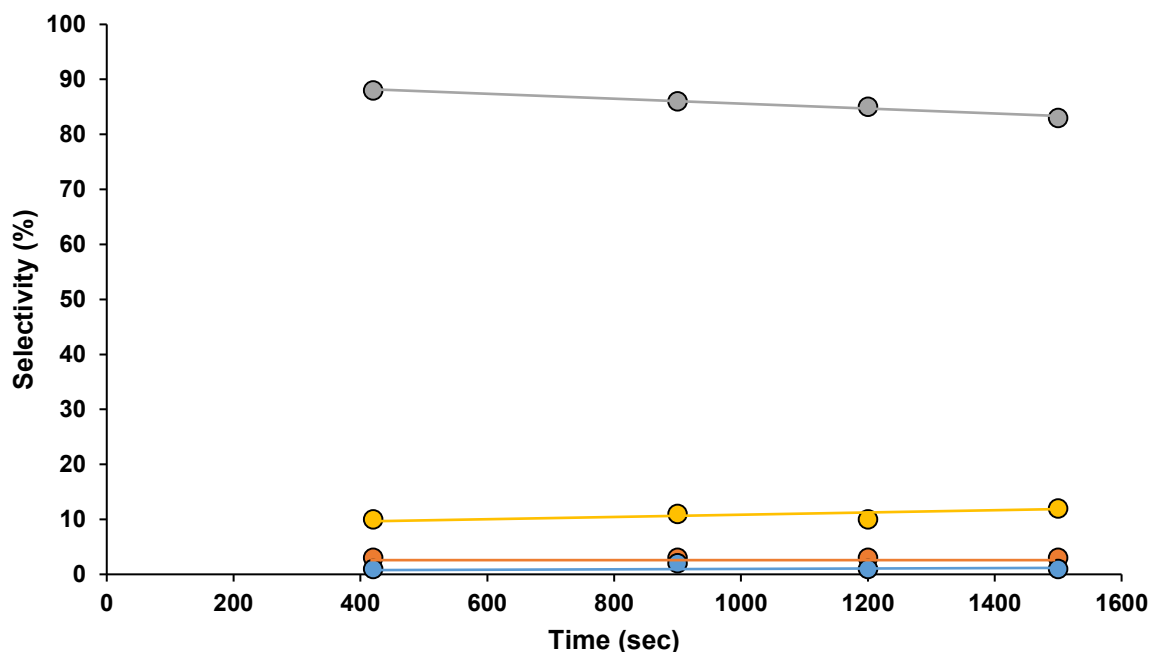


**Figure 5-19** Graph to show selectivity for the reaction of 1 g of cinnamyl alcohol with a 1%(1:9 Au: Pd) AuPd/TiO<sub>2</sub> catalyst in 3 g toluene, 20 mg catalyst at 120 °C, cinnamaldehyde (●), Benzaldehyde (●), methyl styrene (●), phenyl propanol (●), 2 bar (g) O<sub>2</sub>.

The selectivity of the reaction of a 1:9 Au: Pd molar ratio catalyst supported on TiO<sub>2</sub> is shown in Figure 5-19, immediately obvious is that cinnamaldehyde selectivity is very low and *trans*-β-methylstyrene production has been highly promoted in this system. As stated earlier, *trans*-β-methylstyrene is either produced via hydrogenation reactions in the catalytic system or through a disproportionation reaction. The disproportionation pathway is deactivated in AuPd systems when they are supported on MgO therefore further work is required to further elucidate this aspect of the reaction. Pd rich catalysts supported on TiO<sub>2</sub> possess high selectivity towards *trans*-β-methylstyrene. The available palladium in the 1:9 Au: Pd/TiO<sub>2</sub> system would be greater than the 1:1 AuPd/TiO<sub>2</sub> catalyst as these are molar ratios based on a 1% metal loading for 2 g of catalyst. Hydrogenation may therefore be promoted by palladium under these reaction conditions when cinnamyl alcohol is used as a substrate.

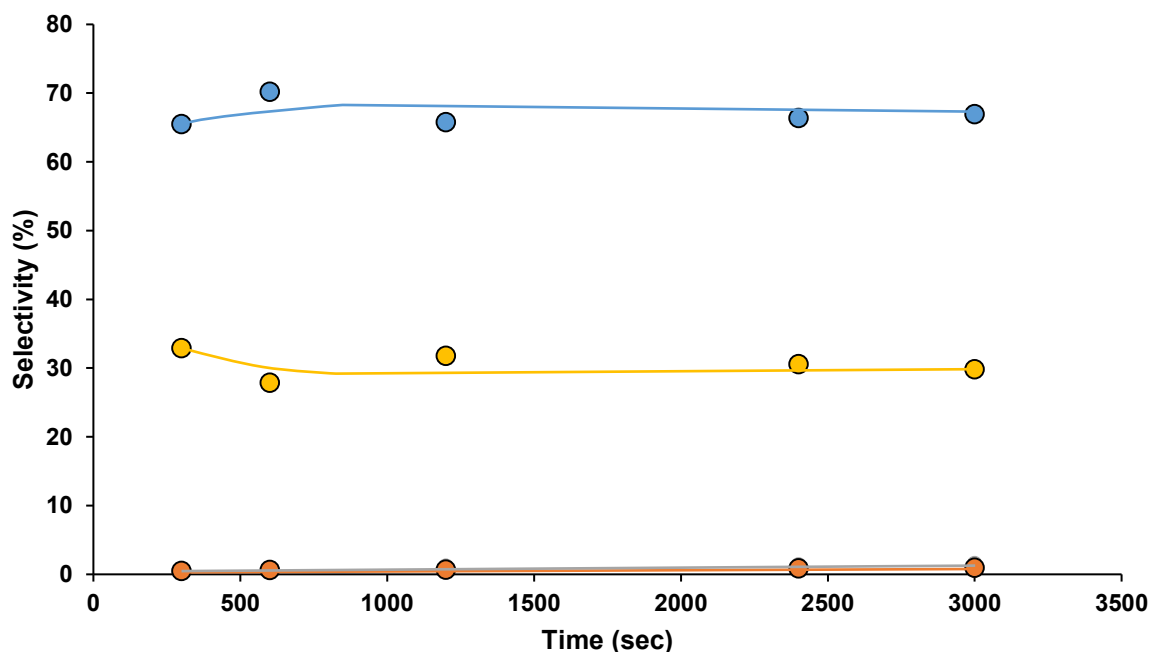


**Figure 5-20 Selectivity of 1 g benzyl alcohol oxidation with a 1%(1:9 Au:Pd)AuPd/TiO<sub>2</sub> catalyst at 120 °C 2 bar (g) O<sub>2</sub> Benzaldehyde (●), toluene (●), benzene (●), benzyl benzoate (●) benzoic acid (●)**

Figure 5-20 shows the selectivity of a 1:9 Au:Pd molar ratio catalyst when reacted with benzyl alcohol, which should display a similar result to Figure 5-19 due to benzyl alcohol and cinnamyl alcohol being vinylogous to each other. The major product in this reaction was benzaldehyde but a significant amount of toluene was also produced. A trace amount of benzene was also detectable in this system. Benzaldehyde can be produced via two reaction pathways, a direct oxidation pathway and a disproportionation pathway. It is this latter pathway that would be significant in this system due to the amount of toluene detected. It can be concluded therefore, that Pd promoted disproportionation and the small addition of Au would promote this. Further work would investigate the metal ratios on MgO support which does not exhibit this disproportionation pathway.

## 5.5. Conclusion

From this work, it can be concluded that cinnamyl alcohol oxidation is dependent on a complex set of parameters and their influence plays an interlinked part in the reaction scheme. The effect of support on the reaction is an important consideration and is one that must be planned

if one is to achieve the desired outcome. Whilst AuPd supported on ZnO is the least active catalyst, it is not markedly so and remains a suitable support for cinnamyl alcohol oxidation. TiO<sub>2</sub> and graphite supports are of similar activity however, the selectivity of the catalysts is different. Carbon supported AuPd produces more side reaction products compared with TiO<sub>2</sub>, consequently, to promote cinnamaldehyde selectivity, one should use TiO<sub>2</sub> instead of graphite.

Combining what is known about anaerobic conditions for these catalysts and the effect of temperature, the ideal temperature to run aerobic oxidation is 120 °C as this temperature is when the catalyst seems to be the most active, even if it does promote disproportionation as this can be countered by using a support that does not have this pathway. Metal loading is also a consideration, 1:1 Au:Pd ratio is the most beneficial to the oxidation of cinnamyl alcohol and benzyl alcohol as reducing the Au loading, based on this limited study, seemed to promote the formation of *trans*- $\beta$ -methylstyrene which isn't generally the desired product. Further research is needed to conclusively identify some aspects of this research but a foundation in its understanding has been achieved.

## Chapter 5 References

1. Rodríguez-Reyes JCF, Friend CM, Madix RJ. Origin of the selectivity in the gold-mediated oxidation of benzyl alcohol. *Surface Science* 2012, **606**(15–16): 1129-1134.
2. Hartung WH, Simonoff R. Hydrogenolysis of benzyl groups attached to oxygen, nitrogen, or sulfur. *Organic Reactions* 1953.
3. Pritchard J, Kesavan L, Piccinini M, He Q, Tiruvalam R, Dimitratos N, Lopez-Sanchez JA, Carley AF, Edwards JK, Kiely CJ, Hutchings GJ. Direct Synthesis of Hydrogen Peroxide and Benzyl Alcohol Oxidation Using Au–Pd Catalysts Prepared by Sol Immobilization. *Langmuir* 2010.
4. Keresszegi C, Burgi T, Mallat T, Baiker A. On the Role of Oxygen in the Liquid-Phase Aerobic Oxidation of Alcohols on Palladium. *Journal of Catalysis* 2002, **211**(1): 244-251.
5. Mori K, Hara T, Mizugaki T, Ebitani K, Kaneda K. Hydroxyapatite-Supported Palladium Nanoclusters: A Highly Active Heterogeneous Catalyst for Selective Oxidation of Alcohols by Use of Molecular Oxygen. *Journal of the American Chemical Society* 2004, **126**(34): 10657-10666.
6. Williams RM, Medlin JW. Benzyl Alcohol Oxidation on Pd(111): Aromatic Binding Effects on Alcohol Reactivity. *Langmuir* 2014, **30**(16): 4642-4653.
7. Guo Z, Liu B, Zhang Q, Deng W, Wang Y, Yang Y. Recent advances in heterogeneous selective oxidation catalysis for sustainable chemistry. *Chemical Society Reviews* 2014, **43**(10): 3480-3524.
8. Marx S, Baiker A. Beneficial Interaction of Gold and Palladium in Bimetallic Catalysts for the Selective Oxidation of Benzyl Alcohol. *The Journal of Physical Chemistry C* 2009, **113**(15): 6191-6201.

9. van Bokhoven JA, Miller JT. d Electron Density and Reactivity of the d Band as a Function of Particle Size in Supported Gold Catalysts. *The Journal of Physical Chemistry C* 2007, **111**(26): 9245-9249.
10. Choudhary VR, Dhar A, Jana P, Jha R, Uphade BS. A green process for chlorine-free benzaldehyde from the solvent-free oxidation of benzyl alcohol with molecular oxygen over a supported nano-size gold catalyst. *Green Chemistry* 2005, **7**(11): 768-770.
11. Dong Y-Y, Liao W-P, Suo Z-H. Uranium oxide-supported gold catalyst for water–gas shift reaction. *Fuel Processing Technology* 2015, **137**: 164-169.
12. Costa JCS, Corio P, Rossi LM. Catalytic oxidation of cinnamyl alcohol using Au-Ag nanotubes investigated by surface-enhanced Raman spectroscopy. *Nanoscale* 2015, **7**(18): 8536-8543.
13. Caravati M, Meier DM, Grunwaldt J-D, Baiker A. Continuous catalytic oxidation of solid alcohols in supercritical CO<sub>2</sub>: A parametric and spectroscopic study of the transformation of cinnamyl alcohol over Pd/Al<sub>2</sub>O<sub>3</sub>. *Journal of Catalysis* 2006, **240**(2): 126-136.
14. Niklasson IB, Delaine T, Islam MN, Karlsson R, Luthman K, Karlberg AT. Cinnamyl alcohol oxidizes rapidly upon air exposure. *Contact Dermatitis* 2013, **68**(3): 129-138.
15. Aver'yanov VA, Vlasov DV, Svechnikova AA, Ermakov AI. Relationship of the selectivity effect of aromatic solvents with their electron-donor ability and organic reactant structure in free radical chlorination. *Kinet Catal* 2000, **41**(2): 152-158.
16. Conte M, Miyamura H, Kobayashi S, Chechik V. Enhanced acyl radical formation in the Au nanoparticle-catalysed aldehydeoxidation. *Chemical Communications* 2010, **46**(1): 145-147.
17. Ionita P, Gilbert BC, Chechik V. Radical Mechanism of a Place-Exchange Reaction of Au Nanoparticles. *Angewandte Chemie* 2005, **117**(24): 3786-3788.

18. Chen J, Jiang T, Wei G, Mohamed AA, Homrighausen C, Krause Bauer JA, Bruce AE, Bruce MRM. Electrochemical and Chemical Oxidation of Gold(I) Thiolate Phosphine Complexes: Formation of Gold Clusters and Disulfide. *Journal of the American Chemical Society* 1999, **121**(39): 9225-9226.
19. Cuervo MR, Asedegbega-Nieto E, Díaz E, Ordóñez S, Vega A, Dongil AB, Rodríguez-Ramos I. Modification of the adsorption properties of high surface area graphites by oxygen functional groups. *Carbon* 2008, **46**(15): 2096-2106.
20. Axet MR, Dechy-Cabaret O, Durand J, Gouygou M, Serp P. Coordination chemistry on carbon surfaces. *Coordination Chemistry Reviews* 2016, **308**: 236-345.
21. Li Y, Zhao Y, Cheng H, Hu Y, Shi G, Dai L, Qu L. Nitrogen-doped graphene quantum dots with oxygen-rich functional groups. *J Am Chem Soc* 2012, **134**(1): 15-18.
22. Jalkanen JP, Halonen M, Fernandez-Torre D, Laasonen K, Halonen L. A computational study of the adsorption of small Ag and Au nanoclusters on graphite. *J Phys Chem A* 2007, **111**(49): 12317-12326.
23. Akola J, Häkkinen H. Density functional study of gold atoms and clusters on a graphite (0001) surface with defects. *Physical Review B* 2006, **74**(16): 165404.
24. Okazaki-Maeda K, Akita T, Tanaka S, Kohyama M. First-Principles Calculations of M<sub>10</sub>/Graphene (M = Au, Pt) Systems - Atomic Structures and Hydrogen Adsorption -. *Materials Transactions* 2008, **49**(11): 2441-2444.
25. Tronconi E, Crisafulli C, Galvagno S, Donato A, Neri G, Pietropaolo R. Kinetics of liquid-phase hydrogenation of cinnamaldehyde over a platinum-tin/nylon catalyst. *Industrial & Engineering Chemistry Research* 1990, **29**(9): 1766-1770.
26. Dimitratos N, Edwards J, Kiely C, Hutchings G. Gold catalysis: helping create a sustainable future. *Appl Petrochem Res* 2012, **2**(1-2): 7-14.



27. Chambers A, David Jackson S, Stirling D, Webb G. Selective Hydrogenation of Cinnamaldehyde over Supported Copper Catalysts. *Journal of Catalysis* 1997, **168**(2): 301-314.
28. Hájek J, Wärnå J, Murzin DY. Liquid-Phase Hydrogenation of Cinnamaldehyde over a Ru–Sn Sol–Gel Catalyst. 2. Kinetic Modeling. *Industrial & Engineering Chemistry Research* 2004, **43**(9): 2039-2048.
29. Ponec V. On the role of promoters in hydrogenations on metals;  $\alpha,\beta$ -unsaturated aldehydes and ketones. *Applied Catalysis A: General* 1997, **149**(1): 27-48.
30. Sankar M, Nowicka E, Tiruvalam R, He Q, Taylor SH, Kiely CJ, Bethell D, Knight DW, Hutchings GJ. Controlling the Duality of the Mechanism in Liquid-Phase Oxidation of Benzyl Alcohol Catalysed by Supported Au–Pd Nanoparticles. *Chemistry – A European Journal* 2011, **17**(23): 6524-6532.
31. Mallat T, Baiker A. Oxidation of alcohols with molecular oxygen on platinum metal catalysts in aqueous solutions. *Catalysis Today* 1994, **19**(2): 247-283.
32. Abad A, Corma A, García H. Catalyst Parameters Determining Activity and Selectivity of Supported Gold Nanoparticles for the Aerobic Oxidation of Alcohols: The Molecular Reaction Mechanism. *Chemistry – A European Journal* 2008, **14**(1): 212-222.
33. Griffin MB, Rodriguez AA, Montemore MM, Monnier JR, Williams CT, Medlin JW. The selective oxidation of ethylene glycol and 1,2-propanediol on Au, Pd, and Au–Pd bimetallic catalysts. *Journal of Catalysis* 2013, **307**: 111-120.
34. Villa A, Ferri D, Campisi S, Chan-Thaw CE, Lu Y, Kröcher O, Prati L. Operando Attenuated Total Reflectance FTIR Spectroscopy: Studies on the Different Selectivity Observed in Benzyl Alcohol Oxidation. *ChemCatChem* 2015, **7**(16): 2534-2541.

35. Dimitratos N, Villa A, Wang D, Porta F, Su D, Prati L. Pd and Pt catalysts modified by alloying with Au in the selective oxidation of alcohols. *Journal of Catalysis* 2006, **244**(1): 113-121.

# Chapter 6

## 6. General Discussion, Conclusion and Future Work

### 6.1. General Discussion and Conclusions

#### 6.1.1. Effects of solvent and metal ratio on benzyl alcohol oxidation

Monometallic Au, Pd and AuPd bimetallic catalysts were used to carry out a series of investigations involving the oxidation of benzyl alcohol, cinnamyl alcohol and a range of substituted benzyl alcohols. Benzyl alcohol oxidation is a test reaction used to assess the performance of catalysts<sup>1</sup>. It has been used as a benchmark when comparing similar reactions, such as when modifying the catalyst used to oxidise benzyl alcohol. It has also been used as a standard reaction to elucidate the reaction mechanism since it has been extensively studied.

Chapter 3 introduced the catalysts to be used in this study and demonstrated their effect on benzyl alcohol oxidation whereas chapter 2 introduced how these catalysts were synthesised. As a recap, the catalysts were prepared via sol immobilisation and produced in a range of molar ratios (Au:Pd) but the standard catalyst is the equimolar Au:Pd catalyst. These catalysts were supported on a range of metal oxides, such as TiO<sub>2</sub> and MgO. The non-metal-oxide graphite was also used as a support. TiO<sub>2</sub> and graphite required acidification of the sol to facilitate immobilising the sol onto the metal oxide. The supports ZnO and MgO were not acidified as this would cause the support to change into a soluble compound. To ascertain whether the methodology in this study was creating catalysts with the correct molar ratio, MP-AES was employed to accurately calculate the metal loading of the catalysts, and it was found that most the catalysts were at a loading consistent with the intended levels. One caveat to this finding was catalysts with higher Pd loading, however XPS analysis did suggest the metal ratios were satisfactory.

Further XPS analysis on the catalysts indicated that the nanoparticles supported on  $\text{TiO}_2$  were metallic in nature due to  $\text{Au}_{77/2}$  peak and  $\text{Pd}_{3d}$  peak being at 83.4 eV and 335 eV respectively. Supporting this observation in metallic binding energies was the fact XPS analysis performs two scans during analysis, any  $\text{Pd}^{n+}$  and  $\text{Au}^{n+}$  species would show up as a reduction in binding energy intensity which did not occur. This is in consensus with established research<sup>1,2</sup>. Lastly, XPS analysis indicated a  $\text{TiO}_2$  ratio of Ti:O exceeding the expected 1:2 ratio and this was rationalised to be due to the presence of PVA, a stabiliser ligand used in the catalyst preparation. These ligands bind to the metal oxide surface along with the metal nanoparticles and so are contributing to the intensity of the O binding energy during analysis. As Prati *et al.*<sup>3</sup> suggested, this stabiliser ligand can obscure the active sites on the catalyst by blocking active sites on the catalyst. If these PVA ligands could be removed whilst the AuPd nanoparticles were bonded to the surface, then one would assume the activity to increase. When THPC was employed as a stabiliser in the reaction of sol immobilised catalysts with glycerol, activity did increase.

A literature search was conducted to assess surface chemistry of these catalysts and TEM results were commented on. The sol immobilisation catalyst preparation produces nanoparticles with a narrow size distribution between 1-9 nm with a mean particle size of 4 nm. Thermal studies into these catalysts found mild sintering of the nanoparticles but the particle size distribution remained relatively narrow. When sols were immobilised onto activated carbon, calcination caused severe sintering of the nanoparticles immobilised on activated carbon<sup>2</sup>.

The next step in investigating AuPd catalysts in the oxidation of benzyl alcohol was to assess if solvent affected the catalysts' activity. It was found that oxidising benzyl alcohol over AuPd/ $\text{TiO}_2$  in the presence of water greatly increased its reaction rate with a high selectivity to the desired benzaldehyde when compared to solvent free conditions. Replacing water with  $\text{D}_2\text{O}$  slowed the rate of reaction and introduced an induction period into the system. Further work would be needed to determine why  $\text{D}_2\text{O}$  had this effect but work continued with investigating water's role in reaction, with literature discussing the role of deuterated benzyl alcohol.

Previous research<sup>4</sup> suggests benzyl alcohol forms an alcoholate on the Au metal cluster which may be affected by deuterium in the deuterated benzyl alcohol through kinetic isotope effects but this would need further study. Water was suggested<sup>5</sup> to be able to activate molecular oxygen over catalysts containing Au, creating a promotion effect in the system even with the partial solubility of benzyl alcohol in water. Mass transport effects were assessed by changing the solvent to benzene to fully solvate the substrate and ensure homogeneous mixing of the reacting mixture. In this scenario, reaction rate was significantly reduced and this trend was repeated using toluene as a solvent.

When methanol was employed as a solvent, its activity was very low relative to water, but was higher than either toluene or benzene. This seemed to suggest polar solvents had a promotional effect on the oxidation of benzyl alcohol due to their stabilising nature on charges created on the catalyst surface. As the reaction was highly inhibited when benzene was used as a solvent, it could be suggested that benzene is a poison to this catalytic system. In order to test this, a series of reactions were conducted in which water and benzene were combined such that the reaction mixture went from exclusively water to exclusively benzene over a range of water:benzene ratios. From this work, it was evident that increasing the amount of benzene in the system led to a decrease in activity when about 30% of water volume was substituted with benzene. After this, reactivity decreased markedly. This supports the idea that benzene is a poison to this catalyst.

While solvent played a key role in the activity of AuPd catalysts in benzyl alcohol oxidation, so too did the AuPd metal ratio of the catalysts. Au has a promotional effect on Pd catalysts with an Au:Pd ratio of 1:2 having the most positive effect on the oxidation reaction and work by Enache *et al.*<sup>6</sup> found Au rich AuPd catalysts to be less active than their Pd rich counterparts. A brief study was conducted in chapter 3 of substituted benzyl alcohol oxidation using 4-methoxybenzyl alcohol on the varying metal ratio catalysts. For 4-methoxybenzyl alcohol, 0.5:9.5 Au:Pd was found to be the most active species and chapter 4 studied substituted benzyl alcohols in more detail. The conclusions can be found later in this chapter.

In conclusion, the presence of water promotes the oxidation of benzyl alcohol and other polar solvents seem to have a promotional affect in this system. This arises from the possibility of formal surface charges forming on the catalyst surface. Organic solvents seem to have an inhibitory effect on benzyl alcohol oxidation, with benzene seemingly acting as a catalytic

poison by completely inhibiting the reaction when used as a solvent on its own. Au:Pd ratio has an effect on reaction whereby Au rich catalysts are lower in activity than Pd rich catalysts highlighting the synergistic effect Au and Pd have in metal alloys.

### 6.1.2. Effects of substituent groups on the oxidation of benzyl alcohol

As benzyl alcohol is used as a model reaction for studying the activity of catalysts, it makes an ideal reaction to subtly modify to ascertain further information on the catalytic system. This is achievable in a way that does not negate the principles established in existing literature. One way of achieving this was to substitute benzyl alcohol with secondary functional groups with the aim of modifying the behaviour in a more predictable way. Reactions were conducted using a 1:1 Au:Pd molar ratio on MgO.

Initially, benzyl alcohol was substituted with a methoxy group in the *para*- position to increase electron density into the aromatic system. By doing this, the rate of reaction increased compared to the rate for standard benzyl alcohol oxidation and selectivity remained high to the desired benzaldehyde molecule. Additional methoxy groups in the *meta*- position did not have a promotional effect on the rate of reaction but decreased the rate of reaction. This was thought to arise from the electron directing nature of the methoxy group in each position. As methoxy is an electron donating group, it will affect the benzyl alcohol resonance structures. Whilst in the *para*- position, this additional electron density can resonate adjacent to the reacting alcohol moiety. When methoxy is in the *meta*- position, electron density is maintained around the benzene ring and formal charges arise on carbons not related to the alcohol moiety. Additionally, methoxy groups add increasing bulk to the substrate which would decrease its ability to adsorb to the catalyst surface and proceed with oxidation.

The next structure to be investigated was *para*-fluorobenzyl alcohol. The substitution of a halide group has the reverse effect of the methoxy groups. Fluorine is highly electronegative, perturbing the electron density by attracting the delocalised electrons to the opposite end of the molecule that the alcohol moiety occupies. In this system, catalyst activity is reduced when compared to the standard benzyl alcohol oxidation reaction.

### 6.1.3. Effect of Au and Pd ratio on the oxidation of substituted benzyl alcohols

The Au:Pd ratio was varied to observe whether this had an effect on catalyst activity as it does for the standard reaction. Neither *para*-methoxybenzyl alcohol nor *para*-fluorobenzyl alcohol oxidation was greatly affected by varying the metal loading of the catalyst. This could be due to *para*-fluorobenzyl alcohol being less active, therefore it was less sensitive to the varying metal ratios present in the catalyst. *para*-Methoxybenzyl alcohol was higher in activity and was also insensitive to Au:Pd ratio. It may be that the promotion effect from the electron donating nature of the methoxy group is dominant compared to any effect the metal ratio has. Additionally, as will be seen in the next section, formal charges factor within the catalytic system. Substituted benzyl alcohol oxidation reactions carried out in water display evidence of formal charge formation. These formal charges seem to be the dominant effect in determining the rate of reaction compared to the Au and Pd metal ratios within the catalyst system.

### 6.1.4. Hammett methodology on the reaction of substituted benzyl alcohols

By implementing the Hammett methodology, mechanistic information for the reaction could be elucidated. *Para*-fluorobenzyl alcohol did not fit with the Hammett plot and was omitted for the purposes of analysis, which led to a  $\rho$  value of -2.47 by using the  $\sigma^-$  values. There was no correlation with  $\sigma^+$  values which ruled out a reaction involving radical intermediates. These observations were in keeping with previous work by Baiker *et al.*<sup>7</sup> in substituted benzyl alcohol oxidation using organically modified ruthenium-hydroxyapatite complexes. Christensen *et al.*<sup>8</sup> found a  $\rho < 0$  in their work which is in agreement of this research. Combining the two observations made by Christensen and Baiker, it can be surmised that a common reaction pathway exists in Ru and Au based catalysts which now extends to bimetallic AuPd catalysts as this work suggests.

By further analysing the results of the Hammett study, benzyl alcohol and its derivatives seemingly undergo reaction via generation of a cation in the benzylic position with oxidation proceeding via  $\beta$ -hydride elimination. Literature relating to this reaction indicated a Kinetic

Isotope Effect (KIE) was present, with  $K_H/K_D$  being around 2.8 suggesting bond breakage of the neighbouring hydrogen atom occurs in the reaction's rate determining step. Of note, this KIE was lower than that for a fully broken bond in the transition state, suggesting this transition state was stabilised by compounds present in the reaction medium. As formal charges are involved in the mechanism with the transition state involving partial bonding, it seems electron donating groups contribute to a stabilising factor in the reaction, allowing the transition state to form and proceed to oxidation. By removing electron density away from the reaction site, this charged intermediate is destabilised and so oxidation is inhibited.

### 6.1.5. Cinnamyl alcohol oxidation and the effect of support

Cinnamyl alcohol oxidation is also used as a model reaction to study aromatic alcohol oxidation and was employed here to assess how AuPd catalysts affect its oxidation. Initially, the effect of support was investigated using 1%AuPd (1:1 Au:Pd ratio) on ZnO, graphite and TiO<sub>2</sub>. From these reactions, it was concluded that oxidation of cinnamyl alcohol was highly selective to cinnamaldehyde for AuPd supported on all the supports studied. However, it was *trans*- $\beta$ -methylstyrene and 3-phenylpropan-1-ol oxidation products that showed the most variability between the differing supports. When ZnO was used as a support, more 3-phenylpropan-1-ol was produced compared to *trans*- $\beta$ -methylstyrene, however, this was reversed when graphite was used for the support material. Additionally, AuPd supported on graphite produced substantially more benzaldehyde when compared to ZnO and TiO<sub>2</sub>.

It was elucidated that benzaldehyde could be produced via an additional reaction pathway present in graphite supported catalysts, when compared to ZnO and TiO<sub>2</sub>, with one pathway potentially being radical in nature. As no initiators were used in this study, there would either need to be a trace compound in graphite or cinnamyl alcohol starting material, or an activation pathway within the catalyst. This later assumption is possible as previous work has suggested Au catalysts can activate molecular oxygen, which would allow a radical mechanism to commence<sup>9</sup>. As graphite has varying surface chemistry based on its production, the graphite source in this study might have had multiple surface oxygen compounds present which could easily be activated by the Au or Au:Pd nanoparticles immobilised on its surface.



Finally, for AuPd supported on TiO<sub>2</sub> a similar trend to graphite was observed as more *trans*- $\beta$ -methylstyrene was produced compared to 3-phenylpropan-1-ol. Production of both compounds arises from hydrogenation of either cinnamyl alcohol or cinnamaldehyde. Using ZnO as a support, hydrogenation of cinnamaldehyde can lead to the formation of 3-phenylpropan-1-ol, whereas for the TiO<sub>2</sub> support *trans*- $\beta$ -methylstyrene is produced via hydrogenation.

AuPd supported on MgO was briefly studied and was highly selective to cinnamaldehyde and produced a significant amount of 3-phenylpropan-1-ol. It is known that when MgO is used as a support in AuPd catalysts, it displays a unique property whereby it can switch off disproportionation reactions in organic alcohol oxidation<sup>10</sup>. AuPd supported on MgO produced trace amounts of *trans*- $\beta$ -methylstyrene, suggesting it does not have a hydrogenation pathway and that *trans*- $\beta$ -methylstyrene does indeed mainly arise from hydrogenation of cinnamaldehyde as observed in the other supports.

#### 6.1.6. Effect of temperature on cinnamyl alcohol oxidation

Previously cited work by Hutchings *et al.*<sup>10</sup> found that increasing temperature promoted disproportionation reaction and this team found that a temperature of 120 °C significantly promoted disproportionation. Consequently, standard reactions in this research were conducted at a temperature known to promote disproportionation of aromatic alcohols. Lowering the temperature to 100 ° and 80 °C also lowered the activity of the AuPd catalysts used in this study. No temperatures above 120 °C were used due to limitations in the reaction equipment used.

At 120 °C, cinnamyl alcohol conversion reached a maximum of ca. 86% when catalysed with AuPd supported on TiO<sub>2</sub>. Conversion remained at ca. 86% with increased reaction time suggesting the catalyst has been deactivated. This deactivation was also observed for benzyl alcohol at 120 °C but not at 100 °C. Deactivation was observed again at 80 °C for both cinnamyl alcohol and benzyl alcohol as the reaction rate started to decrease at longer reaction times. At longer reaction times at 120 °C and 80 °C, deactivation of the catalyst could be occurring due to the catalyst being poisoned from the build-up of by-products building up on

the catalyst surface. As 100 °C kept to a linear increase in conversion at extended reaction times, these by-products seemingly were either not produced, or were easily able to dissociate from the catalyst surface.

Organic solvents have been shown to deactivate catalysts, as well as the presence of carboxylic groups<sup>11</sup> but carboxylic compounds were not detected in this study. Molecular oxygen has been shown to be able to deactivate catalysts<sup>12</sup>, especially if there's a deviation away from the initial rate of reaction, which was detected in this study. Finally, only bimetallic AuPd catalysts were used in this study, which have been shown to have a tendency ability to easily dissociate catalytic by-products<sup>13</sup>.

### 6.1.7. Effect of metal loading on the oxidation of cinnamyl alcohol

All reactions between AuPd catalysts and cinnamyl alcohol were carried out at a 1:1 metal ratio between the Au and Pd on TiO<sub>2</sub>. Metal loading was considered briefly with the Au to Pd ratio being varied to 1:9. This ratio was found to increase the initial rate of reaction for cinnamyl alcohol oxidation. A small amount of Au added to Pd catalysts is needed to promote the oxidation of cinnamyl alcohol however, by analysing the time on line study, selectivity in this system is greatly altered. The major product is now *trans*- $\beta$ -methylstyrene. As *trans*- $\beta$ -methylstyrene is formed via hydrogenation, Pd seemingly plays a dominant part in hydrogenation with small additions of Au promoting this pathway. Using 1:9 AuPd catalyst on TiO<sub>2</sub> for benzyl alcohol oxidation, it was observed that while benzaldehyde was still the major oxidation product, a significant amount of toluene was produced along with trace amounts of benzene. In this system, Pd rich bimetallic AuPd catalysts seemingly promote disproportionation of benzyl alcohol.

## 6.2. Future work

Aromatic alcohol oxidation and gold catalysis in general are fertile grounds for future research and since the discovery of gold catalysis, there has been a dramatic rise in research in this

area. Contextualising the research presented in this thesis to potential future work, one would focus on the following areas:

- Different supports for benzyl alcohol oxidation
  - Only a small selection of supports was used in this study, but there exists a wide range of supports available such as  $\text{Nb}_2\text{O}_3$ , differing activated carbons with the potential to expand to graphite and/or graphene
  - One area that is of personal interest and one that did not get covered is the area of using  $\text{U}_2\text{O}_3$  and other uranium oxides as supports for benzyl alcohol oxidation
  - Varying the catalyst preparation method; sol immobilisation was used exclusively but other techniques exist such as wet impregnation. Additionally, modifying the sol immobilisation technique to implement sequential reduction of the metal clusters is an area to produce core shell nanoparticles instead of the homogeneous alloys created in the simultaneous reduction employed in this study
  - Further surface studies of the Au, Pd and AuPd catalysts
- Effects of substituent groups on benzyl alcohol oxidation
  - A wider set of substituent groups are available for benzyl alcohol and using these will allow one to further assess any impact these have on the oxidation mechanism, expanding on electron withdrawing groups.
  - Conducting the study on substituted benzyl alcohols in different reaction conditions such as different solvents and different metal oxide supports to see if formal charges can be further stabilised or if the mechanism changes
- Cinnamyl alcohol oxidation
  - Testing a wider range of catalysts supports
  - Varying the metal loading of the nanoparticles such as that used in this study's investigation into benzyl alcohol oxidation.

- Conducting the reaction at temperatures exceeding 120 °C however, this would involve in changing the methodology of the reaction as the glass reactors used in this study are not suitable for temperatures exceeding 120 °C.
  - Further reactions under anaerobic conditions
- Catalyst reuse studies
  - Catalysts were only used once in the reactions conducted in this study, future work could consider the stability of the catalysts by using used catalyst in fresh reaction mixtures. Additionally, it would be useful to check metal leaching, research suggests sol immobilised catalysts are stable and can be re-used but this was not investigated here<sup>14</sup>.

## Chapter 6 References

1. Dimitratos N, Lopez-sanchez J, Morgan D, Carley A, Prati L, Hutchings G. Solvent free liquid phase oxidation of benzyl alcohol using Au supported catalysts prepared using a sol immobilization technique. *Catalysis Today* 2007, **122**(3-4): 317-324.
2. Dimitratos N, Lopez-Sanchez JA, Morgan D, Carley AF, Tiruvalam R, Kiely CJ, Bethell D, Hutchings GJ. Solvent-free oxidation of benzyl alcohol using Au-Pd catalysts prepared by sol immobilisation. *Phys Chem Chem Phys* 2009, **11**(25): 5142-5153.
3. Villa A, Wang D, Su DS, Prati L. Gold Sols as Catalysts for Glycerol Oxidation: The Role of Stabilizer. *ChemCatChem* 2009, **1**(4): 510-514.
4. Abad A, Corma A, Garcia H. Catalyst parameters determining activity and selectivity of supported gold nanoparticles for the aerobic oxidation of alcohols: the molecular reaction mechanism. *Chemistry* 2008, **14**(1): 212-222.
5. Yang X, Wang X, Liang C, Su W, Wang C, Feng Z, Li C, Qiu J. Aerobic oxidation of alcohols over Au/TiO<sub>2</sub>: An insight on the promotion effect of water on the catalytic activity of Au/TiO<sub>2</sub>. *Catalysis Communications* 2008, **9**(13): 2278-2281.
6. Enache DI, Barker D, Edwards JK, Taylor SH, Knight DW, Carley AF, Hutchings GJ. Solvent-free oxidation of benzyl alcohol using titania-supported gold–palladium catalysts: Effect of Au–Pd ratio on catalytic performance. *Catalysis Today* 2007, **122**(3–4): 407-411.
7. Opre Z, Ferri D, Krumeich F, Mallat T, Baiker A. Aerobic oxidation of alcohols by organically modified ruthenium hydroxyapatite. *Journal of Catalysis* 2006, **241**(2): 287-295.
8. Fristrup P, Johansen L, Christensen C. Mechanistic Investigation of the Gold-catalyzed Aerobic Oxidation of Alcohols. *Catalysis Letters* 2008, **120**(3-4): 184-190.

9. Conte M, Miyamura H, Kobayashi S, Chechik V. Enhanced acyl radical formation in the Au nanoparticle-catalysed aldehydeoxidation. *Chemical Communications* 2010, **46**(1): 145-147.
10. Sankar M, Nowicka E, Tiruvalam R, He Q, Taylor SH, Kiely CJ, Bethell D, Knight DW, Hutchings GJ. Controlling the Duality of the Mechanism in Liquid-Phase Oxidation of Benzyl Alcohol Catalysed by Supported Au–Pd Nanoparticles. *Chemistry – A European Journal* 2011, **17**(23): 6524-6532.
11. Abad A, Corma A, García H. Catalyst Parameters Determining Activity and Selectivity of Supported Gold Nanoparticles for the Aerobic Oxidation of Alcohols: The Molecular Reaction Mechanism. *Chemistry – A European Journal* 2008, **14**(1): 212-222.
12. Griffin MB, Rodriguez AA, Montemore MM, Monnier JR, Williams CT, Medlin JW. The selective oxidation of ethylene glycol and 1,2-propanediol on Au, Pd, and Au–Pd bimetallic catalysts. *Journal of Catalysis* 2013, **307**: 111-120.
13. Villa A, Ferri D, Campisi S, Chan-Thaw CE, Lu Y, Kröcher O, Prati L. Operando Attenuated Total Reflectance FTIR Spectroscopy: Studies on the Different Selectivity Observed in Benzyl Alcohol Oxidation. *ChemCatChem* 2015, **7**(16): 2534-2541.
14. Dimitratos N, Lopez-Sanchez JA, Morgan D, Carley AF, Tiruvalam R, Kiely CJ, Bethell D, Hutchings GJ. Solvent-free oxidation of benzyl alcohol using Au–Pd catalysts prepared by sol immobilisation. *Physical Chemistry Chemical Physics* 2009, **11**(25): 5142.